DIGITAL WALSH-FOURIER ANALYSER FOR PERIODIC WAVEFORMS

DIGITAL WALSH-FOURIER ANALYSER FOR PERIODIC WAVEFORMS

by

Karl-Hans Siemens

A Thesis

Submitted to the Faculty of Graduate Studies

in Partial Fulfillment of the Requirements

for the Degree

Master of Engineering

McMaster University

May, 1969

MASTER OF ENGINEERING (1969) McMASTER UNIVERSITY
(Electrical Engineering) Hamilton, Ontario

TITLE: Digital Walsh-Fourier Analyser for Periodic Waveforms.

AUTHOR: Karl-Hans Siemens, B.E.E. (General Motors Institute)

SUPERVISOR: Professor R. Kitai

NUMBER OF PAGES: 119

SCOPE AND CONTENTS: This thesis describes a proposed design of a special-purpose digital instrument that will obtain the first 32 coefficients of the Walsh-Fourier series of a low-fundamental frequency periodic voltage. The mathematics are developed for applying Walsh functions to obtain a Walsh-Fourier series in the same manner as sinusoidal waves are used to obtain a Fourier series of a periodic wave. It is shown how Walsh-Fourier coefficients are employed to obtain a Fourier series. Some familiar waveforms are shown as examples. The mathematical concepts are applied to the design of the instrument, of which two major portions have been constructed using integrated circuits. The Walsh-Fourier coefficients are available at the end of the second cycle of the input. The upper fundamental frequency limit of the instrument is approximately 60 Hz. There is no low-frequency limit.

ACKNOWLEDGMENTS

I would like to thank Professor R. Kitai for his constant encouragement and assistance during the course of this work and in the preparation of this thesis.

The financial assistance provided by McKinnon Industries Limited is gratefully acknowledged.

Finally, I would like to thank Miss Olga Pawluk for typing this thesis.

Table of Contents

Table of Contents (continued)

List of Illustrations

List of Illustrations (continued)

List of Tables

List of Symbols

A_n, B_n	= Walsh-Fourier coefficients of a periodic wave
a_n, b_n	= Fourier coefficients of a periodic wave
$a_n(cm)$, $b_n(sm)$	= Fourier coefficients of Walsh functions
k, m, n	= integers
T	= period of a wave
t	= time
f	= frequency
f_c	= clock frequency feeding pulse burst generator
f_s	= sample frequency
V	= voltage
Vmax	= maximum voltage
Vcc	= integrated circuit power supply voltage
w	= frequency (in radians)
$\Phi_n(x)$, $\Phi_n(t)$	= general orthogonal function
r(x), r(t)	= weighting function
θ	= phase
zps.	= zero crossings per second
r	= quantization level number
p	= total number of quantization levels
M	= total number of samples
P_n	= binary weighted pulses from A/D converter
q	= integral portion of T/64
e_t	= remainder of division, T/64 (error in Walsh function timing)

1. Introduction

Conventional wave analysers have long been used to determine the harmonic content of signals by analogue methods. These instruments operate by tuning to the signal component that is to be measured. Generally, the lower limit of fundamental frequency that can be handled is 20 Hz. For waves that have fundamental frequencies far less than 20 Hz., accurate tuning becomes increasingly difficult and a great deal of time would be required to average, say, 20 periods for each signal component that is to be measured.

Consequently, it was decided that a digital instrument would perhaps be more suitable for measurements of low frequency waves. Samples need be taken from only one cycle of the wave. The samples would then be manipulated to derive information concerning the harmonic content of the signal. Thus, the purpose of the project was to devise a low-cost, minimum storage, digital instrument for calculating the Fourier series of a low-frequency periodic input wave.

If a_n and b_n are the coefficients of the Fourier series, then these quantities are calculated by the following equations:

$$a_n = \frac{2}{T} \int_0^T f(t) \cos n w_o t \, dt$$

and $$b_n = \frac{2}{T} \int_0^T f(t) \sin n w_o t \, dt$$

where T is the period of the signal, f(t). The equations require that the signal, f(t), be multiplied by cosine and sine waves and that these quantities be integrated over one period of f(t). In a digital instrument, sinusoidal waves are very difficult to handle. Either the waves would have to be generated according to the fundamental frequency of f(t) and then sampled at the same time as f(t), or each individual value of the waves that would be used in any calculations would have to be stored in a memory.

It was found that an array of functions, called Walsh functions,[3] would adapt themselves to a digital instrument much better than sinusoidal waves. The Walsh functions have only two values, +1 and -1, and hence can be represented by logic "1"'s and "0"'s. They can be used to represent a waveform in a Walsh-Fourier series in much the same way as sinusoidal waves are used to form a Fourier series. Once the Walsh-Fourier series has been found, the method of superposition can be used to convert the series into a Fourier series.

This thesis is written to outline the mathematical principles involved in obtaining a Walsh-Fourier series of a periodic waveform and converting it into a Fourier series. A proposed scheme for a digital instrument to obtain the Walsh-Fourier series of a periodic input signal and the construction of two portions of the instrument are also

described in this thesis. The instrument can analyse waveforms with fundamental frequencies up to 60 Hz. There is no theoretical lower frequency limit.

The second chapter establishes the mathematical basis for the design of the instrument. It shows how the properties of orthogonal functions are used to derive the Fourier series and the Walsh-Fourier series. Conversion of Walsh-Fourier to Fourier series is then explained. The following chapter shows how the mathematical expressions in Chapter II must be modified for use in a digital instrument.

Chapter IV describes the proposed scheme for the instrument with detailed descriptions of those portions of the system that are not commercially available. A partial error analysis providing examples of error arising from use of a finite number of terms in the conversion from Walsh-Fourier to Fourier series and describing the error in producing Walsh functions is given in Chapter V. The final chapter on conclusions discusses the limitations of the instrument and future work to be done on the Walsh-Fourier analyser.

II. Mathematical Basis for Design

Conventional steady state network analysis leads directly to a representation of network performance in terms of the response to sinusoidal signals of different frequencies. The calculation of the output signal from such a network is therefore simplified if the input signal is expressed in these same terms. The Fourier series representation of the input thus reveals the signal in a form particularly well-adapted to providing insight into the behaviour of networks and systems stimulated with signals of various types.

On the market there are many wave analysers which can be used to determine the harmonic content of the waveform which is being tested. However, these instruments are generally analogue devices which have a low frequency response limit of approximately 20 Hz. or higher. In the domain of ultra-low frequencies, digital instruments, which would sample the waveform and process the samples, seem to be preferable to analogue instruments, which would require circuits tuned to these very low frequencies and would require averaging periods of, say, 20 times the reciprocal of the lowest frequency component.

However, in the design of a digital instrument, sinusoidal waves, such as are normally used to calculate and to represent a Fourier series, present some difficulty.

Calculations involving sines and cosines would require that any particular value of the sine or cosine which is used in the calculations be stored or generated in a form that can be used in digital logic. It would be advantageous if another set of functions, more suitable to digital logic, could be used in place of the sinusoidal functions. It has been found that functions, known as Walsh functions, can be employed in place of sines and cosines in order to find the Fourier series of a periodic waveform.

Both sinusoidal waves and Walsh functions are orthogonal. In order to show the mathematical basis for using Walsh functions to obtain the Fourier series, this chapter first discusses the properties of orthogonal functions. It is then shown how a specific case of orthogonal functions, sinusoidal waves, are used to represent a periodic waveform by a series of these waves, commonly known as the Fourier series. A similar analysis is performed using Walsh functions. The final section of this chapter shows how a representation of a periodic waveform using Walsh functions can be converted into an equivalent Fourier series.

Properties of Orthogonal Functions

A periodic signal, f(x), may be expanded into a series of orthogonal functions. A group of functions

$$\Phi_1(x),\ \Phi_2(x),\ \Phi_3(x),\ \text{------}\Phi_n(x)\text{-----}$$

are defined to be orthogonal over the interval [a, b] with respect to a non-negative weighting function, r(x), if

$$\int_a^b r(x)\phi_n(x)\phi_m(x)dx = T_n \quad \text{if } n = m \qquad (2\text{-}1)$$
$$= 0 \quad \text{if } n \neq m$$

where T_n is a constant relating to the interval [a,b]. The function, f(x), may be expressed as the sum of such a group of orthogonal functions as follows:

$$f(x) = a_1\phi_1(x) + a_2\phi_2(x) + a_3\phi_3(x) + \text{----} \qquad (2\text{-}2)$$

Requiring the functions $\phi_n(x)$ to be orthogonal results in the relative ease with which the coefficients a_n may be evaluated. Both sides of Equation (2-2) should be multiplied by $r(x)\phi_n(x)$ and integrated over the interval of orthogonality [a,b].

$$\int_a^b f(x)r(x)\phi_n(x)dx = \int_a^b [a_1 r(x)\phi_1(x)\phi_n(x) + \text{----}$$
$$+a_m r(x)\phi_m(x)\phi_n(x)$$
$$+ a_n r(x)\phi_n^2(x) + \text{----}]dx \qquad (2\text{-}3)$$

By the basic definition of orthogonality as stated in Equation (2-1), all terms on the right-hand side of (2-3) vanish except for the nth term. Therefore,

$$\int_a^b f(x)r(x)\phi_n(x)dx = a_n \int_a^b r(x)\phi_n^2(x)dx = a_n T_n \qquad (2\text{-}4)$$

Thus, the general expression for evaluating the coefficients for an expansion in terms of orthogonal functions is:

$$a_n = \frac{1}{T_n} \int_a^b f(x)r(x)\phi_n(x)dx \qquad (2\text{-}5)$$

Many sets of orthogonal functions could be used to approximate a periodic signal. The Fourier series, which consists of the orthogonal functions, sines and cosines, is the most commonly used series in signal analysis. However, sinusoidal waves are not as suitable to perform calculations

in a digital instrument as are another set of orthogonal functions called Walsh functions. In the following sections, it is shown how both sinusoidal waves and Walsh functions can be used in a series expansion representation of a periodic signal.

Fourier Series

Many of the signals encountered in electric networks are periodic in time. A signal is defined as periodic if

$$f(t) = f(nT + t) \tag{2-6}$$

where: T = period,

n = any integer.

Therefore, it follows that if the signal is known in the interval $[t_1, t_1 + T]$, it is defined for all time. (See Figure II-1).

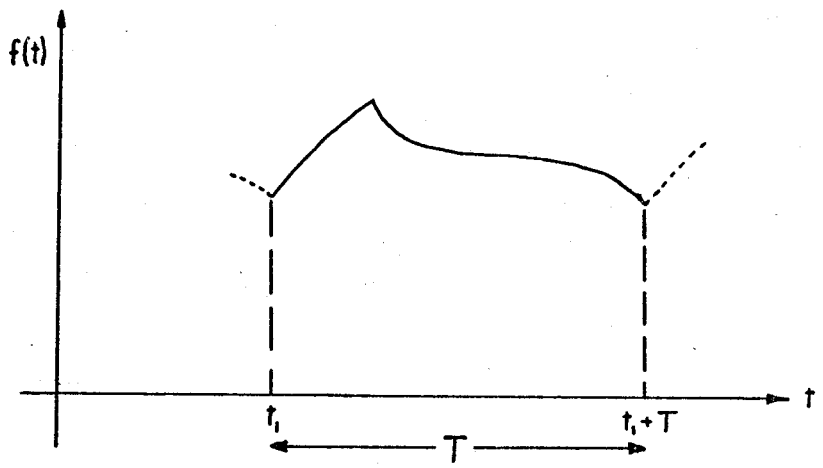

Figure II-1. Periodic Function with Period T

In practical applications in the field of electronics, all signals will be real (rather than complex) functions of time.

To expand f(t) into a series of simple orthogonal functions, it would make sense to choose functions which are themselves periodic and simple in form. The simplest type of periodic function which displays the required characteristics for orthogonality is the sinusoid. That is:

$$\int_o^T \cos(mw_o t)\cos(nw_o t)dt = \begin{cases} 0 & \text{for } m \neq n \\ T/2 & \text{for } m = n \neq 0 \\ T & \text{for } m = n = 0 \end{cases} \qquad (2\text{-}7)$$

where $w_o = \frac{2\pi}{T}$,

and m and n are positive integers.

Likewise,

$$\int_o^T \sin(mw_o t)\sin(nw_o t)dt = \begin{cases} 0 & \text{for } m \neq n \\ T/2 & \text{for } m = n \neq 0 \\ 0 & \text{for } m = n = 0 \end{cases} \qquad (2\text{-}8)$$

and $$\int_o^T \cos(mw_o t)\sin(nw_o t)dt = 0 \text{ for all m and n.} \qquad (2\text{-}9)$$

Thus, sinusoidal signals are orthogonal over the interval, T, with respect to a weighting function, r(t) = 1.0. Therefore, the general orthogonal function can be chosen as

$$\phi_n(t) = \cos(nw_o t - \theta_n) \qquad (2\text{-}10)$$

The function f(t) can be expressed as follows:

$$f(t) = C_o\phi_o(t) + C_1\phi_1(t) + C_2\phi_2(t) + \text{---} \qquad (2\text{-}11)$$

$$= \sum_{n=o}^{\infty} C_n\phi_n(t)$$

The first term in the expansion, (for n=o), represents the

average value or zero frequency term of f(t) and, as such, is somewhat unique in terms of evaluating the coefficient C_o. It may be noted in Equation (2-7) that the value of the integral for m = n = 0 is twice that for m = n ≠ 0. To develop a general expression for the coefficient which applies equally well to all terms, it is necessary to define

$$\phi_o(t) = \frac{1}{2}.$$

The series in Equation (2-11) can then be rewritten:

$$f(t) = \frac{C_o}{2} + \sum_{n=1}^{\infty} C_n \phi_n(t) \qquad (2\text{-}12)$$

$$= \frac{C_o}{2} + \sum_{n=1}^{\infty} C_n \cos(nw_o t - \theta_n)$$

To simplify further the evaluation of the coefficients, the following substitution may be made;

$$C_n \cos(nw_o t - \theta_n) = a_n \cos(nw_o t) + b_n \sin(nw_o t)$$

where $C_n = \sqrt{a_n^2 + b_n^2}$

and $\theta_n = \arctan\left(\frac{b_n}{a_n}\right)$.

The function f(t) may now be expressed in the alternate form

$$f(t) = \frac{a_o}{2} + \sum_{n=1}^{\infty} a_n \cos(nw_o t) + \sum_{n=1}^{\infty} b_n \sin(nw_o t) \qquad (2\text{-}13)$$

where $a_o = C_o$

The forms shown in Equations (2-12) and (2-13) are entirely equivalent. Equation (2-12) is more compact, and for that reason is often used as the final form for representing the function. However, since Equation (2-12) contains two unknowns, C_n and θ_n, it is convenient to convert it to the form of Equation (2-13) and evaluate separately the

coefficients a_n and b_n. Equations (2-12) and (2-13) are known as the trigonometric forms of the Fourier series.

It is necessary to point out that there are some types of functions which may not be expanded successfully into a Fourier series. However, in practice, almost every function that is encountered may be expressed as a Fourier series. Functions with the following properties are Fourier expandable:

1. The function has at most a finite number of discontinuities in one period.

2. It has a finite number of maxima and minima in one period.

3. The integral of the squared magnitude of f(t) over one period is finite. That is,

$$\int_0^T |f(t)|^2 \, dt < \infty$$

Following the procedure indicated in Equations (2-3) through (2-5), the coefficients may be evaluated. To obtain a_o multiply both sides of Equation (2-13) by $\phi_o(t)$ and integrate over one period. Since $\phi_o(t) = \frac{1}{2}$,

$$\frac{1}{2}\int_0^T f(t)dt = \int_0^T \frac{a_o}{4}\,dt + \int_0^T \frac{1}{2}\left\{\sum_{n=1}^{\infty}\left[a_n\cos(nw_ot) + b_n \sin(nw_ot)\right]\right\} dt$$

All terms in the second integral on the right will integrate to zero. Therefore,

$$\frac{1}{2}\int_0^T f(t)dt = \frac{a_oT}{4}$$

and

$$a_o = \frac{2}{T}\int_0^T f(t)dt \qquad (2\text{-}14)$$

To evaluate the remainder of the a_n coefficients, multiply both sides of Equation (2-13) by $\cos(nw_o t)$ and integrate.

$$\int_o^T f(t)\cos(nw_o t)dt = \int_o^T \left\{\frac{a_o}{2}\cos(nw_o t) + \cos(nw_o t)\sum_{m=1}^{\infty}[a_m \cos(mw_o t) + b_m \sin(mw_o t)]\right\} dt$$

In accordance with Equations (2-7), (2-8), and (2-9), all terms on the right will integrate to zero except for the product of the cosine terms when n = m. Thus

$$\int_o^T f(t)\cos(nw_o t)dt = a_n \int_o^T \cos^2(nw_o t)dt = \frac{a_n T}{2}$$

Therefore, $a_n = \frac{2}{T}\int_o^T f(t)\cos(nw_o t)dt$ (2-15)

To evaluate the coefficients b_n, the same procedure as above is followed except that now both sides of Equation (2-13) are multiplied by $\sin(nw_o t)$. Upon integration, all terms but one will again disappear, so that

$$b_n = \frac{2}{T}\int_o^T f(t)\sin(nw_o t)\,dt \qquad (2\text{-}16)$$

The Fourier series representation of the function f(t) is now complete with the coefficients defined. Recapitulating,

$$f(t) = \frac{a_o}{2} + \sum_{n=1}^{\infty}[a_n \cos(nw_o t) + b_n \sin(nw_o t)] \qquad (2\text{-}13)$$

where $a_o = \frac{2}{T}\int_o^T f(t)\,dt$ (2-14)

and $a_n = \frac{2}{T}\int_o^T f(t)\cos(nw_o t)dt$ (2-15)

and $b_n = \frac{2}{T}\int_o^T f(t)\sin(nw_o t)dt$ (2-16)

or $$f(t) = \frac{a_0}{2} + \sum_{n=1}^{\infty} C_n \cos(nw_o t - \theta_n) \qquad (2\text{-}12)$$

where $$C_n = \sqrt{a_n^2 + b_n^2}$$

and $$\theta_n = \arctan\left(\frac{b_n}{a_n}\right) .$$

Walsh-Fourier Series

The concept of frequency in electronics is based on the complete orthogonal system of sine and cosine functions. Other orthogonal systems may be used to describe periodic signals, but only the Walsh functions, several of which are shown in Figure 11-2 on page 13, have been found so far to have comparably good features.[3][4] Since these functions assume only the two values, +1 and -1, it is plausible that they may be more useful in digital circuitry than would sinusoidal functions.

Sine and cosine functions are characterized by their frequency, which is given in terms of oscillations per second. Walsh functions are characterized by their sequency, which is defined by:

$\left(\frac{1}{2}\right)$ (average number of zero crossings per second)

= sequency measured in zps.

The concept of sequency is applicable to sine and cosine functions and is identical with frequency in that case.

The terminology given the Walsh functions, sal (n,θ) and cal (n,θ), is made so that they can be compared easily to the terminology of the sinusoidal functions, $\sin(n\theta)$ and $\cos(n\theta)$. For the Walsh functions, the n denotes the multiple of sequency, whereas for the sine and cosine, n denotes the

Figure II-2. Walsh Functions

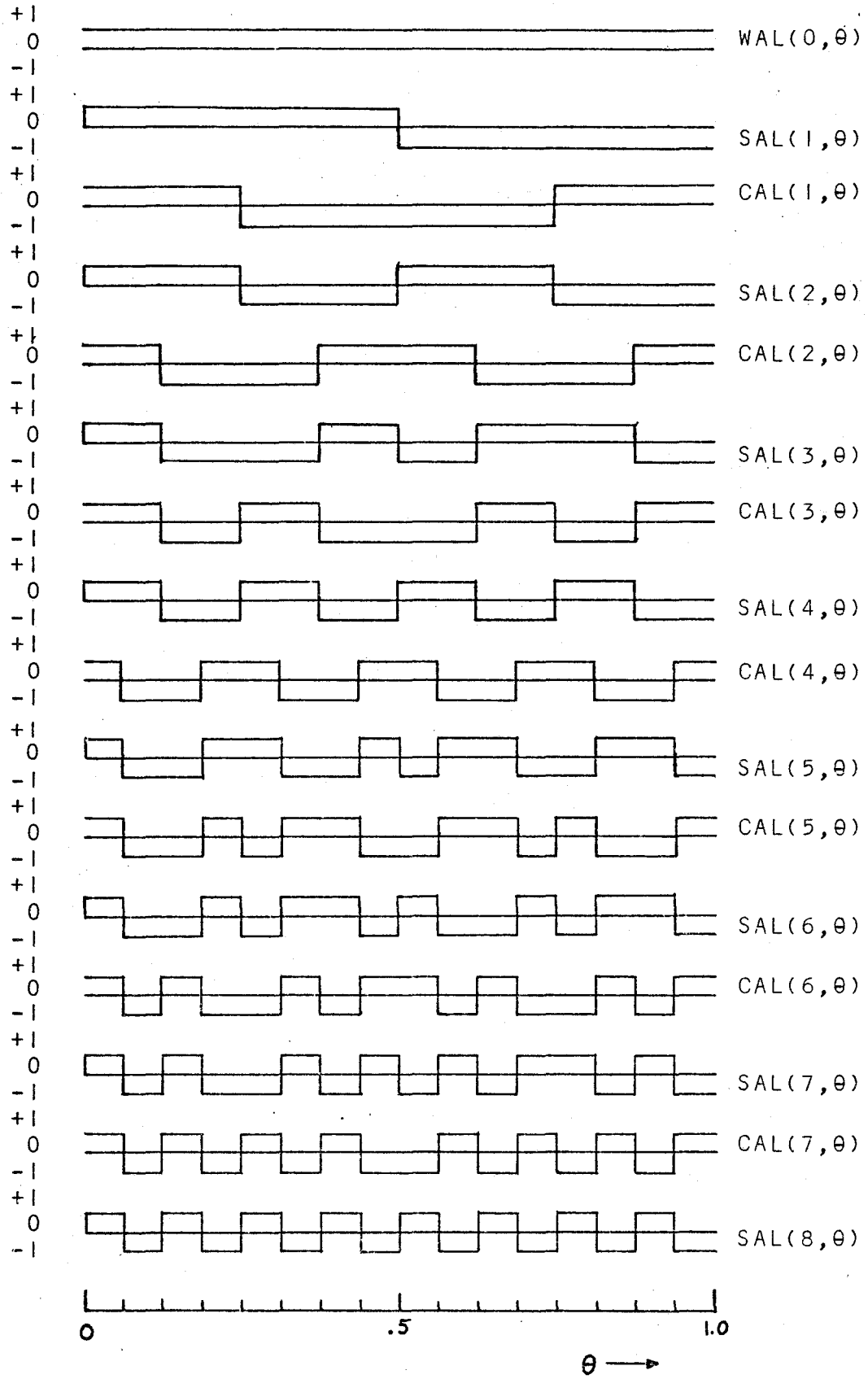

multiple of frequency. The Walsh functions become functions of time by letting $\theta = t/T$, where T is one period. For sinusoidal functions, $\theta = 2\pi ft$. Since $f = 1/T$, θ becomes $\frac{2\pi t}{T}$. Occasionally, wal (n,θ) is used to denote the Walsh functions in general. The function wal$(0,\theta)$ has a constant value of +1. The sinusoidal functions have no comparable function. An explanation of the formation of Walsh functions is given in Appendix A.

In order to use Walsh functions to form a series expansion of a signal, it can be shown (5) that they display the required characteristics of orthogonality. That is,

$$\int_0^T \text{cal}\,(m,\theta)\ \text{cal}(n,\theta)\,dt = 0 \quad \text{for } m \neq n \qquad (2\text{-}17)$$
$$= T \text{ for } m = n \neq 0$$

where m and n are positive integers.

Likewise,

$$\int_0^T \text{sal}(m,\theta)\ \text{sal}(n,\theta)\,dt = 0 \quad \text{for } m \neq n \qquad (2\text{-}18)$$
$$= T \quad \text{for } m = n \neq 0$$

and $$\int_0^T \text{cal}(m,\theta)\ \text{sal}(n,\theta)\,dt = 0 \qquad (2\text{-}19)$$

for all m and n except $m = n = 0$.

The sal and cal functions are not defined as such when m or n equals zero. When m or n becomes zero, the functions become wal$(0,\theta)$, or merely 1 for all time. Wal$(0,\theta)$ also equals $\text{sal}^2(n,\theta)$ or $\text{cal}^2(n,\theta)$. Thus, each of the Equations (2-17), (2-18), and (2-19) becomes

$$\int_0^T \text{wal}\,(0,\theta)\,dt = T \quad \text{when } m = n = 0 \qquad (2\text{-}20)$$

Therefore, according to Equation (2-1), Walsh functions are orthogonal over a period T, with respect to a weighting

function, $r(t) = 1.0$.

Consequently, as in Equation (2-13) for the Fourier series, the function $f(t)$ may be expanded into a sum of mutually orthogonal series as follows:

$$f(t) = A_o + \sum_{n=1}^{\infty} A_n \, cal(n,\theta) + \sum_{n=1}^{\infty} B_n \, sal(n,\theta) \quad (2\text{-}21)$$

A_o is the average value of $f(t)$. The convention which has been adopted in this thesis is that capital letters, A and B, are used for all coefficients of the Walsh-Fourier series, whereas the lower case letters, a and b, apply to the Fourier series coefficients.

In the expression in Equation (2-11), the general orthogonal function, $\phi_n(t)$, for the Fourier series, consists of a function which contains both sine and cosine terms. When $n = 0$, the sine portion is zero leaving cos 0 equal to 1. Therefore $\phi_o(t)$ should be 1 for the Fourier series. However, so that the general expression for the coefficient would apply equally well to all terms, $\phi_o(t)$ was arbitrarily set at 1/2. For the Walsh-Fourier series, when $n = 0$, $\phi_o(t)$ becomes wal $(0,\theta)$. $Wal(0,\theta)$ can be used directly to find the coefficient A_o and no arbitrary value need by assigned to $\phi_o(t)$.

Again, following the procedure of Equations (2-3) through (2-5), the coefficients of the Walsh-Fourier series may be obtained. To evaluate A_o, multiply both sides of Equation (2-21) by $\phi_o(t)$, or $wal(0,\theta)$, and integrate over one period. Since $wal(0,\theta) = 1$ for all t,

$$\int_0^T f(t)dt = \int_0^T A_0 dt + \int_0^T \left(\sum_{n=1}^{\infty} [A_n cal(n,\theta) + B_n sal(n,\theta)] \right) dt$$

All terms in the second integral on the right side integrate to zero. Therefore,

$$\int_0^T f(t)\, dt = \int_0^T A_0 dt = A_0 T$$

and $$A_0 = \frac{1}{T} \int_0^T f(t)dt \qquad (2\text{-}22)$$

To evaluate the remainder of the A_n coefficients, multiply both sides of Equation (2-21) by $cal(n,\theta)$ and integrate.

$$\int_0^T f(t)cal(n,\theta)dt = \int_0^T \Big\{ A_0 cal(n,\theta) + cal(n,\theta) \sum_{m=1}^{\infty} [A_m cal(m,\theta) + B_m sal(m,\theta)] \Big\} dt$$

According to Equations (2-17), (2-18), and (2-19), all terms on the right will integrate to zero except for the product of the cal terms when n = m. Then,

$$\int_0^T f(t)cal(n,\theta)dt = A_n \int_0^T cal^2(n,\theta)dt = A_n T$$

Therefore, $$A_n = \frac{1}{T} \int_0^T f(t)cal(n,\theta)dt \qquad (2\text{-}23)$$

To evaluate the B_n coefficients, the same procedure as above is followed except that now both sides of Equation (2-21) are multiplied by $sal(n,\theta)$. Upon integration, all terms but the $sal^2(n,\theta)$ term will disappear, so that

$$B_n = \frac{1}{T} \int_0^T f(t)sal(n,\theta)dt \qquad (2\text{-}24)$$

The Walsh-Fourier series expansion of f(t) is now complete with the coefficients defined. As a summary,

$$f(t) = A_o + \sum_{n=1}^{\infty} A_n cal(n,\theta) + \sum_{n=1}^{\infty} B_n sal(n,\theta) \qquad (2\text{-}21)$$

where $$A_o = \frac{1}{T}\int_o^T f(t)dt \qquad (2\text{-}22)$$

and $$A_n = \frac{1}{T}\int_o^T f(t)cal(n,\theta)dt \qquad (2\text{-}23)$$

and $$B_n = \frac{1}{T}\int_o^T f(t)sal(n,\theta)dt \qquad (2\text{-}24)$$

Conversion of Walsh-Fourier to Fourier Series

In order to make use of Walsh functions in an instrument that is designed to calculate the Fourier series of a waveform which is being sampled, it must be possible to convert a Walsh-Fourier series representation of the wave into an equivalent Fourier series. This is accomplished by using the principle of superposition. Each term of the Walsh-Fourier series has its own Fourier series. When these series are added together, and the like terms are grouped; then the Fourier series of the waveform being analysed is the result.

The Walsh-Fourier series representation of a periodic wave is

$$f(t) = A_o + \sum_{m=1}^{\infty} A_m cal(m,\theta) + \sum_{m=1}^{\infty} B_m sal(m,\theta) \qquad (2\text{-}21)$$

The Fourier series of the same wave is

$$f(t) = \frac{a_o}{2} + \sum_{n=1}^{\infty} a_n \cos n\theta + \sum_{n=1}^{\infty} b_n \sin n\theta \qquad (2\text{-}13)$$

Since Equation (2-21) equals (2-13) for the same wave,

$$A_o = a_o/2$$

and $$\sum_{m=1}^{\infty} A_m cal(m,\theta) + \sum_{m=1}^{\infty} B_m sal(m,\theta) = \sum_{n=1}^{\infty} a_n \cos n\theta + \sum_{n=1}^{\infty} b_n \sin n\theta \qquad (2\text{-}25)$$

The Fourier series of cal (m,θ) and sal(m,θ), respectively, are

$$cal(m,\theta) = \sum_{n=1}^{\infty} a_n(cm)\cos n\theta \qquad (2\text{-}26)$$

$$sal(m,\theta) = \sum_{n=1}^{\infty} b_n(sm)\sin n\theta \qquad (2\text{-}27)$$

where $a_n(cm)$ and $b_n(sm)$ denote the nth coefficient of the Fourier series of cal(m,θ) and sal(m,θ), respectively.

Substituting Equations (2-26) and (2-27) into Equation (2-25), one obtains

$$\sum_{m=1}^{\infty} A_m \sum_{n=1}^{\infty} a_n(cm)\cos n\theta + \sum_{m=1}^{\infty} B_m \sum_{n=1}^{\infty} b_n(sm)\sin n\theta$$

$$= \sum_{n=1}^{\infty} a_n \cos n\theta + \sum_{n=1}^{\infty} b_n \sin n\theta \qquad (2\text{-}28)$$

In Equation (2-28), let n have a particular value N. Then the equation becomes,

$$\sum_{m=1}^{\infty} A_m a_N(cm)\cos N\theta + \sum_{m=1}^{\infty} B_m b_N(sm)\sin N\theta$$

$$= a_N \cos N\theta + b_N \sin N\theta \qquad (2\text{-}29)$$

Coefficients of the cos Nθ and sin Nθ terms, respectively, can then be equated.

$$a_N = \sum_{m=1}^{\infty} A_m a_N(cm) \qquad (2\text{-}30)$$

$$b_N = \sum_{m=1}^{\infty} B_m b_N(sm) \qquad (2\text{-}31)$$

Therefore, the Fourier series of f(t), in terms of Walsh-Fourier series coefficients, is:

$$f(t) = A_o + \sum_{n=1}^{\infty} \sum_{m=1}^{\infty} (A_m a_n(cm)\cos n\theta + B_m b_n(sm)\sin n\theta) \qquad (2\text{-}32)$$

Appendix B contains calculations for numerical values of the Fourier series of several Walsh functions and shows how these

values are applied to a conversion from a Walsh-Fourier to a Fourier series.

III. Concepts of Instrument Design

The apparatus to be designed must be capable of providing information leading readily to the values of the Walsh-Fourier coefficients, A_o, A_n, and B_n, for a periodic input signal which has a low fundamental frequency, say, under 60 Hz. It must be able to collect all the necessary data in as few cycles of the input signal as possible. This chapter is devoted to a description of how information on the input signal is manipulated in order to yield the desired output information.

The Walsh-Fourier coefficients of a periodic wave are calculated by using the following equations;

$$A_o = \frac{1}{T}\int_o^T f(t)dt \qquad (2\text{-}22)$$

$$A_n = \frac{1}{T}\int_o^T f(t)cal(n,\theta)dt \qquad (2\text{-}23)$$

$$B_n = \frac{1}{T}\int_o^T f(t)sal(n,\theta)dt \qquad (2\text{-}24)$$

where T is the period of the input signal, f(t).
The instrument is digital, so that data from a wave is in the form of quantized samples. Since discrete samples are used to describe f(t), a true integration as indicated by Equations (2-22) to (2-24) is impossible. These equations must be changed into a summation. If there are M samples of f(t) during the period T,

$$dt = \frac{T}{M} \tag{3-1}$$

and the equations (2-22) to (2-24) may be rewritten as

$$A_o = \frac{1}{M} \sum_{m=1}^{M} f(t)_m \tag{3-2}$$

$$A_n = \frac{1}{M} \sum_{m=1}^{M} f(t)_m cal(n,\theta)_m \tag{3-3}$$

$$B_n = \frac{1}{M} \sum_{m=1}^{M} f(t)_m sal(n,\theta)_m \tag{3-4}$$

where $f(t)_m$, $cal(n,\theta)_m$, and $sal(n,\theta)_m$ are the values of the respective functions at the time of the mth sample.

The most obvious way to process a continuous wave, $f(t)$, for use in a digital instrument, is to use an analogue-to-digital converter. It is the nature of this device to sample $f(t)$, to quantize the samples into various levels, and to use a straight binary code for level designation. The A/D converter uses a binary number of levels. Quantization of the waveform means that all of the samples within the range of voltages specified for any given level are given the same value. For example, in Figure III-1 on page 22, if the A/D converter has a range of 0 to + Vmax volts and has p quantization levels, then the signal, $f(t)$, is considered to have the quantized value $Vmax\left(\frac{2r-1}{2p}\right)$ volts when $f(t)$ is between the levels r-1 and r. Figure III-1 shows that $f(t)$ lies within this range during the time t_1 to t_2. However, since the A/D converter gives only a binary-coded signal for each sample, any sample of the wave, $f(t)_m$, which is taken during the time t_1 to t_2, is represented by the binary value

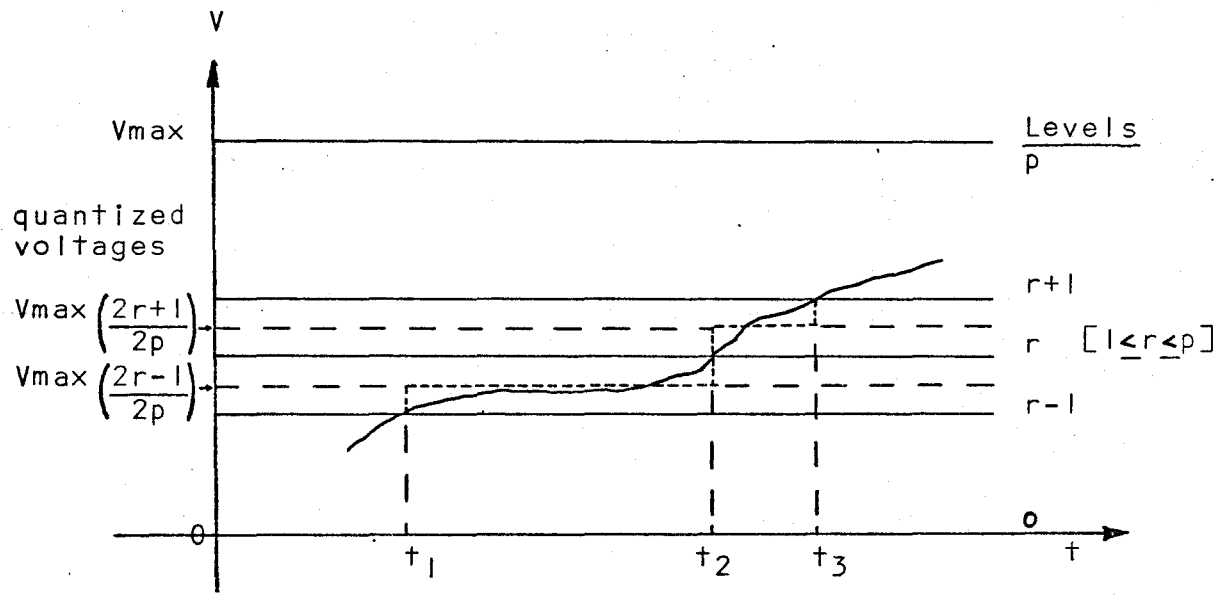

Figure III-1. Quantization

of r-1. Let this value be designated by $f(t)_{qm}$. To change the coded value back into a voltage value, it must be multiplied by $\frac{Vmax}{p}$. Thus

$$f(t)_m = \frac{Vmax}{p} f(t)_{qm} \qquad (3\text{-}5)$$

The analogue-to-digital converter which is being used can accept waveforms which have voltage extremes of zero to +10 volts. An AC input signal, limited to ± 5 volts, would need to be given a +5 volt DC shift in order to be processed by the A/D converter. Alternatively, the AC signal could be rectified, in which case a ± 10 volt signal could be handled without requiring a DC shift. Without rectification, the number of quantization levels would have to be doubled to provide the same degree of accuracy as in the rectified case. This would necessitate handling an additional binary bit and would consequently slow down the sample processing. Further difficulties would be encountered in changing the binary-coded output of the A/D converter so that the codes given to equivalent levels above and below the zero level would be identical. Therefore, it is preferable to rectify the input signal. In this way, samples with the same absolute value are automatically given the same coding. However, an additional signal is necessary to indicate the sign of f(t). A logic "1" is used to represent the positive portion of the signal and a logic "0" is used for the negative portion. Now $f(t)_m$ can be rewritten as

$$f(t)_m = \frac{Vmax}{p} \left| f(t)_{qm} \right| \operatorname{sgn} f(t)_m \qquad (3\text{-}6)$$

In addition to changing the input into a series of binary-coded samples, the instrument must provide an array of Walsh functions of the sequencies necessary to calculate all the desired Walsh-Fourier coefficients. The Walsh functions must have the same period and be in phase with the periodic input wave. The first cycle of the input can be used to determine the period. This information is required so that the Walsh functions can be generated correctly during the second cycle. Logic 1's and 0's are used to represent the positive and negative portions, respectively, of the Walsh functions.

Sampling of the input starts at the beginning of the second period. Figure III-2 on page 25, illustrates an example of a periodic signal, f(t), and the signals which are required to find the Walsh-Fourier coefficient B_3 of f(t). Part (a) of the Figure contains two cycles of the waveform to be analyzed. This input is broken down into two portions, $|f(t)|$ and sgn f(t), illustrated in part (b). The function sal(3,θ) is the Walsh function by which f(t) must be multiplied to obtain B_3. The actual function and its representative signal, as produced in the instrument, sgn sal(3,θ), are shown in parts (c) and (d), respectively. The Walsh functions are not produced until the second cycle of f(t), since the first cycle is required to determine the period of the input.

A combinational logic circuit is needed to produce the signal sgn f(t) sgn sal(n,θ). The proper signal for the example in Figure III-2 is shown in part (e). Thus, the

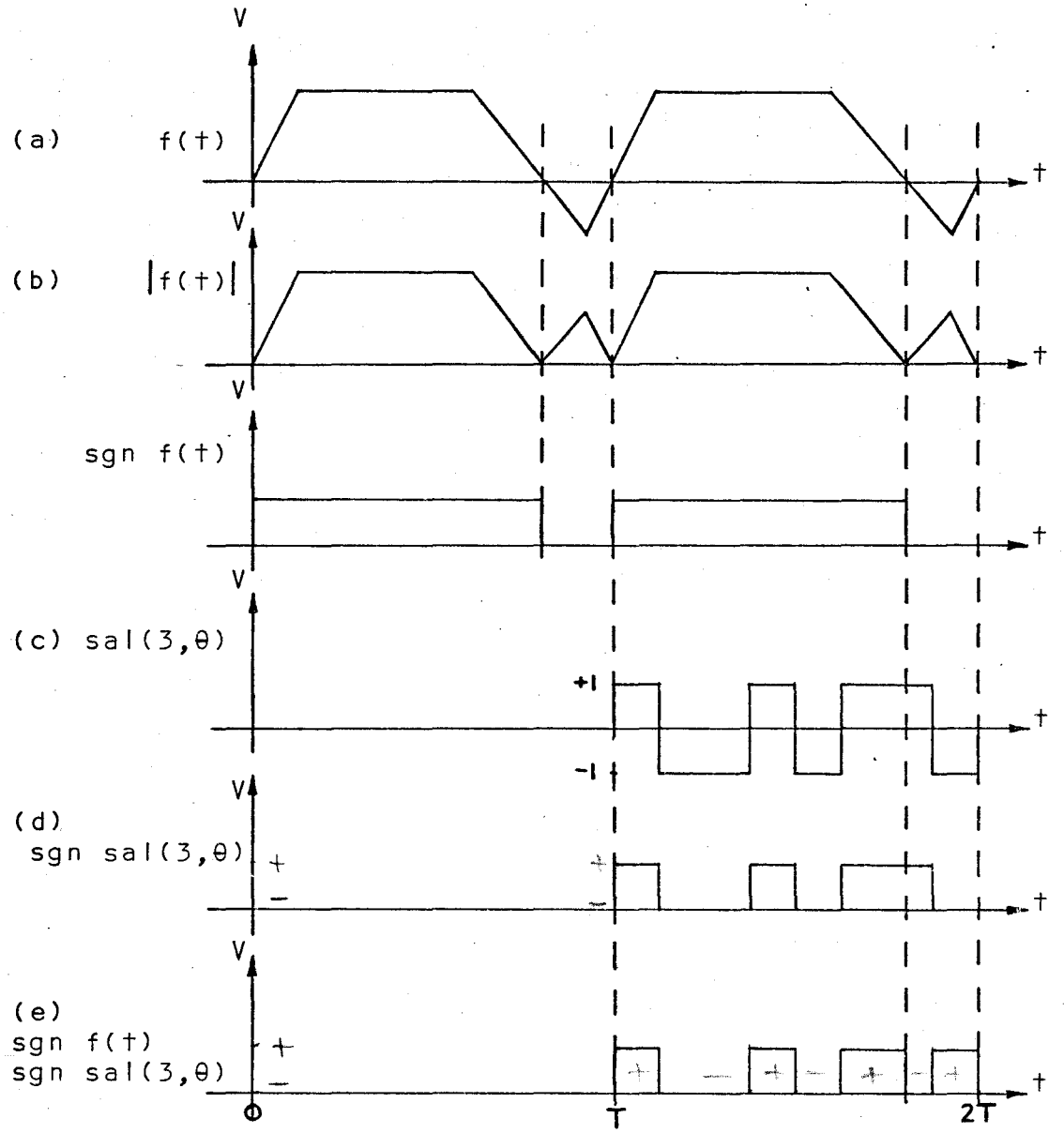

Figure III-2. Example of Functions Used to Calculate B_3

samples, $|f(t)_{qm}|$, taken from the wave $|f(t)|$, are added to or subtracted from an accumulation of previous samples, the addition or subtraction being dependent on the value of the signal sgn f(t) sgn sal(n,θ) at the time the samples are taken. The instrument has to be able to accumulate a summation for each of the Walsh-Fourier coefficients that is desired. The number of samples that are made during one period must also be counted.

The final forms in which the Equations (2-22) to (2-24) are written so that they can be processed by the digital instrument are;

$$A_o = \frac{Vmax}{pM} \sum_{m=1}^{M} |f(t)_{qm}| \text{ sgn } f(t)_m \qquad (3\text{-}7)$$

$$A_n = \frac{Vmax}{pM} \sum_{m=1}^{M} |f(t)_{qm}| \text{ sgn } f(t)_m \text{sgn cal}(n,\theta)_m \qquad (3\text{-}8)$$

$$B_n = \frac{Vmax}{pM} \sum_{m=1}^{M} |f(t)_{qm}| \text{ sgn } f(t)_m \text{sgn sal}(n,\theta)_m \qquad (3\text{-}9)$$

Since p is a binary number and the summations are performed in binary, the instrument can easily perform the division by p by ignoring the number of least significant binary bits of the summation as are used to represent p in the binary system. Therefore, in the instrument that is described in this thesis, only the factor $\frac{Vmax}{M}$ is not incorporated into the calculations. However, if the readout for each of the Walsh-Fourier coefficients is in decimal code, each value need only be divided by M and the decimal point of the answer shifted one place to the right, since Vmax = 10, in order to obtain the proper values of the Walsh-Fourier coefficients. The following

chapter discusses in detail the actual instrumentation which has been designed to realize Equations (3-7) to (3-9).

IV. Instrumentation

In the preceeding two chapters, the mathematics and the concepts of applying those mathematics to the development of an instrument which provides the Walsh-Fourier coefficients of a periodic signal have been formulated. This chapter describes the proposed design of the instrument and the construction of two portions, the Walsh function generator and the pulse burst generator, both of which have been completed and tested. The majority of the logic systems described in this chapter, whether or not they have been constructed in final form, have been simulated on a Digital Equipment Corporation Computer Lab. Sections of this chapter are devoted to each of the following topics;

(a) Complete System,

(b) A/D Conversion,

(c) Walsh Function Generator,

(d) Pulse Burst Generator,

(e) Sample Processing System.

Certain portions of the instrument, such as a precision rectifier and a Schmitt trigger, are not described in detail, since these are commercially available items.

Complete System

The block diagram of the complete system is shown in Figure IV-1 on page 29. Due to the type of A/D converter

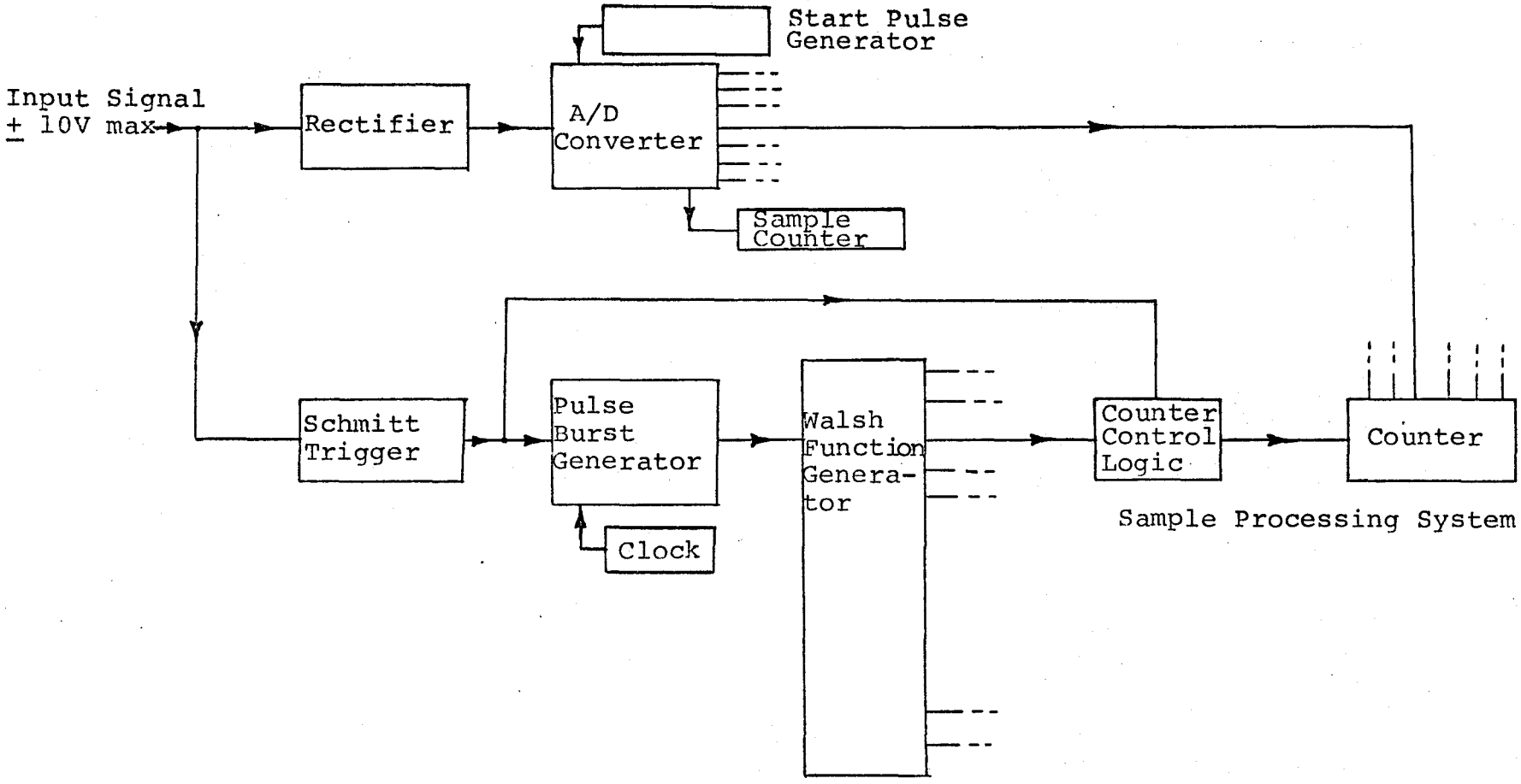

Figure IV-1. System Block Diagram

which is being used, the input signal, f(t), is limited to the range of ±10 volts. The input is directed along two paths. One of these leads to the conversion of the input into a series of quantized, binary-coded samples. The other path leads to controls, which use information concerning the period of the input, and process the binary-coded samples from the first path.

The first path consists only of two major items, a rectifier, and an A/D converter. Rectification is positive so that the input to the A/D converter is restricted to 0 to +10 volts. The output of the rectifier, $|f(t)|$, is sampled by the converter. The samples, $|f(t)_m|$, are quantized and given a binary coding. Each binary digit of the coding appears on a separate output lead. Since the first cycle of the input signal is used only to determine the period of the fundamental frequency, the output logic of the A/D converter is designed to provide sample information during the second cycle only. A counter is used to total the number of samples.

Concurrently, in the second input path, the input signal passes through a Schmitt trigger which detects zero voltage crossings. This information is necessary because all of the system operations are to begin with the first positive-going zero crossing of the input. The output of the Schmitt trigger is a logic "1" when f(t) is positive, and a logic "0" when f(t) is negative, thus representing the function sgn f(t).

Two parts of the system are controlled by sgn f(t). First, there is a pulse burst generator. It uses the signal

from the Schmitt trigger to calculate the period of one cycle of the input, measured between successive positive-going zero crossings, and uses that information to produce a series of pulses which feed into the Walsh function generator. This generator, which operates only during the second cycle of the input, produces an array of Walsh functions, from wal(0,θ) to sal(32,θ) and cal (31,θ), which have the same period and phase as the incoming signal. Since logic units are used, the outputs of the Walsh function generator are really representations of the sign of the Walsh functions, or sgn wal(n,θ).

The second place that sgn f(t) is used is in conjunction with each of the Walsh functions. By means of simple combinational logic, an array of signals are produced to represent

sgn f(t) sgn wal(n,θ)

as required by Equations (3-7) to (3-9).

The final stage of the instrument contains counters, one for each of the Walsh-Fourier coefficients. For any particular coefficient, addition or subtraction of the samples from the A/D converter is determined by the signal sgn f(t) sgn wal(n,θ). Each counter is designed to divide the accumulation of sample values by the number of quantization levels. Thus, the final stages of the counters hold the quantities determined by each of the following equations:

$$A_o = \frac{1}{p} \sum_{m=1}^{M} |f(t)_{qm}| \operatorname{sgn} f(t)_m \qquad (4\text{-}1)$$

$$A_n = \frac{1}{p} \sum_{m=1}^{M} |f(t)_{qm}| \operatorname{sgn} cal(n,\theta)_m \qquad (4\text{-}2)$$

$$B_n = \frac{1}{P} \sum_{m=1}^{M} |f(t)_{qm}| \operatorname{sgn} sal(n,\theta)_m \qquad (4\text{-}3)$$

The above equations differ from Equations (3-7) to (3-9) only by the factor $\frac{Vmax}{M}$. Vmax = 10, and M is supplied by a separate counter. It is left to the operator of the instrument to multiply Equations (4-1) and (4-3) by $\frac{10}{M}$. M is also used to determine the fundamental frequency of the input. If the sample frequency is f_s, then the time between samples is $1/f_s$. The time for M samples is $M/f_s = T$. Therefore, the fundamental frequency of the input $f_1 = f_s/M$.

The instrument was designed to the point where the Walsh-Fourier coefficients of a low-frequency periodic input wave could be obtained readily. In order to obtain the Fourier series of the input, the equations derived in Appendix B can be used.

A/D Conversion

After rectification of the input has been performed, the waveform being analysed must be sampled and quantized. The samples are to be given a binary code, with each bit of the code appearing on a separate lead. Several methods of analogue-to-digital conversion have been made realizable on modules produced by Digital Equipment Corporation (D.E.C.). These modules are described in the D.E.C. "Digital Logic Handbook". In all cases, the methods involve formation of quantized analogue voltages corresponding to the digital states, and comparison of these with the incoming analogue

signal. The principal types of A/D conversion are;

(a) Simultaneous conversion,

(b) Counter conversion,

(c) Continuous conversion,

(d) Successive approximation conversion.

Considering speed, accuracy, and cost, it has been decided to use 6-bit successive-approximation conversion. D.E.C. supplies a complete 10-bit successive approximation, A/D converter with a built-in reference supply (Model number A801). The circuit is arranged so that any number of bits, up to 10, may be used. The complete converter is contained on one D.E.C. double logic module. The block diagram of the A/D converter is shown in Figure IV-2 on page 34. The actual circuit diagram is illustrated in Figure IV-3 on page 35.

Conversion by successive approximation is realized by a series of decisions on approximations that converge rapidly on the correct digital state. Since an example of A/D conversion with 6 bits becomes rather lengthy, only a 16-level, or 4-bit, case is described. The first approximation would be the eight level, that is, state 1000. The analogue conversion of this state is compared with the input, and if it exceeds the input, the eight-weighted bit is reset to "0". If the approximation is too small, the bit remains a "1". The first 4 bits of the register, shown in Figure IV-3 by the flip-flops E14 and E13, now contain either 1000 or 0000. Next, the four-weighted bit is set to "1", giving an approximation of either 4 (0100) or 12(1100), depending on the first decision. A second decision, similar to the first is then

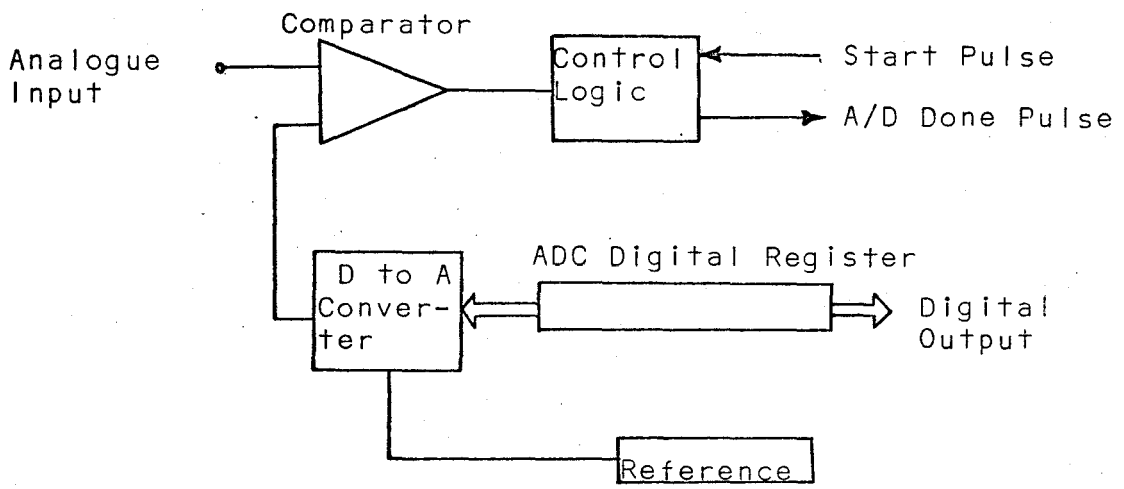

Figure IV-2. A801 10-Bit Analogue-to-Digital Converter.

- 1968 Digital Logic Handbook

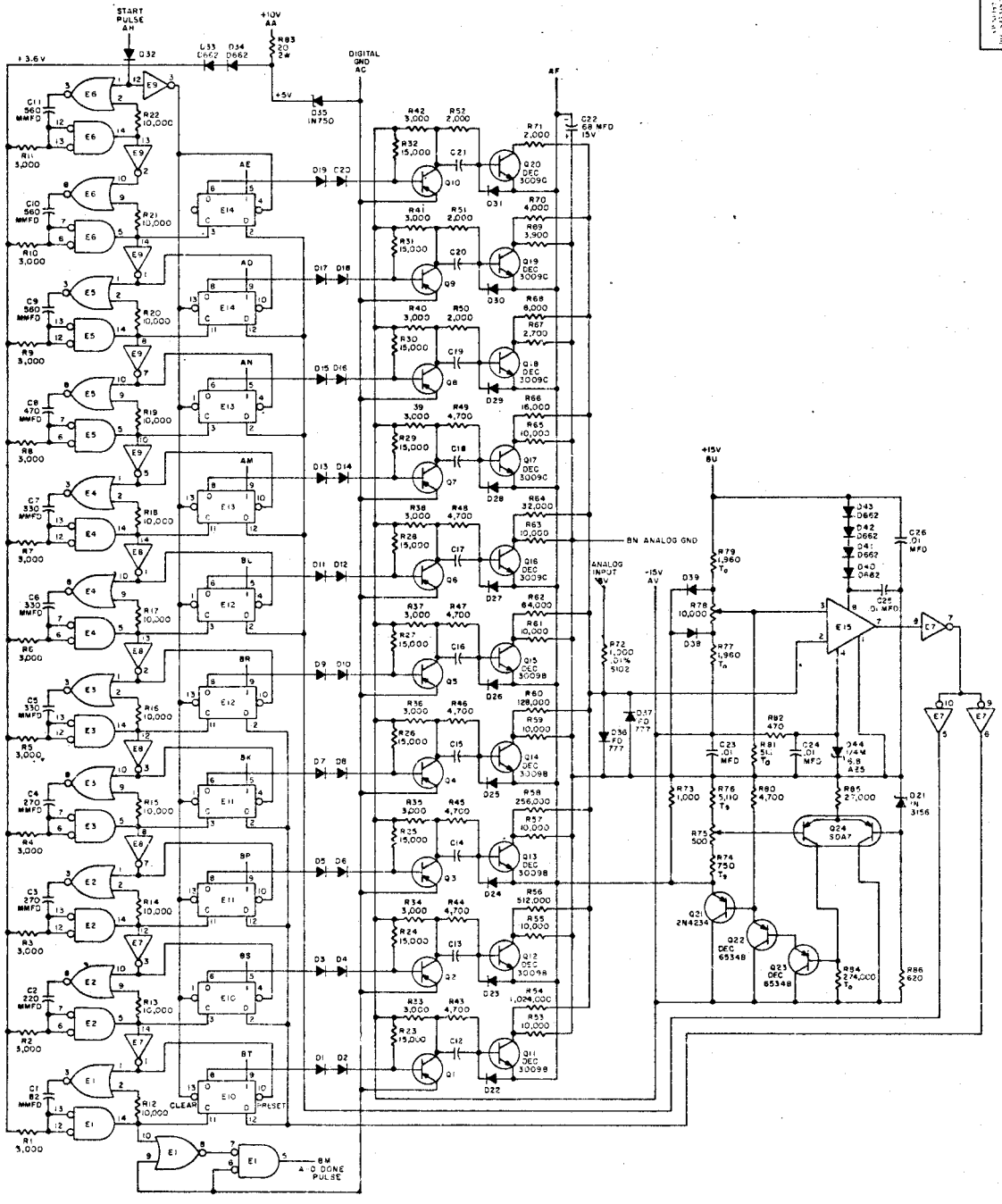

UNLESS OTHERWISE INDICATED:
TRANSISTORS ARE DEC3894-38
RESISTORS ARE 1/4W, 5%
DIODES ARE D664
CAPACITORS ARE 47 MMFD
PIN 7 = GND ON E10, E11, E12, E13 & E14
PIN 14 = +5V ON E10, E11, E12, E13 & E14
PIN 4 = GND ON E1, E2, E3, E4, E5, E6, E7, E8 & E9
PIN 11 = +3.6V ON E1, E2, E3, E4, E5, E6, E7, E8 & E9
E1, E2, E3, E4, E5 & E6 ARE MC724
E7, E8 & E9 ARE MC789
E10, E11, E12, E13 & E14 ARE DEC7474N
E15 IS UA710
R66, R68, R70 & R71 ARE VISHAY M.F. .01% 5PPM
R58, R60, RE2, R64, R74 & R76 ARE M.F., 1/8W, 25 PPM.1%
R56 IS 1/4W, M.F. 25 PPM 1%
R54 IS 1/2 W, M.F. 25 PPM 1%
R77, R79, R81 & R84 ARE M.F., 1/8W, 100 PPM 1%
R75 IS A BOURNS TRIMPOT TYPE 224L DEC PART #13-5156
R78 IS A BOURNS TRIMPOT TYPE 224L DEC PART #13-0519

Figure IV-3. A801 A/D Converter

TRANSISTOR & DIGITAL CONVERSION CHART			
digital EQUIPMENT CORPORATION	A-D CONVERTER 10 BIT A801	SIZE D	DWG NO A801-0-1
		SCALE	REV
		SHEET	

performed on this approximation. This cycle is repeated for a number of decisions equal to the desired number of bits, for this example, 4. Figure IV-4 on page 37 shows the state diagram for a 4-bit successive approximation conversion. The numbers in the circles are states which represent the levels about which the decisions are made, and the numbers over the leaders show the final states of the binaries involved.

The determination of each bit occurs serially in time, the value of the most signifigant bit being determined first. Normally, the entire A/D conversion is completed before any output from the converter is used. However, with reference to the sample processing method which is described in a later section of this chapter, it is advantageous to process each bit serially in time as well. A minor addition to the A/D converter circuit in Figure IV-3 is needed to obtain the desired outputs.

After the start pulse is applied to input AH, it is propagated through the circuit so that after each decision, the pulse sets the flip-flop which is to hold the result of that decision and also presets the flip-flop involved in the next decision. Extra outputs can be added to tap this pulse at the appropriate points, as indicated by Equations (4-4) to (4-9), and use them for control purposes, thus yielding information on each digit of the A/D converter output very shortly after it is available.

For example, with the required 6-bit conversion, when the pulse reaches lead 5 of the logic module E6 (let this

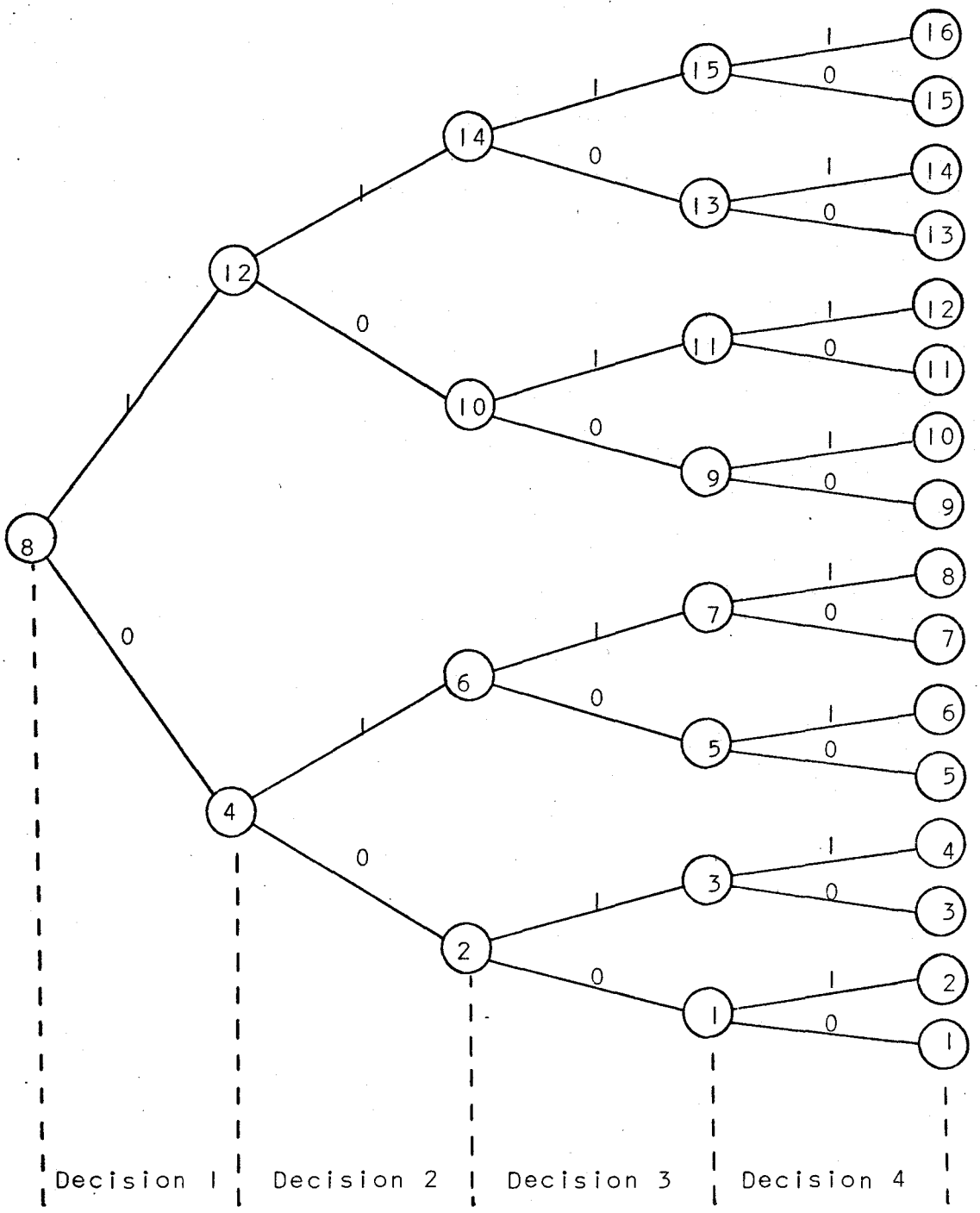

Figure IV-4. State Diagram for 4-Bit Successive-Approximation Conversion

point be called E6-5), in the circuit in Figure IV-3, it is used to set the flip-flop which determines the most significant bit (let this bit be called P_{32}). The pulse also presets the next flip-flop and is then passed through a delay circuit, containing delay elements C_9 and R_9, while the next decision is being made. After the pulse has passed through the delay circuit to set the next flip-flop, all operations concerning the first bit have been completed so that at that time the pulse can be combined with the output of the first flip-flop (AE at the output of E14) to yield P_{32}. The logic required is simply an AND gate. A/D converter output terminals which are used to obtain the information on each of the bits serially in time are then

(AE)(E5-14)	for P_{32}	(4-4)
(AD)(E5-5)	for P_{16}	(4-5)
(AN)(E4-14)	for P_8	(4-6)
(AM)(E4-5)	for P_4	(4-7)
(BL)(E3-14)	for P_2	(4-8)
(BR)(E3-5)	for P_1	(4-9)

as labelled in the circuit diagram in Figure IV-3. At the end of each complete A/D conversion, a pulse from terminal E3-5 is fed into a counter which records the number of samples, M, that have been taken.

The A801 A/D converter must be triggered by a pulse which has a width between 100 and 500 nsec. The complete 10-bit conversion requires 10 μsec. With 6-bit conversion requiring approximately 6 μsec., and allowing roughly

another 1 μsec. to complete the sample processing, the maximum sampling rate is about 140 kHz. For the analysis of extremely long-period waves, a sampling rate as low as, say, 1 Hz. may be used. Since the first cycle of the input is used to determine the period, samples must start only at the beginning of the second cycle and stop at the end of that cycle.

A scheme for the complete system of controls for the sampling rate, the A/D converter with its output logic, and the sample counter is shown in Figure IV-5 on page 40. An M401 variable clock, supplied by D.E.C., supplies the pulses to start the A/D conversion. Depending on the connection between N2 and S2, T2, or P2, the clock rate can be varied from 175 kHz. down to 175 Hz. Each of three ranges can be set to certain rates, say, 100 kHz., 10 kHz., and 1 kHz. respectively. To obtain lower sampling rates, let the output be set to the 1 kHz. position. Three decade counters can be added in series to the output, D2. The outputs of each of the 3 counters can be tapped to produce pulses at rates of 100, 10, and 1 Hz., respectively. The rotary switch that is used to obtain each of the pulse rates is shown in Figure IV-5.

The leads, FF1, $\overline{\text{FF1}}$, and FF2, to the input and output logic of the counter come from the pulse burst generator described in a later section. This logic allows the first A/D conversion "start" pulse to arrive just after the second cycle of the input has begun. The "sample start" pulses end when the second cycle is over.

One small modification is necessary with the above system of providing A/D start pulses. Whereas the start

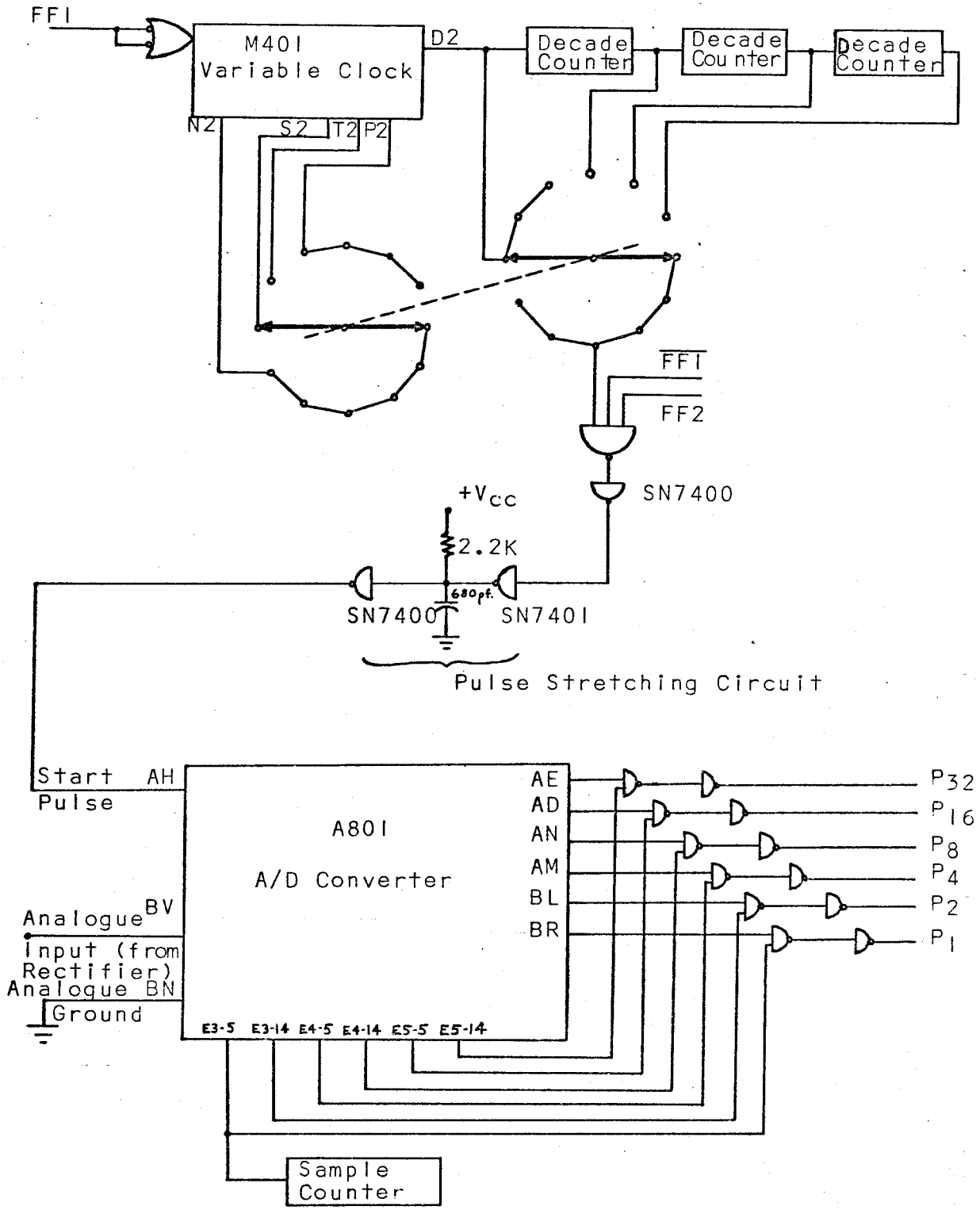

Figure IV-5. A/D Conversion

pulses must have a width of 100 to 500nsec., the maximum pulse width from an M401 clock is 80 nsec. Consequently, the clock pulse width must be increased. The pulse stretching circuit in Figure IV-5 uses a NAND gate with an open collector so that a 2.2 KΩ resistor and a 680 pf. capacitor can be attached to increase the rise time of the inverted pulse. The second NAND gate re-inverts and sharpens the pulse. This circuit has been found to maintain the pulse width at approximately 350 nsec. in the range from 1 Hz. to over 100 kHz.

Walsh Function Generator

While samples of the second cycle of the periodic input wave are being taken, a Walsh function for each Walsh-Fourier coefficient that is to be determined is produced with the same phase and period as the incoming wave. The circuitry to produce the Walsh functions up to sal(32,θ) and cal(31,θ) has been designed. However, only that portion of the generator which provides up to sal(24,θ) and cal(23,θ) has as yet been constructed.

Since Walsh functions are bipolar, sequencesof logic "1"'s and "0"'s can be used to represent the positive and negative portions, respectively, of the functions. For the sake of simplicity in determining the logic required to produce the Walsh functions, calculations are shown only for functions up to and including sal(8,θ). In this section of the thesis only, a letter designation is given to each of the Walsh functions.

Table IV-1 on page 42 shows the binary sequences used

Letter Designation	Walsh Function	Binary Sequence
a	sal(1,θ)	1111111100000000
b	cal(1,θ)	1111000000001111
c	sal(2,θ)	1111000011110000
d	cal(2,θ)	1100001111000011
e	sal(3,θ)	1100001100111100
f	cal(3,θ)	1100110000110011
g	sal(4,θ)	1100110011001100
h	cal(4,θ)	1001100110011001
i	sal(5,θ)	1001100101100110
j	cal(5,θ)	1001011001101001
k	sal(6,θ)	1001011010010110
l	cal(6,θ)	1010010110100101
m	sal(7,θ)	1010010101011010
n	cal(7,θ)	1010101001010101
o	sal(8,θ)	1010101010101010

Table IV-1. Binary Sequence Representation of Walsh Functions

to represent sal(1,θ) to sal(8,θ). Since sal(1,θ), sal(2,θ), sal(4,θ), ----- sal(2^k,θ) are rectangular waves having unity mark/space ratio, they can easily be produced by the outputs of a binary down counter. Figure IV-6 on page 44 shows the circuit and its input and outputs for the functions a, c, g, and o, which are sal(1,θ), sal(2,θ), sal(4,θ) and sal(8,θ), respectively. The pulse input comes from the pulse burst generator that is described in the next section of this chapter.

All Walsh functions begin in the positive state. This is achieved by initially clearing each of the flip-flops and using the "0" outputs of the flip-flops to represent the positive functions a, c, g, and o. The "1" outputs produce negative Walsh functions. Since all the positive functions are initially in the "1" state, the first pulse from the pulse burst generator should arrive not at the beginning of the second cycle, but T/16 seconds after the cycle has started. Once the basic sal(2^k,θ) functions, (k= 1,2,3----), are produced, all the other Walsh functions can be constructed by combinational logic involving these basic functions.

The Karnaugh maps for the combinational logic to produce Walsh functions, derived from Table IV-1, are shown in Figure IV-7 on page 45. From these maps, the logic expressions for functions a to o are as follows;

$$a = a \tag{4-10}$$

$$b = ac + \bar{a}\bar{c} \tag{4-11}$$

$$c = c' \tag{4-12}$$

$$d = cg + \bar{c}\bar{g} \tag{4-13}$$

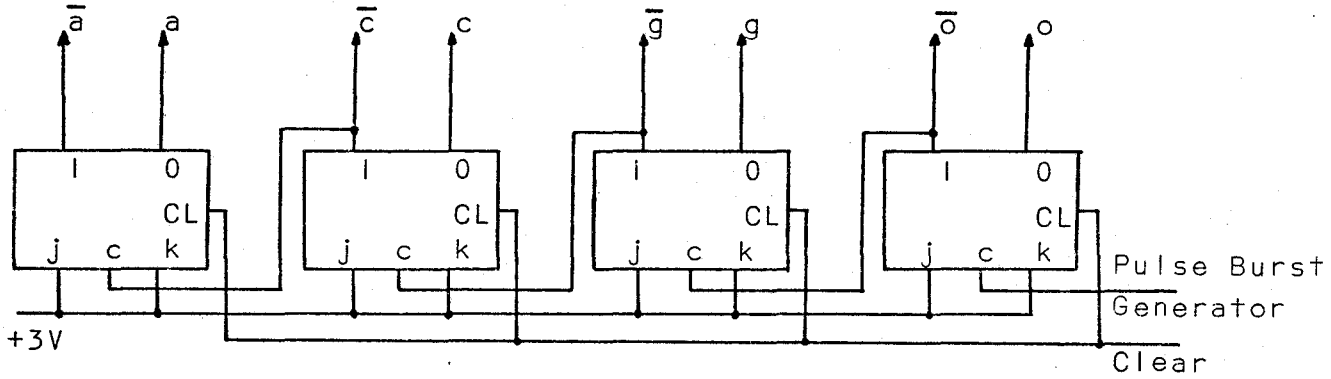

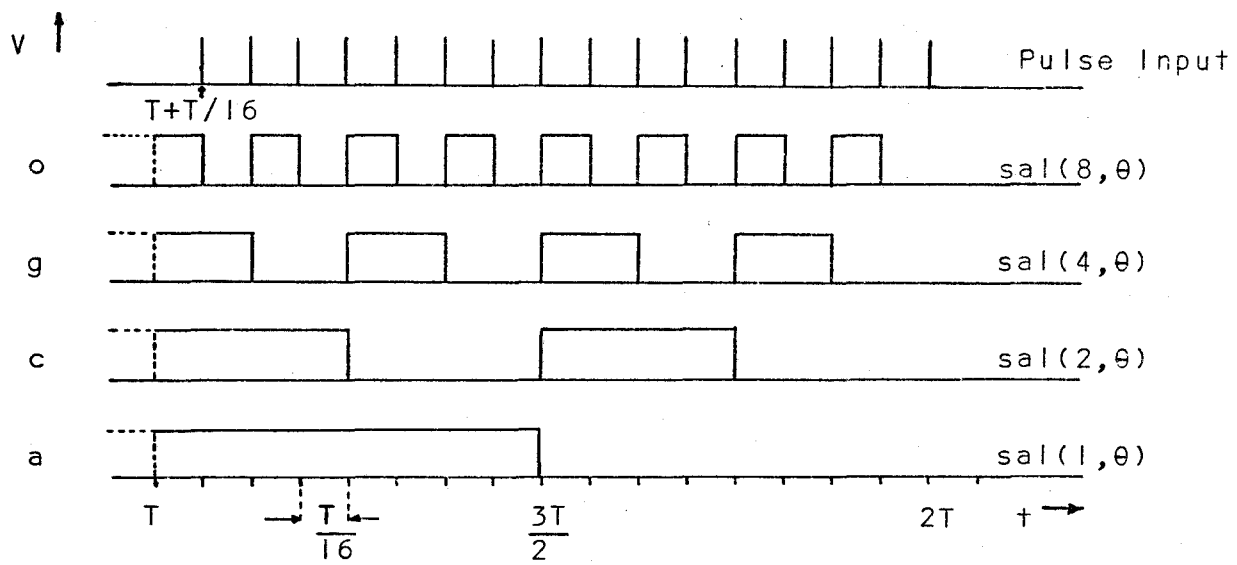

Figure IV-6. Production of $sal(2^k,\theta)$

Inputs				Outputs										
a	c	g	o	b	d	e	f	h	i	j	k	l	m	n
1	1	1	1	1	1	1	1	1	1	1	1	1	1	1
1	1	1	0	1	1	1	1	0	0	0	0	0	0	0
1	1	0	1	1	0	0	0	0	0	0	0	1	1	1
1	1	0	0	1	0	0	0	1	1	1	1	0	0	0
1	0	1	1	0	0	0	1	1	1	0	0	0	0	1
1	0	1	0	0	0	0	1	0	0	1	1	1	1	0
1	0	0	1	0	1	1	0	0	0	1	1	0	0	1
1	0	0	0	0	1	1	0	1	1	0	0	1	1	0
0	1	1	1	0	1	0	0	1	0	0	1	1	0	0
0	1	1	0	0	1	0	0	0	1	1	0	0	1	1
0	1	0	1	0	0	1	1	0	1	1	0	1	0	0
0	1	0	0	0	0	1	1	1	0	0	1	0	1	1
0	0	1	1	1	0	1	0	1	0	1	0	0	1	0
0	0	1	0	1	0	1	0	0	1	0	1	1	0	1
0	0	0	1	1	1	0	1	0	1	0	1	0	1	0
0	0	0	0	1	1	0	1	1	0	1	0	1	0	1

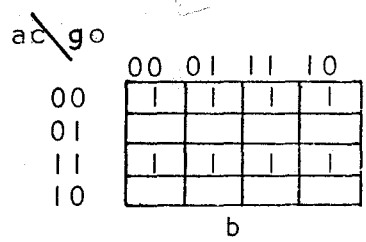

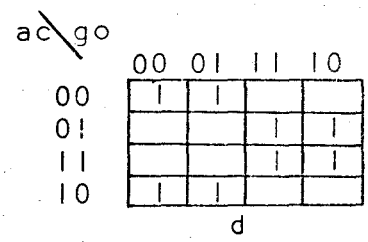

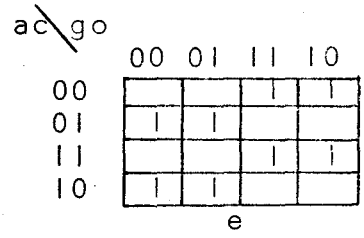

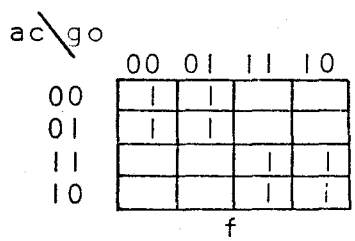

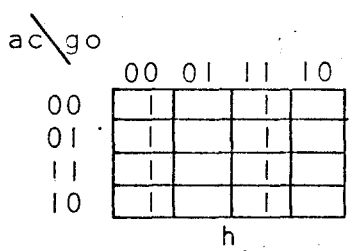

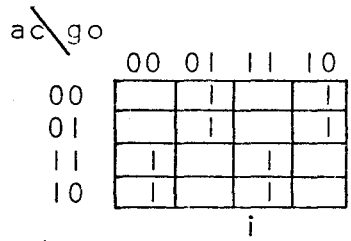

Figure IV-7. Karnaugh Maps for Walsh Function Logic

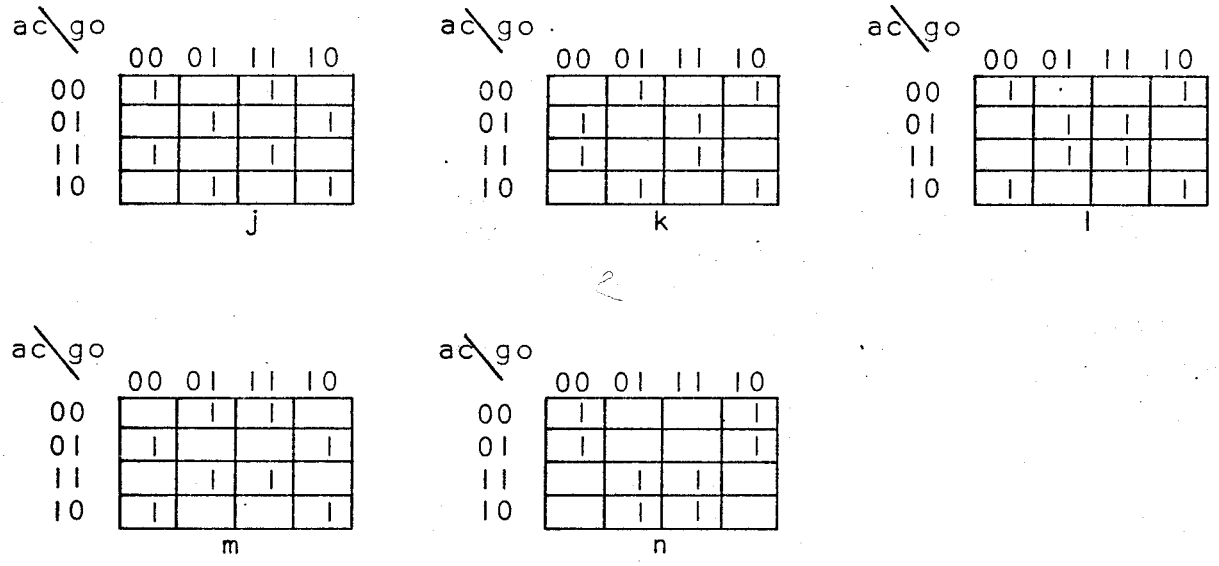

Figure IV-7. (continued) Karnaugh Maps for Walsh Function Logic

$$e = acg + \bar{a}\bar{c}g + \bar{a}c\bar{g} + a\bar{c}\bar{g} = ad + \bar{a}\bar{d} \quad (4\text{-}14)$$

$$f = ag + \bar{a}\bar{g} \quad (4\text{-}15)$$

$$g = g \quad (4\text{-}16)$$

$$h = go + \bar{g}\bar{o} \quad (4\text{-}17)$$

$$i = ago + a\bar{g}\bar{o} + \bar{a}\bar{g}o + \bar{a}g\bar{o} = ah + \bar{a}\bar{h} \quad (4\text{-}18)$$

$$j = acgo + ac\bar{g}\bar{o} + a\bar{c}\bar{g}o + a\bar{c}g\bar{o} + \bar{a}c\bar{g}o + \bar{a}cg\bar{o} + \bar{a}\bar{c}\bar{g}o + \bar{a}\bar{c}g\bar{o} = ci + \bar{c}\bar{i} \quad (4\text{-}19)$$

$$k = cgo + \bar{c}g\bar{o} + \bar{c}\bar{g}o + c\bar{g}\bar{o} = ch + \bar{c}\bar{h} \quad (4\text{-}20)$$

$$l = co + \bar{c}\bar{o} \quad (4\text{-}21)$$

$$m = aco + a\bar{c}\bar{o} + \bar{a}c\bar{o} + \bar{a}\bar{c}o = al + \bar{a}\bar{l} \quad (4\text{-}22)$$

$$n = ao + \bar{a}\bar{o} \quad (4\text{-}23)$$

$$o = o \quad (4\text{-}24)$$

It becomes readily apparent that all the Walsh functions, except the sal($2^k\theta$) functions, can be produced by coincidence logic gates. For example, function b consists of terms involving functions a and c. Therefore, b is produced by the coincidence of a and c, that is $ac + \bar{a}\bar{c}$. (This is the complement of $a \oplus c$). Similarly, functions d and f are produced by $cg + \bar{c}\bar{g}$ and $ag + \bar{a}\bar{g}$, respectively. Each of the above 3 functions consist of terms involving only 2 other functions. The function e, however, has terms containing a, c, and g. It can easily be shown that e could be produced by the coincidence of any one of a, c, or g and the Walsh function which contains all of the remaining functions. That is, e could be produced by $ad + \bar{a}\bar{d}$, $cf + \bar{c}\bar{f}$, or $gb + \bar{g}\bar{b}$. It is apparent that when 3 or more basic sal($2^k,\theta$) functions are contained in the expressions for a Walsh function, several

coincidence gates could be used to produce the same function. In such cases, in determining which coincidence gate to use to form a particular Walsh function, it was decided to involve a sal(2^k,θ) function and an appropriate Walsh function which has a sequency lower than the desired function. Table IV-II on pages 49 and 50 lists the Walsh functions, their letter designations, the functions involved in the logic expressions for the Walsh functions, and the most desirable coincidence expression for each function. (Only the function T, of the functions whose terms contain 3 or more letters, contains an expression involving a higher sequency function. This was resorted to only in order to correct an error in the construction of the Walsh function generator.)

The information in Table IV-II has been used to construct a circuit which generates all the Walsh functions from a to U, that is, sal(1,θ) to sal(24,θ). Texas Instruments TTL integrated circuits were used throughout the circuit. They were mounted on 3 Avnet H5937 circuit boards, each of which can hold up to 20 14-pin dual-in-line integrated circuits and has 22 input-output terminals on each side.

Schematic diagrams of the Walsh function generator are shown in Figures IV-8 to IV-10 on pages 51 to 53 . Each of the Figures displays the circuit contained on one board. Therefore, the labels on each diagram pertain only to the input-output terminals and the integrated circuits positions on the corresponding board. The input-output terminals are labelled with the appropriate number or letter enclosed in

Table IV-II. Logic Expressions for Walsh Function Generation

Letter Designation	Walsh Function	Basic Functions Involved in Walsh Function Logic Terms						Logic Expression for Walsh Functions
		a	c	g	o	E	X	
a	sal(1,θ)	a						a
b	cal(1,θ)	a	c					ac + $\bar{a}\bar{c}$
c	sal(2,θ)		c					c
d	cal(2,θ)		c	g				cg + $\bar{c}\bar{g}$
e	sal(3,θ)	a	c	g				ad + $\bar{a}\bar{d}$
f	cal(3,θ)	a		g				ag + $\bar{a}\bar{g}$
g	sal(4,θ)			g				g
h	cal(4,θ)			g	o			go + $\bar{g}\bar{o}$
i	sal(5,θ)	a		g	o			ah + $\bar{a}\bar{h}$
j	cal(5,θ)	a	c	g	o			ci + $\bar{c}\bar{i}$
k	sal(6,θ)		c	g	o			ch + $\bar{c}\bar{h}$
l	cal(6,θ)		c		o			co + $\bar{c}\bar{o}$
m	sal(7,θ)	a	c		o			al + $\bar{a}\bar{l}$
n	cal(7,θ)	a			o			ao + $\bar{a}\bar{o}$
o	sal(8,θ)				o			o
p	cal(8,θ)				o	E		oE + $\bar{o}\bar{E}$
q	sal(9,θ)	a			o	E		ap + $\bar{a}\bar{p}$
r	cal(9,θ)	a	c		o	E		cq + $\bar{c}\bar{q}$
s	sal(10,θ)		c		o	E		cp + $\bar{c}\bar{p}$
t	cal(10,θ)		c	g	o	E		gs + $\bar{g}\bar{s}$
u	sal(11,θ)	a	c	g	o	E		at + $\bar{a}\bar{t}$
v	cal(11,θ)	a		g	o	E		gq + $\bar{g}\bar{q}$
w	sal(12,θ)			g	o	E		gp + $\bar{g}\bar{p}$
x	cal(12,θ)			g		E		gE + $\bar{g}\bar{E}$
y	sal(13,θ)	a		g		E		ax + $\bar{a}\bar{x}$
z	cal(13,θ)	a	c	g		E		cy + $\bar{c}\bar{y}$
A	sal(14,θ)		c	g		E		cx + $\bar{c}\bar{x}$
B	cal(14,θ)		c			E		cE + $\bar{c}\bar{E}$
C	sal(15,θ)	a	c			E		aB + $\bar{a}\bar{B}$
D	cal(15,θ)	a				E		aE + $\bar{a}\bar{E}$
E	sal(16,θ)					E		E
F	cal(16,θ)					E	X	EX + $\bar{E}\bar{X}$
G	sal(17,θ)	a				E	X	aF + $\bar{a}\bar{F}$
H	cal(17,θ)	a	c			E	X	cG + $\bar{c}\bar{G}$
I	sal(18,θ)		c			E	X	cF + $\bar{c}\bar{F}$
J	cal(18,θ)		c	g		E	X	gI + $\bar{g}\bar{I}$
K	sal(19,θ)	a	c	g		E	X	aJ + $\bar{a}\bar{J}$
L	cal(19,θ)	a		g		E	X	gG + $\bar{g}\bar{G}$
M	sal(20,θ)			g		E	X	gF + $\bar{g}\bar{F}$
N	cal(20,θ)			g	o	E	X	oM + $\bar{o}\bar{M}$
O	sal(21,θ)	a		g	o	E	X	aN + $\bar{a}\bar{N}$
P	cal(21,θ)	a	c	g	o	E	X	cO + $\bar{c}\bar{O}$
Q	sal(22,θ)		c	g	o	E	X	cN + $\bar{c}\bar{N}$
R	cal(22,θ)		c		o	E	X	oI + $\bar{o}\bar{I}$
S	sal(23,θ)	a	c		o	E	X	aR + $\bar{a}\bar{R}$

Table IV-11. (cont'd)
Logic Expressions for Walsh Function Generation

Letter Designation	Walsh Function	Basic Functions Involved in Walsh Function Logic Terms						Logic Expression for Walsh Functions
		a	c	g	o	E	X	
T	cal(23,θ)	a			o	E	X	$aU + \bar{a}\bar{U}$
U	sal(24,θ)				o	E	X	$oF + \bar{o}\bar{F}$
V	cal(24,θ)				o		X	$oX + \bar{o}\bar{X}$
W	sal(25,θ)	a			o		X	$aV + \bar{a}\bar{V}$
Y	cal(25,θ)	a	c		o		X	$cW + \bar{c}\bar{W}$
Z	sal(26,θ)		c		o		X	$cV + \bar{c}\bar{V}$
α	cal(26,θ)		c	g	o		X	$gZ + \bar{g}\bar{Z}$
β	sal(27,θ)	a	c	g	o		X	$a\alpha + \bar{a}\bar{\alpha}$
γ	cal(27,θ)	a		g	o		X	$gW + \bar{g}\bar{W}$
δ	sal(28,θ)			g	o		X	$gV + \bar{g}\bar{V}$
ε	cal(28,θ)			g			X	$gX + \bar{g}\bar{X}$
ζ	sal(29,θ)	a		g			X	$e\varepsilon + \bar{a}\bar{\varepsilon}$
η	cal(29,θ)	a	c	g			X	$c\zeta + \bar{c}\bar{\zeta}$
θ	sal(30,θ)		c	g			X	$c\varepsilon + \bar{c}\bar{\varepsilon}$
λ	cal(30,θ)		c				X	$cX + \bar{c}\bar{X}$
μ	sal(31,θ)	a	c				X	$a\lambda + \bar{a}\bar{\lambda}$
Φ	cal(31,θ)	a					X	$aX + \bar{a}\bar{X}$
X	sal(32,θ)						X	X

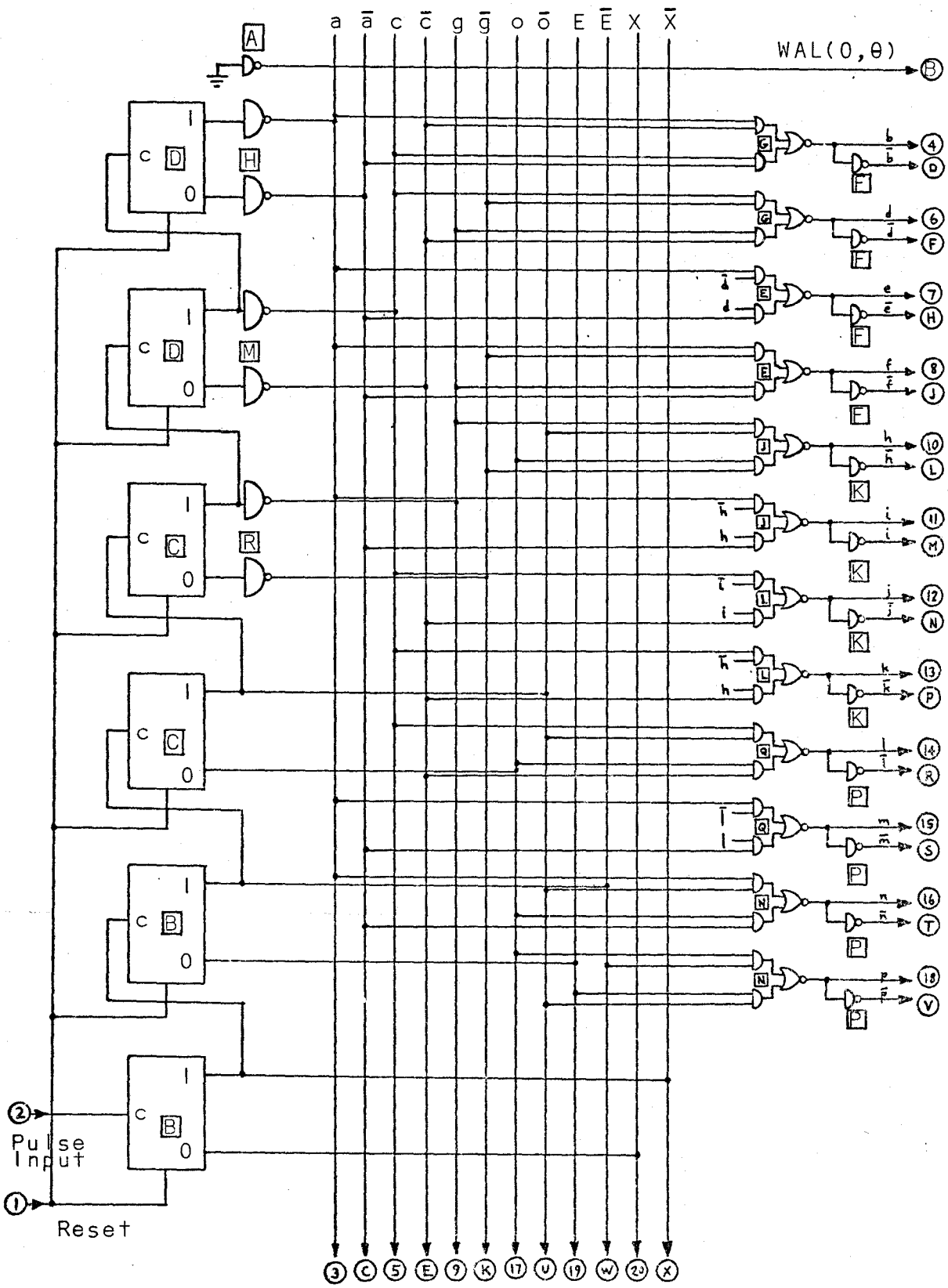

Figure IV-8. Schematic of Walsh Function Generator - Card I.

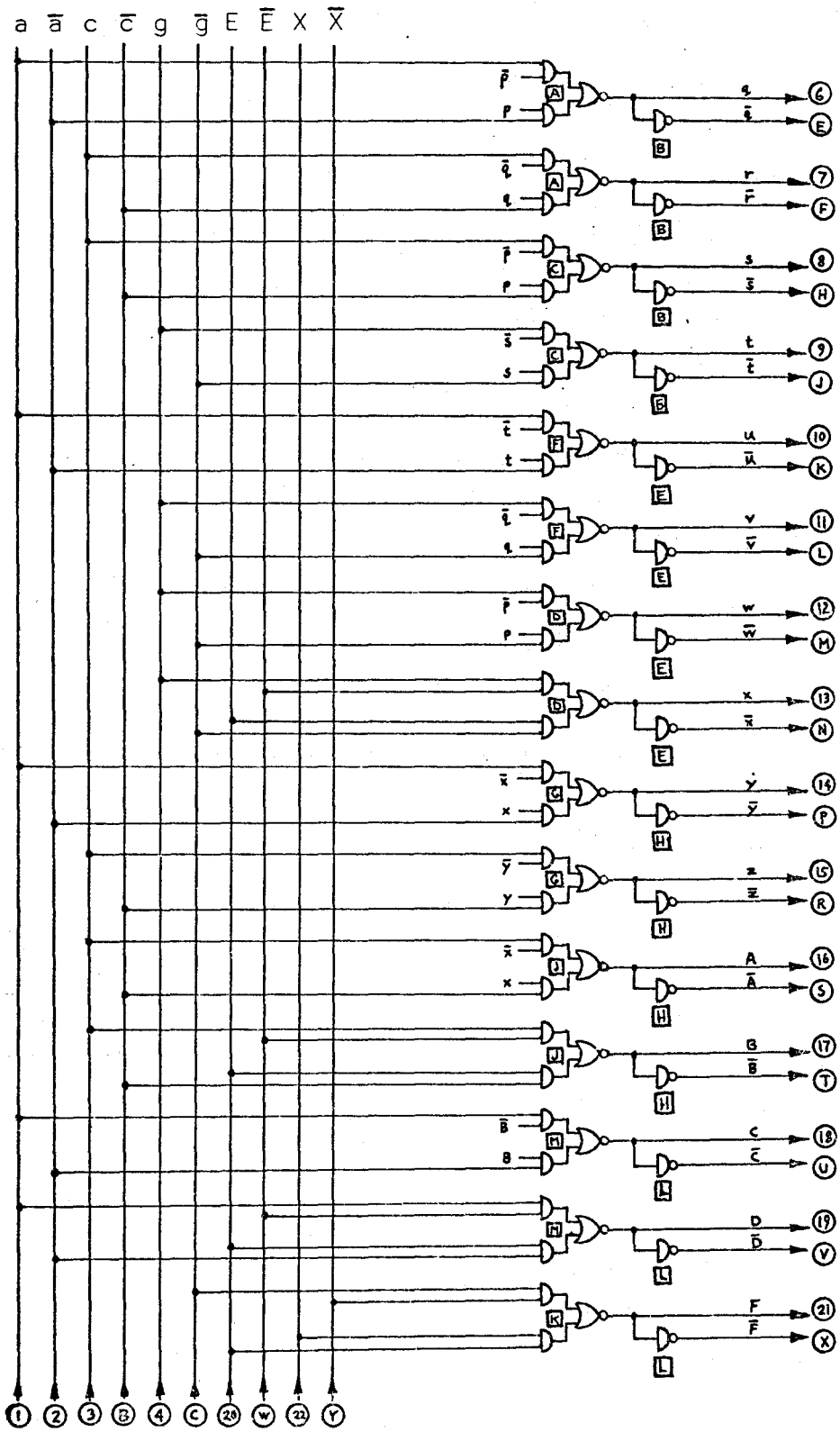

Figure IV-9. Schematic of Walsh Function Generator - Card 2

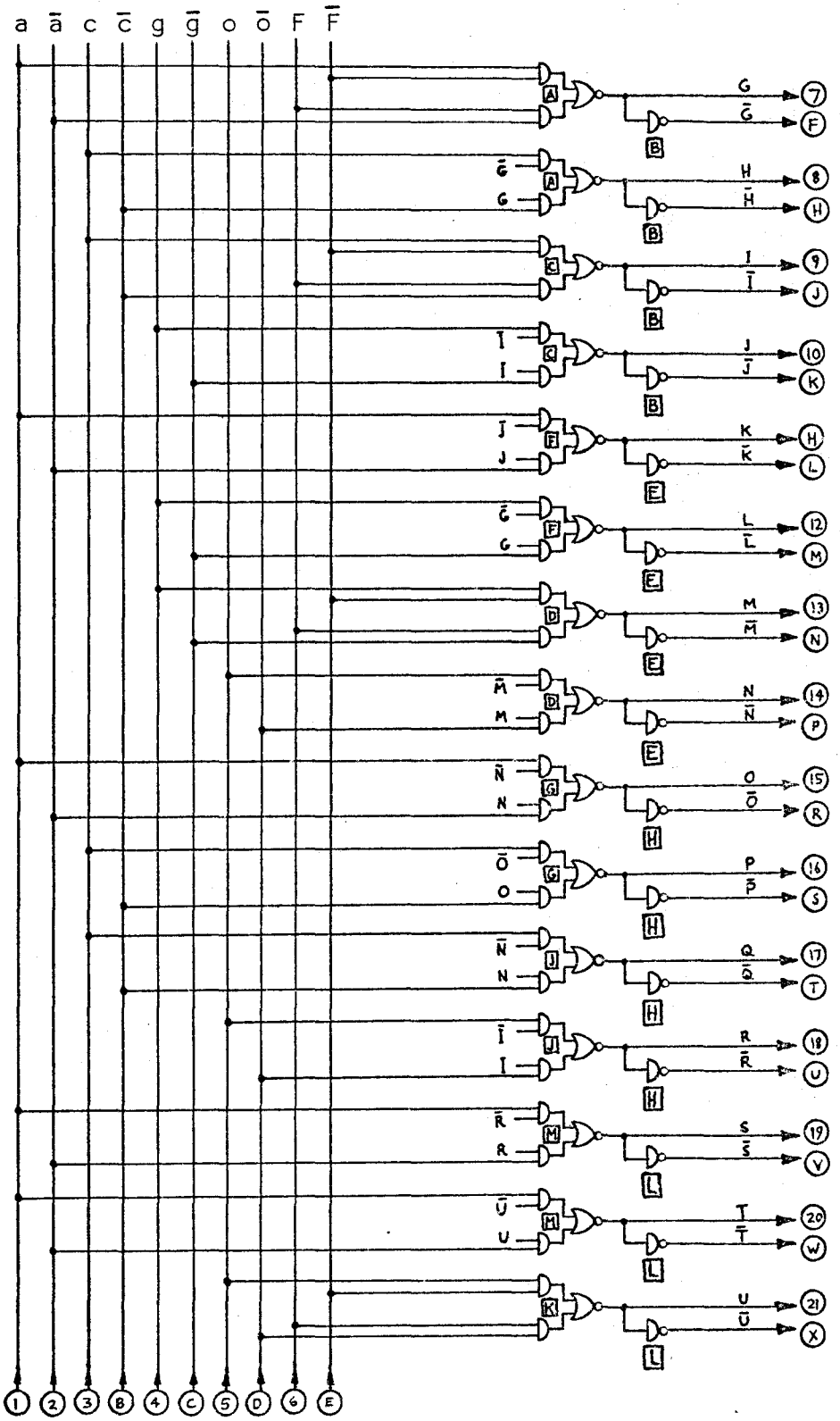

Figure IV-10. Schematic of Walsh Function Generator - Card 3

a circle. The logic functions are labelled with letters enclosed in squares which are used to show the location on the circuit board of the integrated circuit chip housing the logic functions. The layouts of the integrated circuits on each of the boards are shown in the appendix in Figures C-1 and C-2 on pages 107 and 108. The input-output terminal locations for each board are identical, and hence, are shown only in Figure C-1.

The pulse inputs to the Walsh function generator must be provided at the proper times to form the Walsh functions during the second complete cycle of the periodic input wave. The circuit which has been designed to provide the pulses is described in the following section.

Pulse Burst Generator

The highest sequency function that is produced by the Walsh function generator is sal(32,0). It is this function, which is the output of "0" of the first flip-flop in Figure IV-8, which determines the pulse input requirements of the Walsh function generator. Thus, 64 regularly-spaced pulses must be provided during the second period of the input signal. Since all Walsh functions are initially in the "1" condition, and this state is produced naturally by the initial "reset" state of all flip-flops in Figure IV-8, the first input pulse is to be produced T/64 seconds after the beginning of the second cycle. (T is the period of one cycle, and should not be confused with T used in Table IV-II). Starting at that time, a burst of 64 pulses, each spaced T/64 seconds

apart, is required. The last pulse should come at the end of the second cycle.

Figure IV-11 on page 56 shows the block diagram of the system that has been designed to give the 64-pulse burst. The output of a Schmitt trigger and an inverter controls the system. The Schmitt trigger should be one which accurately detects positive-going zero voltage crossings of the input. It has a logic "1" output when the input is positive, and "0" when the input is negative. This signal is fed into a series of 3 flip-flops that are used to control the rest of the pulse burst generator.

Just after the first positive-going zero crossing of the input, the output of FF1 in Figure IV-11 enables the first counter, which contains 20 bits, to admit pulses from a clock. The counter accumulates the pulses throughout the first cycle of the input. At the end of the cycle the counter stops and it now contains a number, in terms of its binary state, representing the period of the first cycle. It is desired to send out pulses every 1/64 of that period throughout the second cycle. A number which represents 1/64 of the period is simply the number stored in the 14 most significant bits of the 20-bit counter. This is so because binary division by 64, or 1000000 in binary, merely means ignoring the 6 least significant bits of the counter.

Thus, a second counter containing 14 bits is enabled during the second cycle of the input. During this cycle, the 7th to 20th bits of the first counter are compared to the

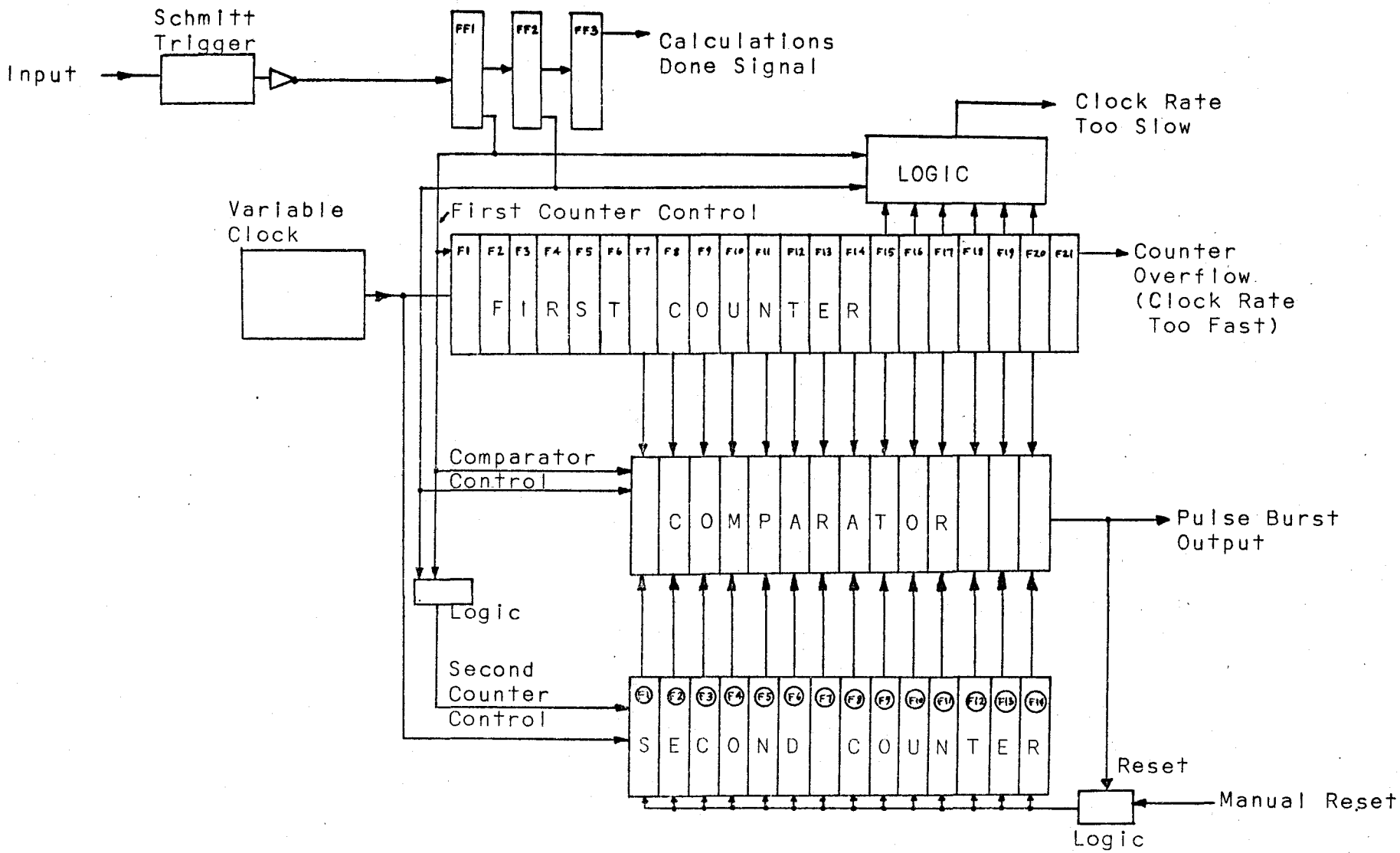

Figure IV-11. Pulse Burst Generator

1st to 14th bits, respectively, of the second counter. When the number in the second counter coincides with that in the last 14 bits of the first counter (this first happens at T/64 seconds after the beginning of the second cycle) the comparator output changes from logic "0" to "1". This signal, which is the output of the pulse burst generator, also feeds back a "clear" signal to the second counter, thereby invalidating the comparison. The output of the comparator switches back to "0", thereby converting the output into a pulse and enabling the "clear" leads of the second counter so that it may resume counting. The width of the output pulses is determined by the propagation delay through the second counter reset logic, the counter itself, and the comparator. In the system which has been built, the pulse width is typically 75 nsec. This is sufficient to switch the flip-flops in the Walsh function generator. The procedure of counting, comparison, and resetting takes place 64 times throughout the second cycle.

The schematic diagrams of the pulse burst generator, which has been constructed on 2 circuit boards, are shown in Figures IV-12 and IV-13 on pages 58 and 59, respectively. The locations of the integrated circuits on the boards are shown in the appendix in Figures C-3 and C-4 on pages 109 and 110, respectively.

Ideally, the 64th pulse should be generated exactly at the end of the second cycle of the input. However, this requires that the number stored in the first counter at the end of the first cycle be divisible exactly by 64. This is

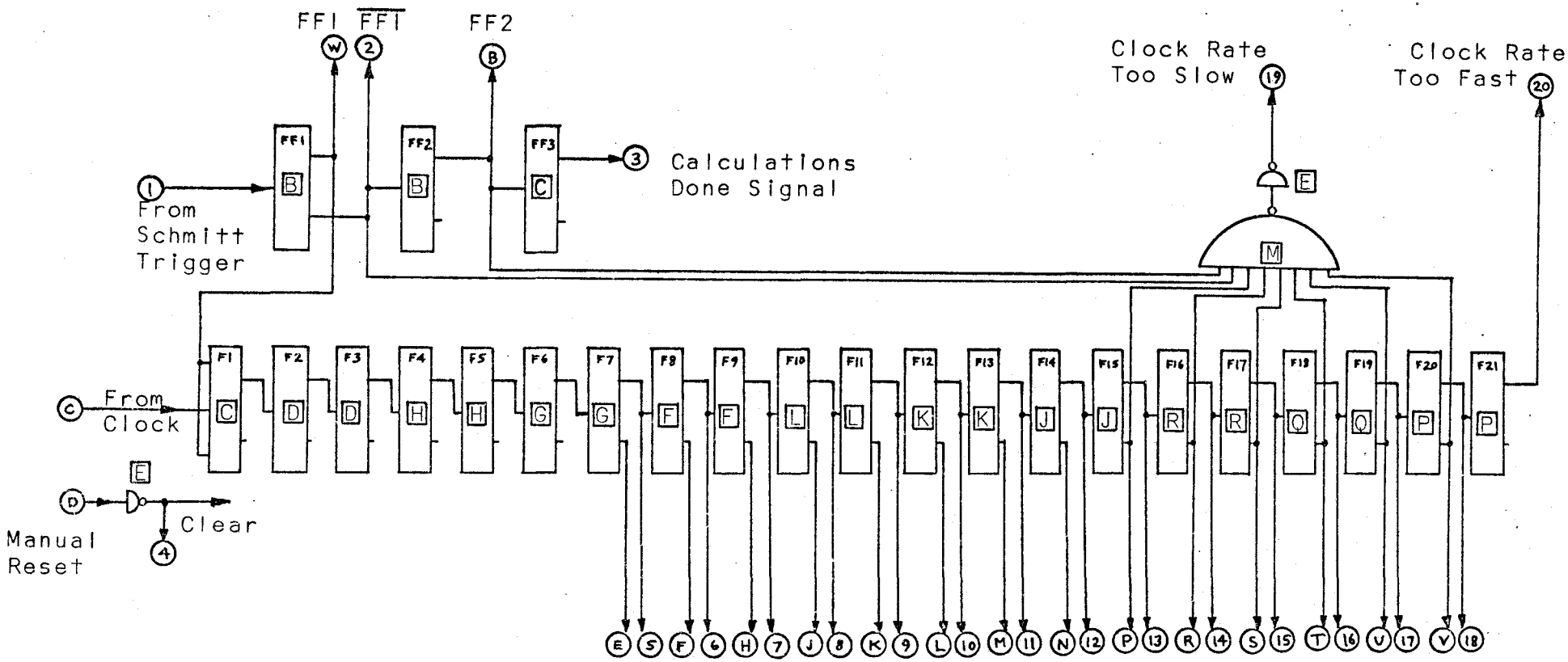

Figure IV-12. Schematic of Pulse Burst Generator - Card 1

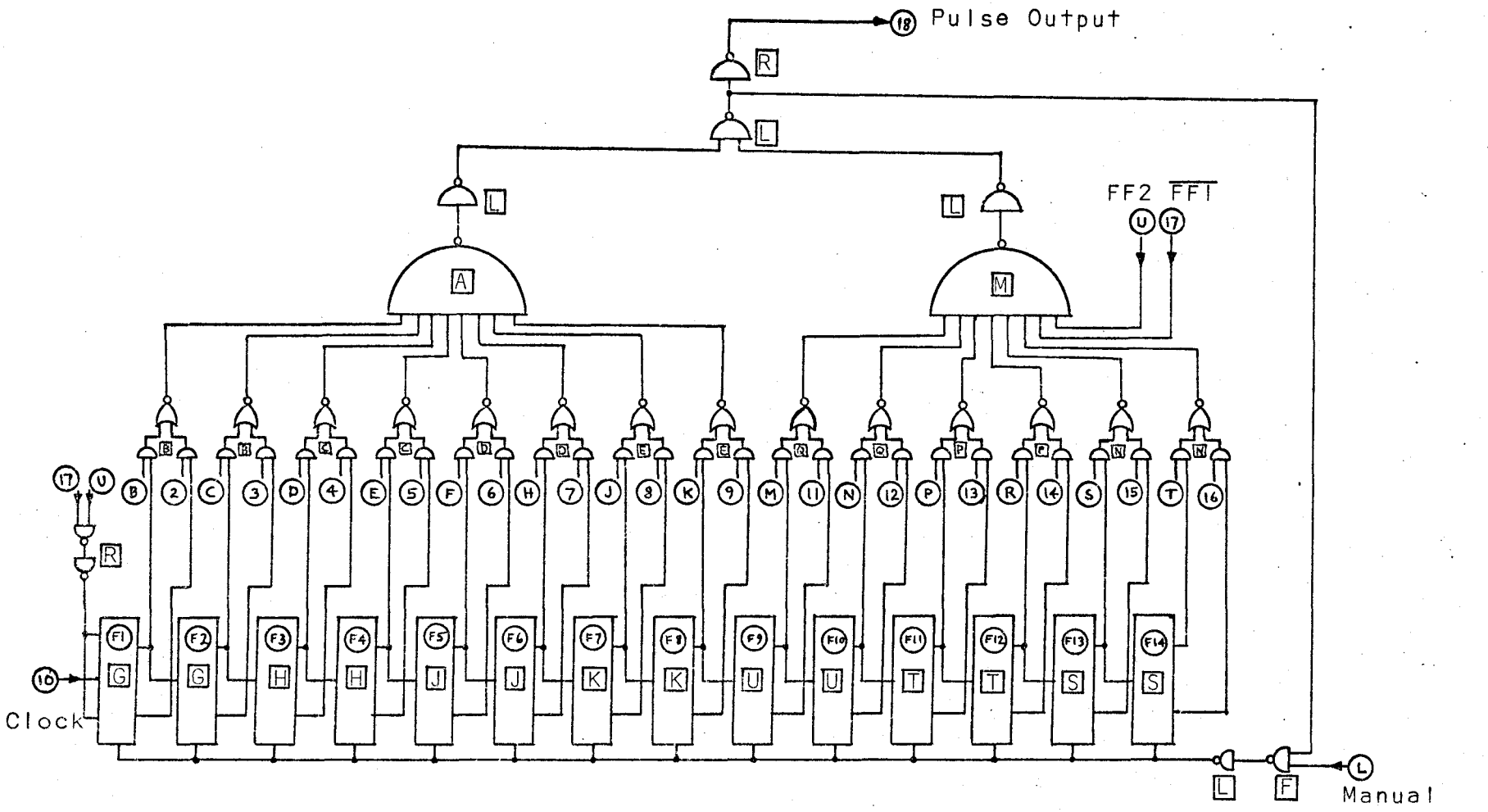

Figure IV-13. Schematic of Pulse Burst Generator -Card 2

seldom the case. The remainder of the division is held in the first 6 flip-flops of the counter. Let this remainder be called e_t pulses. If the integral portion of T/64 in terms of number of pulses is called q, then the length of the first period is

$$T_1 = 64q + e_t \text{ pulses} \tag{4-25}$$

The period of the Walsh functions generated by the pulses from the pulse burst generator during the second period would be

$$T_2 = 64q \text{ pulses} \tag{4-26}$$

Therefore, the error in timing of the period of the Walsh functions is e_t pulses. There is, of course, another small error in timing that amounts to 1 pulse or less due to a lack of synchronization between the counting pulses and the input signal. This error is quite small and is ignored at present.

Since the timing error is represented by the 6 least significant binary bits in the counter, it is obvious that the maximum error would be 63 pulses. This fact can be used to determine the minimum number of flip-flops that are required in the first counter for a maximum error of, say, .4%. The minimum count for this accuracy is calculated by

$$\frac{63(100)}{T_2} = .4\% \tag{4-27}$$

whence $T_2 = 15{,}750.$ (4-28)

The number of flip-flops needed to guarantee at least that large a number is 15. To provide a sufficient range of operation, a 20-bit counter was used. To insure that the count representing the period of the cycle reaches at least the 15th flip-flop, logic gates are used (see Figure IV-12) to

check that at the beginning of the second cycle, there is at least one "1" in the 15th to 20th flip-flops. If there is not, then a light indicates that the rate at which the clock is feeding the pulse burst generator is too low.

On the other hand, if the clock rate is too high, the counter may overflow. A 21st flip-flop is added so that when the count reaches this flip-flop, a light will indicate that the clock rate is too fast. In either case when the lights go on, the entire instrument ceases calculations.

It is apparent that the clock rate feeding the pulse burst generator controls the upper limit of the fundamental frequency of a periodic wave that can be analysed by the system. Table IV-III on page 62, gives a list of recommended clock rates and the maximum and minimum fundamental input frequencies of waves that can be analysed using them.

An upper limit on clock rate of 1 MHz. is recommended, unless very short leads are used in construction, since higher frequencies may result in errors due to radiation and interference with the rest of the system. This means that the maximum fundamental input frequency is 60 Hz. Since the clock rate can be reduced, there is no theoretical lower frequency limit for the system and the upper limit is sufficient to overlap the frequency range of conventional wave analysers.

Sample Processing System

There are two steps involved in the sample processing. Up to this point, the system for producing binary-coded samples of the input, $|f(t)_{qm}|$, and the Walsh functions has been

Table IV-III. Input Frequency Limits with Various Clock Rates

Clock Rate (Hz.)	Maximum Frequency (Hz.)	Minimum Frequency (Hz.)	Period
10,000,000	600	10	.00167 - .1 sec.
1,000,000	60	1	.0167 - 1.0 sec.
100,000	6	.1	.167 - 10 sec.
10,000	.6	.01	1.67 - 100 sec.
1,000	.06	.001	.278 - 16.7 min.
100	.006	.0001	2.78 - 167 min.
10	.0006	.00001	.462 - 27.7 hrs.
1	.00006	.000001	.192 - 11.6 days

described. The step following the production of Walsh functions is to obtain signals representing sgn f(t) sgn wal(n,θ). This signal determines whether the binary-coded samples are to be added or subtracted. A coincidence gate involving the output of the Schmitt trigger, which provides sgn f(t), and the output of the Walsh function generator, which provides sgn wal(n,θ), is all that is necessary. The logic is shown in Figure IV-14 below

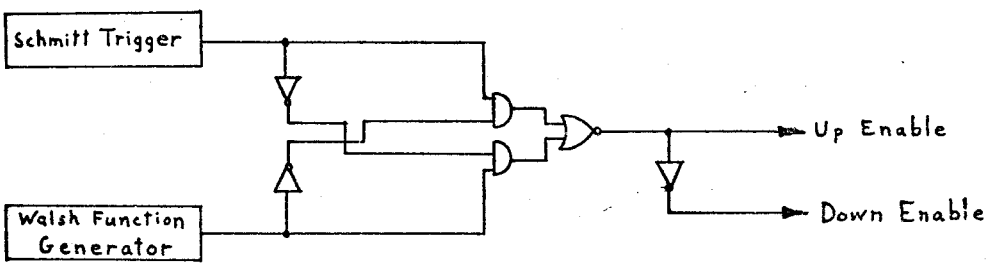

Figure IV-14. Logic for Producing sgn f(t) sgn wal(n,θ)

The "up enable" output is a logic "1" when sgn f(t) sgn wal(n,θ) is positive, and the "down enable" is "1" when sgn f(t) sgn wal(n,θ) is negative. The inverter shown external to the Walsh function generator in Figure IV-14 is shown only for illustrative purposes since the generator produces both positive and negative Walsh functions. One of the logic systems in Figure IV-14 is needed for each of the Walsh functions.

The final stage in the system is the accumulation of the samples from the A/D converter. For each of the Walsh-Fourier coefficients, the binary-coded samples of the input are either added to or subtracted from (depending on sgn f(t)

sgn wal(n,θ),) an accumulation of previous samples. There are several possible methods of performing these calculations. Only one of the methods which have been investigated is shown here. The circuit of the entire sample processing system for one of the Walsh-Fourier coefficients is shown in Figure IV-15 on page 65.

The sample accumulation stage consists mainly of 2 6-bit binary counters with parallel feeds. The upper counter in Figure IV-15 records the samples when it is enabled by the positive sgn f(t) sgn wal(n,θ) lead. Except for the first flip-flop, the clock inputs of each J-K flip-flop are controlled by an exclusive OR of the parallel pulse input or the previous flip-flop. Since the pulse inputs arrive serially in time from the A/D converter, the most significant bit arriving first, there is never any conflict between a pulse input and a level change from a less significant bit. The same procedure is followed in the lower counter, which accumulates samples whenever sgn f(t) sgn wal(n,θ) is negative.

As pulses are accumulated in each of the counters, there will be overflows from the 6th bits. These overflows feed into an A-B mode reversible counter, the A input being the overflow from the positive sample counter, and the B input being the overflow from the negative sample counter. Since each of the counters must reach a count of 64 before they overflow, the number which appears in the reversible counter is 1/64 of the total sample value. But 64 is the number of quantization levels, p, that have been used in the A/D converter. Consequently the number stored in the reversible counter

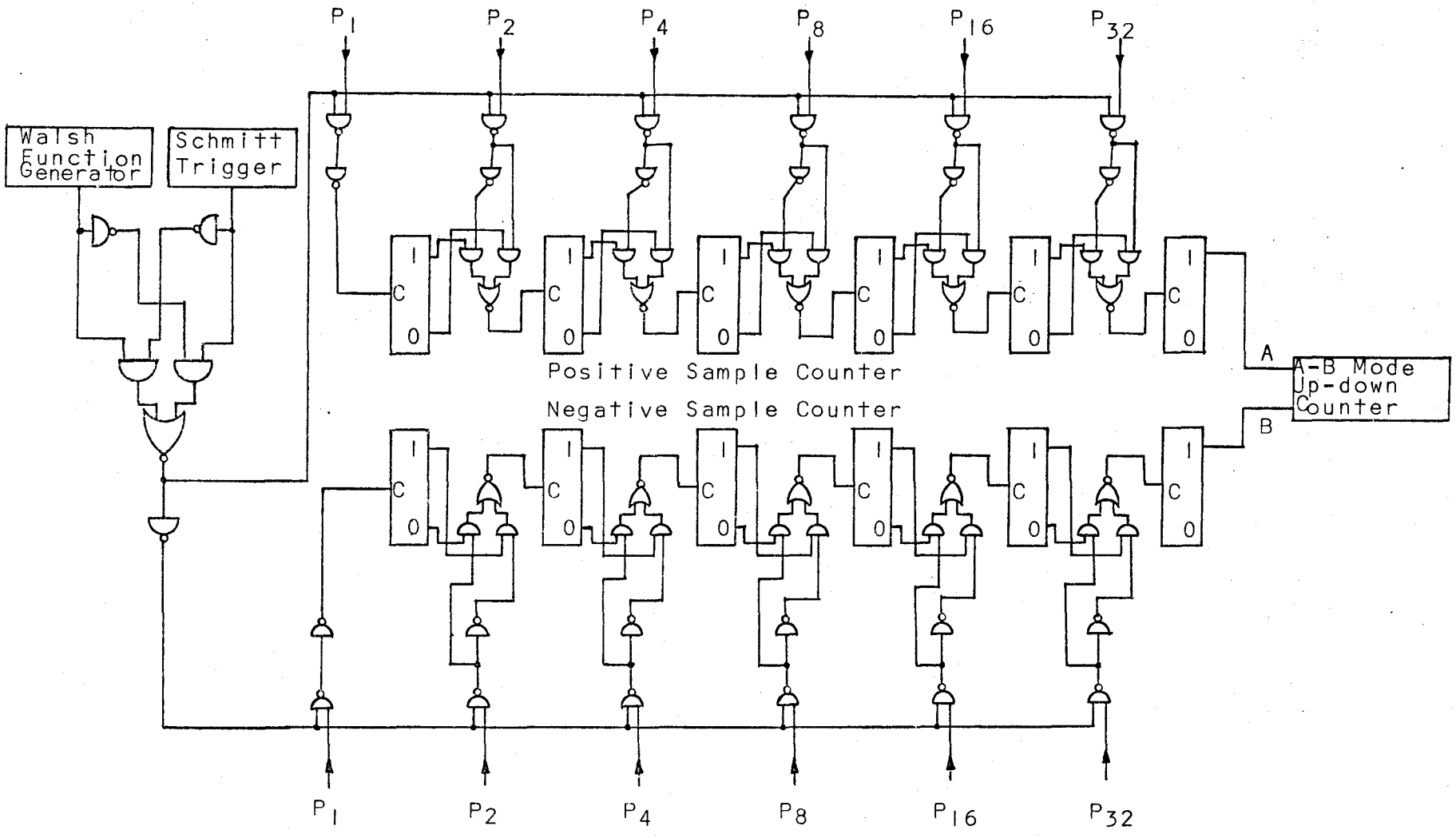

Figure IV-15. Sample Processing System

corresponds, except for a possible small remainder in the two counters feeding the reversible counter, to the desired expressions given in Equations (4-1) to (4-3). At present, a Hewlett-Packard 5280A Reversible Counter is used as the A-B mode reversible counter.

The only remaining operation is a manual one. The numbers in the reversible counters must each be multiplied by 10 and divided by the number contained in the sample counter in Figure IV-5. Thus, the values of the Walsh-Fourier coefficients of the periodic input wave are determined.

V. Partial Error Analysis

The main purpose of this thesis is to show the application of the mathematics for Walsh-Fourier analysis of a low fundamental frequency periodic wave to a digital instrument. Thus, only a small portion of the error analysis has been performed. Only two errors are considered here. The first is the mathematical error involved in the conversion of Walsh-Fourier to Fourier series due to the use of a finite number of terms in an infinite series. The second is a timing error in the Walsh function generator. Since the only completed sections of the instrument are the Walsh function generator and the pulse burst generator, it is the timing error involved in producing Walsh functions of the correct period that is discussed. Other system errors, such as quantization errors, finite sampling rate errors, level inaccuracies, and effect of finite aperture time have not been investigated.

Errors due to Mathematical Approximation

The equation for each Fourier coefficient involves an infinite series of terms containing Walsh-Fourier coefficients. However, the instrument that has been designed is capable of providing only 32 coefficients. Consequently, the equations for the Fourier coefficients, as shown in Table B-IV in the

appendix, must be terminated at the terms involving A_{32} and B_{32}. Therefore, even if the Walsh-Fourier coefficients, A_n and B_n, could be determined precisely, errors would still result in calculating the Fourier coefficients, a_n and b_n.

A general expression for the mathematical errors is not developed. Rather, a number of waveforms, with various amplitude probability distributions, are used as examples. The waveforms that are used are a square wave, pulses with various duty cycles, a sine wave, a sum of several sine waves with equal amplitude, and finally, a triangular wave. Each wave is considered to start with the first positive-going zero voltage crossing. A computer was used to perform all calculations. For each of the waves, the computer calculated the true Fourier coefficients, the Fourier coefficients according to the equations in Table B-IV in the appendix, the actual error, and the per cent error. Several sets of calculations were made for each wave. Each set used a different number of Walsh-Fourier coefficients, beginning with 4 and increasing by a factor of 2 for each set until all 32 coefficients were used in the calculations. Several examples of Walsh-Fourier to Fourier series conversion using 32 coefficients are given in appendix D in Tables D-I to D-VII on pages 112 to 118. Since it was found that for several waveforms calculations of harmonics beyond the 10th, even using all 32 Walsh-Fourier coefficients, became somewhat inaccurate, only values for 10 coefficients are listed in appendix D.

Not all of the waveforms that were investigated are

listed in appendix D. However, the ones that are shown are representative of all the waveforms that were examined. Observations of the calculations show that;

(1) A square wave is to the Walsh-Fourier series what a sine wave is to the Fourier series; i.e. the Walsh-Fourier series of a square wave consists only of $B_1 sal(1,\theta)$ where B_1 is the amplitude of the square wave.

(2) The Walsh-Fourier series of a sine wave contains many terms, whereas the Fourier series has only the one term, $b_1 \sin\theta$.

(3) When the Walsh-Fourier series of a wave contains only a finite number of terms, such as with a square wave or square pulses with duty cycles of 1/2, 1/4, 1/8, 1/16, ..., the conversion to Fourier series can be performed with very small error.

(4) The probability of error in conversion is greater when the Walsh-Fourier series contains a large number of terms.

(5) The per cent error in conversion generally increases for calculations of higher harmonics.

Walsh Function Period Timing Error

At the end of the first cycle of the input, the binary state of the first counter in the pulse burst generator records the period of the cycle in terms of clock pulses. The count is not necessarily precise, for the cycle may start or stop

between the time pulses arrive from the clock. A similar error may occur during the second cycle when the Walsh Functions are generated. However, these errors are negligible if a very high clock rate is used and they are very difficult to measure. Hence, they are ignored in this thesis.

The only main source of timing error is e_t, which is described in Chapter IV. It results from the remainder in the division by 64 of the binary state of the first counter in the pulse burst generator. e_t is the error measured as a pulse count. If f_c is the clock frequency, then the error measured in seconds is e_t/f_c. It is by this amount that the period of the Walsh functions will be less than the period of the input wave, as determined by the first cycle.

The error, e_t, can be measured quite easily by using the circuit shown in Figure V-1 on page 71. An A-B mode reversible counter is used, the A input recording the number of pulses which are used to measure the first period, and the B input recording the period of the Walsh functions. The number which remains in the counter at the end of two periods is e_t. It has been verified that this number corresponds to the remainder in the division by comparing it to the number representing the binary states of the 6 flip-flops which contain the 6 least significant binary digits in the first counter of the pulse burst generator.

A D.E.C. Computer Lab was used to supply the clock pulses and logic units, as shown in Figure V-1. The input from the Schmitt trigger to the pulse burst generator was simulated by using manually controlled switches.

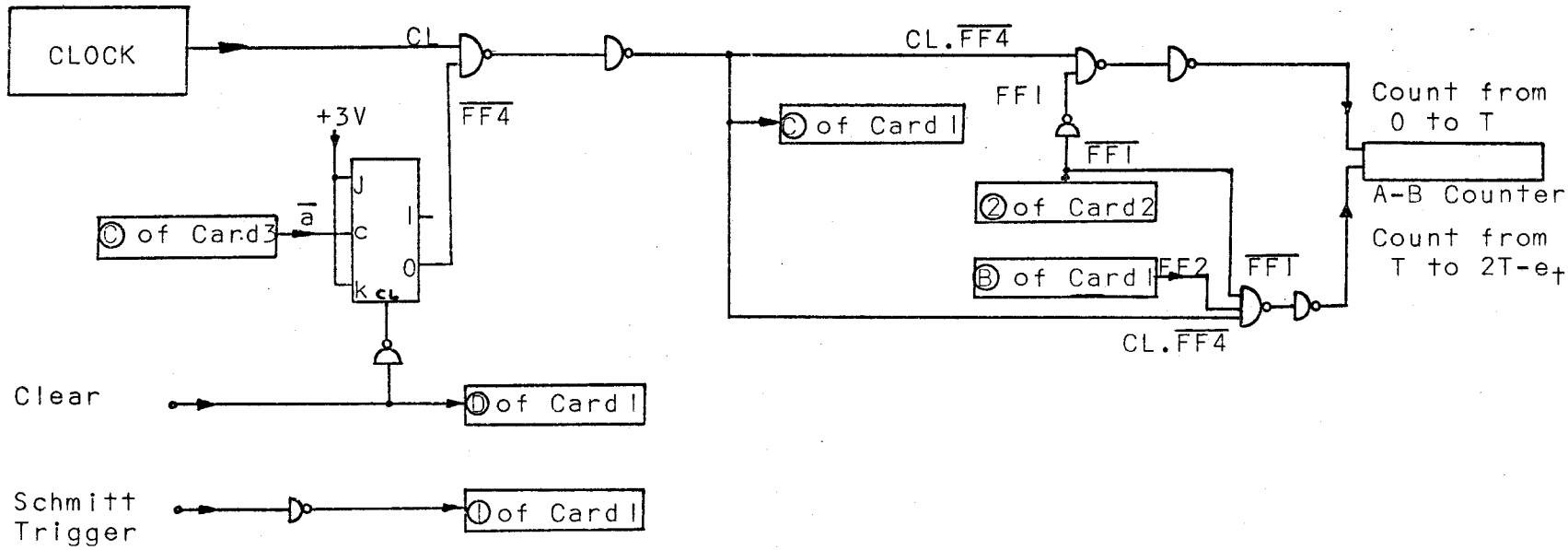

Figure V-1. System to Measure e_+

Since the maximum value of e_t is 63, and the pulse burst generator is set to stop the system if the count at the end of the first cycle has not reached the 15th flip-flop of the first counter, the maximum timing error is 63/16,384, or .384%. However, assuming that the period of the input is random for many tests, then the probability distribution of e_t would be uniform, with all values for e_t from 0 to 63 being equally likely. Since the maximum error would only occur when the 15th flip-flop has barely been reached and e_t = 63, the average error is far less than .384%.

By using the system in Figure V-1, 500 samples of e_t were taken. The distribution of the samples is shown in the histogram in Figure V-2 on page 73. The samples were placed into 16 groups of 4. The average value of e_t was found to be 31.642, whereas the theoretical value is 31.5. The theoretical sample distribution and average value for e_t are also shown in Figure V-2.

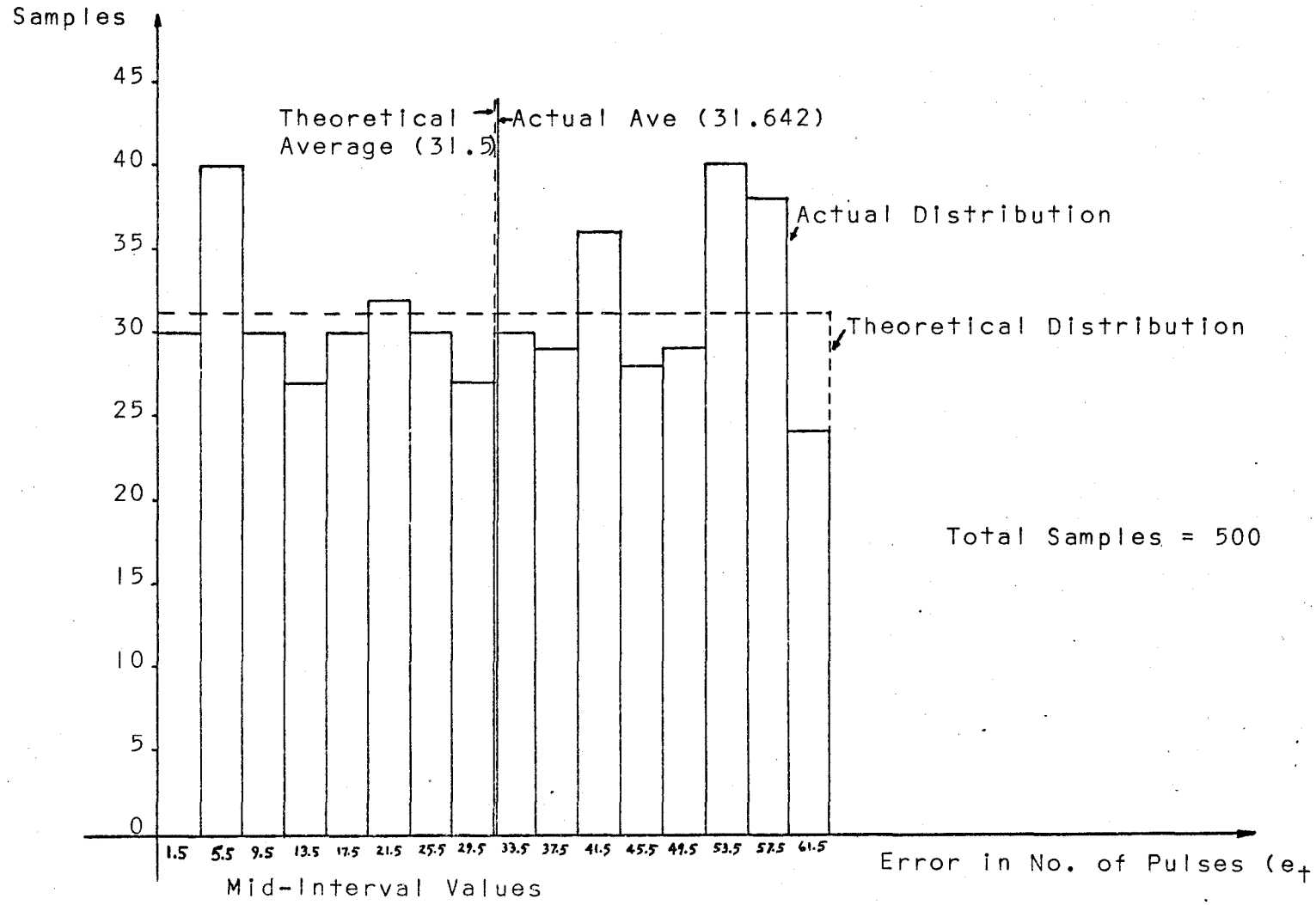

Figure V-2. Sample Distribution of e_t

VI. Conclusions

The design of the Walsh-Fourier analyser which is proposed in this thesis requires that the waveforms to be analyzed be restricted in amplitude to ± 10 volts. The input controls to the pulse burst generator are designed to investigate only those signals which have two zero-voltage crossings per cycle. The upper limit of fundamental frequency that can be handled is approximately 60 Hz. This frequency, which is determined by the clock feeding the pulse burst generator, is sufficient to overlap the lower frequency limit of conventional wave analysers. The Walsh-Fourier analyser has no theoretical lower frequency limit.

It has been concluded that, for many commonly-used waveforms, 32 Walsh-Fourier coefficients can be used to determine 10 Fourier coefficients to a reasonable degree of accuracy. An advantage of the Walsh-Fourier analyser is that the coefficients of both cosine and sine terms of the Fourier series can be determined. Conventional wave analysers can supply only the coefficients of the complex Fourier series, C_n, where $C_n = \sqrt{a_n^2 + b_n^2}$.

Several problems on the Walsh-Fourier analyser remain to be solved. Construction of the proposed design should be completed. Modifications may be made to allow the instrument to analyse waveforms with more than two zero-crossings per

cycle, and possibly to analyse noise. An additional circuit may be designed which performs the Walsh-Fourier to Fourier series conversion electronically. Finally, a complete error analysis of the system must be performed to provide a more adequate comparison with currently available wave analysers, and to establish better design criteria.

APPENDIX

Appendix A. Rules for Determining Walsh Functions

One period of a Walsh function is T seconds. In the general Walsh function, wal(n,θ), θ = t/T, where t is in the range $0 \leq t \leq T$ so that θ is in the range $0 \leq \theta \leq 1$. Sal(1,θ) is a function (see Figure II-2 on page 13) defined as:

$$\begin{aligned} sal(1,\theta) &= +1 \quad 0 \leq \theta < .5 \\ &= -1 \quad .5 \leq \theta < 1 \end{aligned} \qquad \text{(A-1)}$$

Beginning with this initial function, all other Walsh functions can be determined by the following rules;

(1) Let the general terms for the sal and cal functions be represented by;

$sal[(2N+1)2^k, \theta]$

$cal[(2N+1)2^k, \theta]$

with N = 0, 1, 2, 3, ------

and k = 0, 1, 2, 3, -----

k and N are both finite.

(2) Any function which has a sequency 2^k times that of a function with a particular value of n has exactly the same form as that function.

(3) In order to determine the cal function from the corresponding sal function of the same sequency, the following rules apply.

(a) If N is even, and for a particular value of k, the sal function is shifted $\frac{T}{2^{k+2}}$ to the left (or

in the negative direction) to produce the cal function.

(b) If N is odd, then the sal function is shifted $\frac{T}{2^{k+2}}$ to the right (or in the positive direction) to produce the cal function.

(4) For any given cal function, the sal function with a sequency which is one greater than the cal function may be produced as follows:

$$sal[(2N+1)2^k+1,\theta] = +cal[(2N+1)2^k, \theta] \quad 0 \leq \theta < .5 \qquad (A-2)$$

$$sal[(2N+1)2^k+1,\theta] = -cal[(2N+1)2^k, \theta] \quad .5 \leq \theta < 1 \qquad (A-3)$$

Examples (Reference should be made to Figure II-2 on page 13)

Rule(2)- Given $sal[(2N+1)2^k,\theta]$ with N=0 and k=0, 1, 2, 3, ---- the following functions may be produced: $sal(1,\theta)$, $sal(2,\theta)$, $sal(4,\theta)$, $sal(8,\theta)$, -----. Thus, $sal(8,\theta)$ for example, is identical in form to $sal(1,\theta)$, but has 8 times the sequency.

Similarly, if N=1 and k=0, 1, 2, 3, ---, $sal(3,\theta)$, $sal(6,\theta)$, $sal(12,\theta)$, $sal(24,\theta)$, --- are produced. $Sal(24,\theta)$ has 8 times the sequency as $sal(3,\theta)$, but they are identical in form.

Rule(3)- Given $sal[(2N+1)2^k,\theta]$, find $cal[(2N+1)2^k,\theta]$ where N and k are the same for the sal and cal functions.

(a) Let N=0 and k=0, 1, 2, 3, ---

k	Function	Shift required to produce cal functions
0	$sal(1,\theta)$	-T/4
1	$sal(2,\theta)$	-T/8
2	$sal(4,\theta)$	-T/16
3	$sal(8,\theta)$	-T/32
4	$sal(16,\theta)$	-T/64

(b) Let N=1 and k =0, 1, 2, 3, ---

k	Function	Shift required to produce cal functions
0	sal(3,θ)	+T/4
1	sal(6,θ)	+T/8
2	sal(12,θ)	+T/16
3	sal(24,θ)	+T/32
4	sal(48,θ)	+T/64

Rule(4)- Given cal(5,θ), find sal(6,θ).

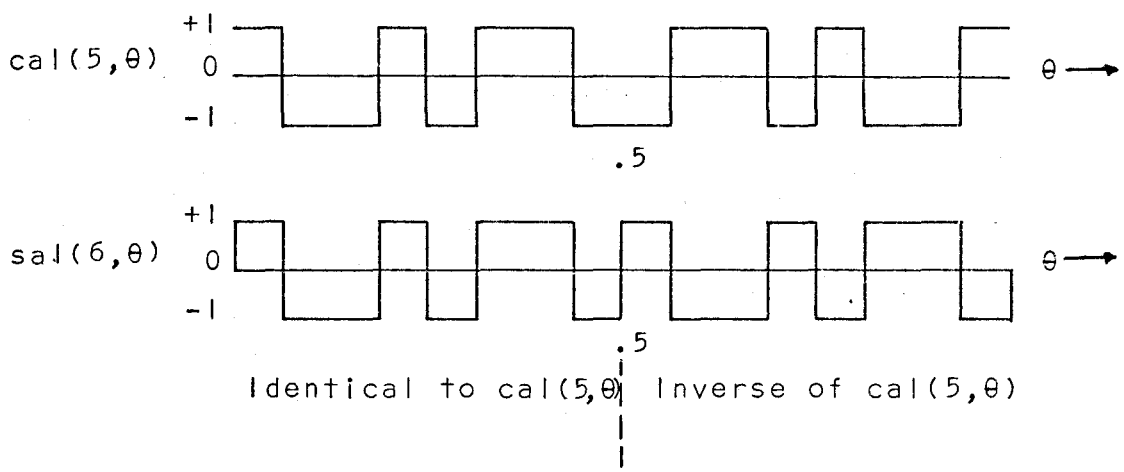

Appendix B. Conversion of Walsh-Fourier to Fourier Series

The Walsh-Fourier series representation of a periodic wave f(t) is

$$f(t) = A_o + \sum_{n=1}^{\infty} A_n cal(n,\theta) + \sum_{n=1}^{\infty} B_n sal(n,\theta) \qquad (2\text{-}21)$$

As stated in Chapter II, the Fourier series of each of the Walsh functions must be known to convert Equation (2-21) into an equivalent Fourier series. In this Appendix, the Fourier coefficients for a number of Walsh functions are derived and used to find equations of the coefficients of the Fourier series of f(t). Only odd sequency multiples of sal(1,θ) and cal(1,θ) need be processed, since the other Walsh functions, and hence their Fourier series can be derived easily from these functions. Subscripts for the coefficients of the Fourier series of the Walsh functions are the same as those defined in Chapter II.

Using Equations (2-14) to (2-16), Fourier coefficients of cal(1,θ) are found as follows;

$$a_o(c1) = 0 \qquad (B\text{-}1)$$

$$a_n(c1) = \frac{1}{\pi}\int_o^{2\pi} cal(1,\theta)\cos n\theta\, d\theta$$

$$= \frac{1}{\pi}\left[\int_o^{\pi/2} \cos n\theta\, d\theta - \int_{\pi/2}^{3\pi/2} \cos n\theta\, d\theta + \int_{3\pi/2}^{2\pi} \cos n\theta\, d\theta\right]$$

$$= \frac{2}{\pi n}\left[\sin\frac{n\pi}{2} - \sin\frac{3n\pi}{2}\right]$$

$$\therefore a_n(c1) = \frac{4\pi}{n}\sin\frac{n\pi}{2} \qquad \text{(B-2)}$$

$$b_n(c1) = \frac{1}{\pi}\int_0^{2\pi} cal(1,\theta)\sin n\theta d\theta$$

$$= \frac{1}{\pi}\left[\int_0^{\pi/2}\sin n\theta d\theta - \int_{\pi/2}^{3\pi/2}\sin n\theta d\theta + \int_{3\pi/2}^{2\pi}\sin n\theta d\theta\right]$$

$$\therefore b_n(c1) = 0 \qquad \text{(B-3)}$$

Only the $a_n(cm)$ coefficients, with $n \neq 0$, of the Fourier series of all cal (m,θ) functions are non-zero.

Fourier coefficients of $sal(1,\theta)$ are found as follows:

$$a_o(s1) = 0 \qquad \text{(B-4)}$$

$$a_n(s1) = \frac{1}{\pi}\int_0^{2\pi} sal(1,\theta)\cos n\theta d\theta$$

$$= \frac{1}{\pi}\left[\int_0^{\pi}\cos n\theta d\theta - \int_{\pi}^{2\pi}\cos n\theta d\theta\right]$$

$$\therefore a_n(s1) = 0 \qquad \text{(B-5)}$$

$$b_n(s1) = \frac{1}{\pi}\int_0^{2\pi} sal(1,\theta)\sin n\theta d\theta$$

$$= \frac{1}{\pi}\left[\int_0^{\pi}\sin n\theta d\theta - \int_{\pi}^{2\pi}\sin n\theta d\theta\right]$$

$$\therefore b_n(s1) = \frac{2}{\pi n}\left[1 - \cos n\pi\right] \qquad \text{(B-6)}$$

Only the $b_n(sm)$ coefficients of the Fourier series of all $sal(m,\theta)$ functions are non-zero.

Similarly, Fourier coefficients of other Walsh functions may be calculated. The equations of several of the coefficients are listed in Table B-I on pages 82 to 84. A computer program was used to calculate the numerical value

Table B-1. Equations of Fourier Coefficients of Walsh Functions

$$a_n(c1) = \frac{4}{\pi n} \sin \frac{n\pi}{2}$$

$$b_n(s1) = \frac{2}{\pi n} [1 - \cos n\pi]$$

$$a_n(c3) = \frac{4}{\pi n} \cos n\pi \sin \frac{n\pi}{2} [1 - 2\cos \frac{n\pi}{4}]$$

$$b_n(s3) = \frac{2}{\pi n} [1 - \cos n\pi + 4\cos n\pi \sin \frac{n\pi}{2} \sin \frac{n\pi}{4}]$$

$$a_n(c5) = \frac{4}{\pi n} \cos n\pi \sin \frac{n\pi}{2} [4\sin \frac{n\pi}{4} \sin \frac{n\pi}{8} - 1]$$

$$b_n(s5) = \frac{2}{\pi n} [1 - \cos n\pi + 8 \cos n\pi \sin \frac{n\pi}{2} \cos \frac{n\pi}{4} \sin \frac{n\pi}{8}]$$

$$a_n(c7) = \frac{4}{\pi n} \cos n\pi \sin \frac{n\pi}{2} [1 + 2 \cos \frac{n\pi}{4} (1 - 2 \cos \frac{n\pi}{8})]$$

$$b_n(s7) = \frac{2}{\pi n} [1 - \cos n\pi + 4 \cos n\pi \sin \frac{n\pi}{2} \sin \frac{n\pi}{4} (2 \cos \frac{n\pi}{8} - 1)]$$

$$a_n(c9) = \frac{4}{\pi n} \cos n\pi \sin \frac{n\pi}{2} [8 \sin \frac{n\pi}{4} \cos \frac{n\pi}{8} \sin \frac{n\pi}{16} - 1]$$

$$b_n(s9) = \frac{2}{\pi n} [1 - \cos n\pi + 16 \cos n\pi \sin \frac{n\pi}{2} \cos \frac{n\pi}{4} \cos \frac{n\pi}{8} \sin \frac{n\pi}{16}]$$

$$a_n(c11) = \frac{4}{\pi n} \cos n\pi \sin \frac{n\pi}{2} [1 - 2 \cos \frac{n\pi}{4} (1 - 4 \sin \frac{n\pi}{8} \sin \frac{n\pi}{16})]$$

Table B-1. (Continued)
Equations of Fourier Coefficients of Walsh Functions

$$b_n(s11) = \frac{2}{\pi n}\left[1 - \cos n\pi + 4\cos n\pi \sin\frac{n\pi}{2}\sin\frac{n\pi}{4}\left(1 - 4\sin\frac{n\pi}{8}\sin\frac{n\pi}{16}\right)\right]$$

$$a_n(c13) = \frac{4}{\pi n}\cos n\pi \sin\frac{n\pi}{2}\left[4\sin\frac{n\pi}{4}\sin\frac{n\pi}{8}\left(2\cos\frac{n\pi}{16} - 1\right) - 1\right]$$

$$b_n(s13) = \frac{2}{\pi n}\left[1 - \cos n\pi + 8\cos n\pi \sin\frac{n\pi}{2}\cos\frac{n\pi}{4}\sin\frac{n\pi}{8}\left(2\cos\frac{n\pi}{16} - 1\right)\right]$$

$$a_n(c15) = \frac{4}{\pi n}\cos n\pi \sin\frac{n\pi}{2}\left[1 + 2\cos\frac{n\pi}{4}\left\{1 + 2\cos\frac{n\pi}{8}\left(1 - 2\cos\frac{n\pi}{16}\right)\right\}\right]$$

$$b_n(s15) = \frac{2}{\pi n}\left[1 - \cos n\pi + 4\cos n\pi \sin\frac{n\pi}{2}\sin\frac{n\pi}{4}\left\{2\cos\frac{n\pi}{8}\left(2\cos\frac{n\pi}{16} - 1\right) - 1\right\}\right]$$

$$a_n(c17) = \frac{4}{\pi n}\cos n\pi \sin\frac{n\pi}{2}\left[16\sin\frac{n\pi}{4}\cos\frac{n\pi}{8}\cos\frac{n\pi}{16}\sin\frac{n\pi}{32} - 1\right]$$

$$b_n(s17) = \frac{2}{\pi n}\left[1 - \cos n\pi + 32\cos n\pi \sin\frac{n\pi}{2}\cos\frac{n\pi}{4}\cos\frac{n\pi}{8}\cos\frac{n\pi}{16}\sin\frac{n\pi}{32}\right]$$

$$a_n(c19) = \frac{4}{\pi n}\cos n\pi \sin\frac{n\pi}{2}\left[1 + 2\cos\frac{n\pi}{4}\left(8\sin\frac{n\pi}{8}\cos\frac{n\pi}{16}\sin\frac{n\pi}{32} - 1\right)\right]$$

$$b_n(s19) = \frac{2}{\pi n}\left[1 - \cos n\pi + 4\cos n\pi \sin\frac{n\pi}{2}\sin\frac{n\pi}{4}\left(1 - 8\sin\frac{n\pi}{8}\cos\frac{n\pi}{16}\sin\frac{n\pi}{32}\right)\right]$$

$$a_n(c21) = \frac{4}{\pi n}\cos n\pi \sin\frac{n\pi}{2}\left[4\sin\frac{n\pi}{4}\sin\frac{n\pi}{8}\left(1 - 4\sin\frac{n\pi}{16}\sin\frac{n\pi}{32}\right) - 1\right]$$

$$b_n(s21) = \frac{2}{\pi n}\left[1 - \cos n\pi + 8\cos n\pi \sin\frac{n\pi}{2}\cos\frac{n\pi}{4}\sin\frac{n\pi}{8}\left(1 - 4\sin\frac{n\pi}{16}\sin\frac{n\pi}{32}\right)\right]$$

Table B-1. (Continued)
Equations of Fourier Coefficients of Walsh Functions

$$a_n(c23) = \frac{4}{\pi n} \cos n\pi \sin \frac{n\pi}{2} \left[1 + 2 \cos \frac{n\pi}{4} \left(1 - 2 \cos \frac{n\pi}{8} \left\{ 1 - 4 \sin \frac{n\pi}{16} \sin \frac{n\pi}{32} \right\}\right)\right]$$

$$b_n(s23) = \frac{2}{\pi n} \left[1 - \cos n\pi + 4 \cos n\pi \sin \frac{n\pi}{2} \sin \frac{n\pi}{4} \left(2 \cos \frac{n\pi}{8} \left\{1 - 4 \sin \frac{n\pi}{16} \sin \frac{n\pi}{32}\right\} - 1\right)\right]$$

$$a_n(c25) = \frac{4}{\pi n} \cos n\pi \sin \frac{n\pi}{2} \left[8 \sin \frac{n\pi}{4} \cos \frac{n\pi}{8} \sin \frac{n\pi}{16} \left(2 \cos \frac{n\pi}{32} - 1\right) - 1\right]$$

$$b_n(s25) = \frac{2}{\pi n} \left[1 - \cos n\pi + 16 \cos n\pi \sin \frac{n\pi}{2} \cos \frac{n\pi}{4} \cos \frac{n\pi}{8} \sin \frac{n\pi}{16} \left(2 \cos \frac{n\pi}{32} - 1\right)\right]$$

$$a_n(c27) = \frac{4}{\pi n} \cos n\pi \sin \frac{n\pi}{2} \left[1 + 2 \cos \frac{n\pi}{4} \left\{ \sin \frac{n\pi}{8} \sin \frac{n\pi}{16} \left(2\cos \frac{n\pi}{32} - 1\right) - 1 \right\}\right]$$

$$b_n(s27) = \frac{2}{\pi n} \left[1 - \cos n\pi + 4 \cos n\pi \sin \frac{n\pi}{2} \sin \frac{n\pi}{4} \left(1 - 4\sin \frac{n\pi}{8} \sin \frac{n\pi}{16} \left\{ 2\cos \frac{n\pi}{32} - 1 \right\}\right)\right]$$

$$a_n(c29) = \frac{4}{\pi n} \cos n\pi \sin \frac{n\pi}{2} \left[4\sin \frac{n\pi}{4} \sin \frac{n\pi}{8} \left(2\cos \frac{n\pi}{16} \left\{ 2\cos \frac{n\pi}{32} - 1 \right\} - 1\right) - 1\right]$$

$$b_n(s29) = \frac{2}{\pi n} \left[1 - \cos n\pi + 8\cos n\pi \sin \frac{n\pi}{2} \cos \frac{n\pi}{4} \sin \frac{n\pi}{8} \left(2\cos \frac{n\pi}{16} \left\{2\cos \frac{n\pi}{32} - 1\right\} - 1\right)\right]$$

$$a_n(c31) = \frac{4}{\pi n} \cos n\pi \sin \frac{n\pi}{2} \left[1 + 2\cos \frac{n\pi}{4} \left\{ 1 + 2\cos \frac{n\pi}{8} \left(1 + 2\cos \frac{n\pi}{16} \left[1 - 2\cos \frac{n\pi}{32}\right]\right)\right\}\right]$$

$$b_n(s31) = \frac{2}{\pi n} \left[1 - \cos n\pi + 4\cos n\pi \sin \frac{n\pi}{2} \sin \frac{n\pi}{4} \left(2\cos \frac{n\pi}{8} \left\{ 2\cos \frac{n\pi}{16} \left[2\cos \frac{n\pi}{32} - 1\right] - 1 \right\} - 1\right)\right]$$

of the first 50 harmonics of the Walsh functions by using the equations listed in Table B-I. The values of the coefficients are shown in Table B-II on pages 86 to 91. By using these values, the Fourier series of sal(1,θ) and cal(1,θ) to sal(32,θ) and cal(32,θ) may be calculated. The Fourier series of these functions are listed in Table B-III on pages 92 to 98.

The final step in the conversion from Walsh-Fourier to Fourier series involves the derivation of the formulae of the Fourier coefficients of the signal, f(t), in terms of the Walsh-Fourier coefficients. The Fourier coefficients, a_n and b_n, are calculated by Equations (2-30) and (2-31), where a_n(cm) and b_m(sm) are constants as determined by the equations in Table B-III. The formulae for the Fourier coefficients are listed in Table B-IV on pages 99 to 105.

Table B-11. Fourier Coefficients of Walsh Functions

EXECUTION

N	ANC1	BNS1	ANC3	BNS3	ANC5	BNS5
1	1.273240	1.273240	0.527393	-0.527393	-0.104905	-0.104905
2	0.000000	-0.000000	0.000000	0.000000	0.000000	-0.000000
3	-0.424413	0.424413	1.024624	1.024624	0.684632	-0.684632
4	-0.000000	-0.000000	-0.000000	-0.000000	0.000000	0.000000
5	0.254648	0.254648	-0.614774	0.614774	0.920075	0.920075
6	0.000000	-0.000000	0.000000	-0.000000	-0.000000	-0.000000
7	-0.181891	0.181891	-0.075342	-0.075342	-0.378769	0.378769
8	-0.000000	-0.000000	0.000000	-0.000000	0.000000	-0.000000
9	0.141471	0.141471	0.058599	-0.058599	0.294598	0.294598
10	0.000000	-0.000000	0.000000	0.000000	-0.000000	-0.000000
11	-0.115749	0.115749	0.279443	0.279443	-0.418216	0.418216
12	-0.000000	-0.000000	-0.000000	-0.000000	0.000000	-0.000000
13	0.097942	0.097942	-0.236452	0.236452	-0.157992	-0.157992
14	0.000000	-0.000000	0.000000	-0.000000	0.000000	0.000000
15	-0.084883	0.084883	-0.035160	-0.035160	0.006994	-0.006994
16	-0.000000	-0.000000	0.000000	-0.000000	0.000000	0.000000
17	0.074896	0.074896	0.031023	-0.031023	-0.006171	-0.006171
18	0.000000	-0.000000	0.000000	0.000000	0.000000	0.000000
19	-0.067013	0.067013	0.161783	0.161783	0.108100	-0.108100
20	-0.000000	-0.000000	-0.000000	-0.000000	0.000000	0.000000
21	0.060630	0.060630	-0.146375	0.146375	0.219065	0.219066
22	0.000000	-0.000000	0.000000	-0.000000	-0.000000	-0.000000
23	-0.055358	0.055358	-0.022930	-0.022930	-0.115278	0.115278
24	-0.000000	-0.000000	0.000000	-0.000000	0.000000	-0.000000
25	0.050930	0.050930	0.021096	-0.021096	0.106055	0.106055
26	0.000000	-0.000000	0.000000	0.000000	-0.000000	-0.000000
27	-0.047157	0.047157	0.113847	0.113847	-0.170384	0.170384
28	-0.000000	-0.000000	-0.000000	-0.000000	0.000000	-0.000000
29	0.043905	0.043905	-0.105996	0.105996	-0.070824	-0.070824
30	0.000000	-0.000000	0.000000	-0.000000	0.000000	0.000000
31	-0.041072	0.041072	-0.017013	-0.017013	0.003384	-0.003384
32	-0.000000	-0.000000	0.000000	-0.000000	0.000000	0.000000
33	0.038583	0.038583	0.015982	-0.015982	-0.003179	-0.003179
34	0.000000	-0.000000	0.000000	0.000000	0.000000	0.000000
35	-0.036378	0.036378	0.087825	0.087825	0.058683	-0.058683
36	-0.000000	-0.000000	-0.000000	-0.000000	0.000000	0.000000
37	0.034412	0.034412	-0.083078	0.083078	0.124334	0.124334
38	0.000000	-0.000000	0.000000	-0.000000	-0.000000	-0.000000
39	-0.032647	0.032647	-0.013523	-0.013523	-0.067984	0.067984
40	-0.000000	-0.000000	0.000000	-0.000000	0.000000	-0.000000
41	0.031055	0.031055	0.012863	-0.012863	0.064668	0.064668
42	0.000000	-0.000000	0.000000	0.000000	-0.000000	-0.000000
43	-0.029610	0.029610	0.071485	0.071485	-0.106985	0.106985
44	-0.000000	-0.000000	-0.000000	-0.000000	0.000000	-0.000000
45	0.028294	0.028294	-0.068308	0.068308	-0.045642	-0.045642
46	0.000000	-0.000000	0.000000	-0.000000	0.000000	0.000000
47	-0.027090	0.027090	-0.011221	-0.011221	0.002232	-0.002232
48	-0.000000	-0.000000	0.000000	-0.000000	0.000000	0.000000
49	0.025984	0.025984	0.010763	-0.010763	-0.002141	-0.002141
50	0.000000	-0.000000	0.000000	0.000000	0.000000	0.000000

Table B-11. (continued) Fourier Coefficients of Walsh Functions

N	ANC7	BNS7	ANC9	BNS9	ANC11	BNS11
1	0.253263	-0.253263	-0.024944	-0.024944	-0.010332	0.010332
2	0.000000	0.000000	0.000000	0.000000	0.000000	-0.000000
3	0.283584	0.283584	0.086024	-0.086024	-0.207681	-0.207681
4	0.000000	0.000000	0.000000	0.000000	0.000000	0.000000
5	0.381108	-0.381108	-0.203706	-0.203706	0.491790	-0.491790
6	0.000000	0.000000	0.000000	0.000000	0.000000	0.000000
7	0.914430	0.914430	0.750453	-0.750453	0.310848	0.310848
8	-0.000000	-0.000000	0.000000	0.000000	0.000000	0.000000
9	-0.711223	0.711223	0.866628	0.866628	0.358969	-0.358969
10	0.000000	-0.000000	-0.000000	-0.000000	0.000000	0.000000
11	-0.173231	-0.173231	-0.324092	0.324092	0.782427	0.782427
12	0.000000	0.000000	0.000000	-0.000000	-0.000000	-0.000000
13	-0.065442	0.065442	0.215735	0.215735	-0.520830	0.520830
14	0.000000	-0.000000	-0.000000	-0.000000	0.000000	-0.000000
15	-0.016884	-0.016884	-0.171428	0.171428	-0.071008	-0.071008
16	0.000000	0.000000	0.000000	-0.000000	0.000000	0.000000
17	0.014898	-0.014898	0.151260	0.151260	0.062654	-0.062654
18	0.000000	0.000000	-0.000000	-0.000000	0.000000	0.000000
19	0.044776	0.044776	-0.147608	0.147608	0.356357	0.356357
20	0.000000	0.000000	0.000000	-0.000000	-0.000000	-0.000000
21	0.090740	-0.090740	0.169762	0.169762	-0.409843	0.409843
22	0.000000	0.000000	-0.000000	-0.000000	0.000000	-0.000000
23	0.278305	0.278305	-0.339115	0.339115	-0.140466	-0.140466
24	-0.000000	-0.000000	0.000000	-0.000000	0.000000	0.000000
25	-0.256040	0.256040	-0.210127	-0.210127	-0.087037	0.087037
26	0.000000	-0.000000	0.000000	0.000000	0.000000	-0.000000
27	-0.070575	-0.070575	0.037723	-0.037723	-0.091072	-0.091072
28	0.000000	0.000000	0.000000	0.000000	0.000000	0.000000
29	-0.029336	0.029336	-0.008899	-0.008899	0.021484	-0.021484
30	0.000000	-0.000000	0.000000	0.000000	0.000000	0.000000
31	-0.008170	-0.008170	0.000805	-0.000805	0.000333	0.000333
32	0.000000	0.000000	0.000000	0.000000	0.000000	0.000000
33	0.007675	-0.007675	-0.000756	-0.000756	-0.000313	0.000313
34	0.000000	0.000000	0.000000	0.000000	0.000000	-0.000000
35	0.024307	0.024307	0.007374	-0.007374	-0.017801	-0.017801
36	0.000000	0.000000	0.000000	0.000000	0.000000	0.000000
37	0.051501	-0.051501	-0.027528	-0.027528	0.066458	-0.066458
38	0.000000	0.000000	0.000000	0.000000	0.000000	0.000000
39	0.164128	0.164128	0.134697	-0.134697	0.055793	0.055793
40	-0.000000	-0.000000	0.000000	0.000000	0.000000	0.000000
41	-0.156122	0.156122	0.190235	0.190235	0.078798	-0.078798
42	0.000000	-0.000000	-0.000000	-0.000000	0.000000	0.000000
43	-0.044315	-0.044315	-0.082907	0.082907	0.200156	0.200156
44	0.000000	0.000000	0.000000	-0.000000	-0.000000	-0.000000
45	-0.018906	0.018906	0.062323	0.062323	-0.150462	0.150462
46	0.000000	-0.000000	-0.000000	-0.000000	0.000000	-0.000000
47	-0.005389	-0.005389	-0.054711	0.054711	-0.022662	-0.022662
48	0.000000	0.000000	0.000000	-0.000000	0.000000	0.000000
49	0.005169	-0.005169	0.052478	0.052478	0.021737	-0.021737
50	0.000000	0.000000	-0.000000	-0.000000	0.000000	0.000000

Table B-11. (continued) Fourier Coefficients of Walsh Functions

N	ANC13	BNS13	ANC15	BNS15	ANC17	BNS17
1	-0.051944	-0.051944	0.125403	-0.125403	-0.006161	-0.006161
2	0.000000	0.000000	0.000000	0.000000	0.000000	0.000000
3	0.310816	-0.310816	0.128744	0.128744	0.019097	-0.019097
4	0.000000	0.000000	0.000000	0.000000	0.000000	0.000000
5	0.328604	0.328604	0.136112	-0.136112	-0.034094	-0.034094
6	-0.000000	0.000000	0.000000	0.000000	0.000000	0.000000
7	-0.061831	0.061831	0.149274	0.149274	0.053411	-0.053411
8	0.000000	0.000000	0.000000	0.000000	0.000000	0.000000
9	-0.071403	-0.071403	0.172383	-0.172383	-0.081531	-0.081531
10	0.000000	0.000000	0.000000	0.000000	0.000000	0.000000
11	0.522801	-0.522801	0.216551	0.216551	0.129796	-0.129796
12	0.000000	0.000000	0.000000	0.000000	0.000000	0.000000
13	0.779477	0.779477	0.322870	-0.322870	-0.239457	-0.239457
14	-0.000000	-0.000000	0.000000	0.000000	0.000000	0.000000
15	-0.356981	0.356981	0.861828	0.861828	0.781115	-0.781115
16	0.000000	-0.000000	-0.000000	-0.000000	0.000000	0.000000
17	0.314983	0.314983	-0.760436	0.760436	0.839012	0.839012
18	-0.000000	-0.000000	0.000000	-0.000000	-0.000000	-0.000000
19	-0.533326	0.533326	-0.220911	-0.220911	-0.297864	0.297864
20	0.000000	-0.000000	0.000000	0.000000	0.000000	-0.000000
21	-0.273848	-0.273848	-0.113432	0.113432	0.189249	0.189249
22	0.000000	0.000000	0.000000	-0.000000	-0.000000	-0.000000
23	0.027940	-0.027940	-0.067454	-0.067454	-0.142620	0.142620
24	0.000000	0.000000	0.000000	0.000000	0.000000	-0.000000
25	0.017313	0.017313	-0.041797	0.041797	0.116814	0.116814
26	-0.000000	0.000000	0.000000	-0.000000	-0.000000	-0.000000
27	-0.060853	0.060853	-0.025206	-0.025206	-0.100628	0.100628
28	0.000000	-0.000000	0.000000	0.000000	0.000000	-0.000000
29	-0.032153	-0.032153	-0.013318	0.013318	0.089785	0.089785
30	0.000000	0.000000	0.000000	-0.000000	-0.000000	-0.000000
31	0.001676	-0.001676	-0.004045	-0.004045	-0.082343	0.082343
32	0.000000	0.000000	0.000000	0.000000	0.000000	-0.000000
33	-0.001574	-0.001574	0.003800	-0.003800	0.077353	0.077353
34	0.000000	0.000000	0.000000	0.000000	-0.000000	-0.000000
35	0.026641	-0.026641	0.011035	0.011035	-0.074393	0.074393
36	0.000000	0.000000	0.000000	0.000000	0.000000	-0.000000
37	0.044406	0.044406	0.018394	-0.018394	0.073431	0.073431
38	-0.000000	0.000000	0.000000	0.000000	-0.000000	-0.000000
39	-0.011098	0.011098	0.026793	0.026793	-0.074881	0.074881
40	0.000000	0.000000	0.000000	0.000000	0.000000	-0.000000
41	-0.015674	-0.015674	0.037840	-0.037840	0.080006	0.080006
42	0.000000	0.000000	0.000000	0.000000	-0.000000	-0.000000
43	0.133740	-0.133740	0.055397	0.055397	-0.092424	0.092424
44	0.000000	0.000000	0.000000	0.000000	0.000000	-0.000000
45	0.225182	0.225182	0.093274	-0.093273	0.125765	0.125765
46	-0.000000	-0.000000	0.000000	0.000000	-0.000000	-0.000000
47	-0.113930	0.113930	0.275051	0.275051	-0.303473	0.303472
48	0.000000	-0.000000	-0.000000	-0.000000	0.000000	-0.000000
49	0.109280	0.109280	-0.263825	0.263825	-0.239117	-0.239117
50	-0.000000	-0.000000	0.000000	-0.000000	0.000000	0.000000

Table B-11. (continued) Fourier Coefficients of Walsh Functions

N	ANC19	BNS19	ANC21	BNS21	ANC23	BNS23
1	-0.002552	0.002552	0.000508	0.000508	-0.001225	0.001225
2	0.000000	-0.000000	0.000000	0.000000	0.000000	-0.000000
3	-0.046105	-0.046105	-0.030807	0.030807	-0.012760	-0.012760
4	0.000000	0.000000	0.000000	-0.000000	0.000000	0.000000
5	0.082311	-0.082311	-0.123187	-0.123187	-0.051026	0.051026
6	0.000000	0.000000	0.000000	0.000000	0.000000	-0.000000
7	0.022124	0.022124	0.111223	-0.111223	-0.268516	-0.268516
8	0.000000	0.000000	0.000000	0.000000	0.000000	0.000000
9	-0.033771	0.033771	-0.169780	-0.169780	0.409884	-0.409884
10	0.000000	-0.000000	0.000000	0.000000	0.000000	0.000000
11	-0.313355	-0.313355	0.468969	-0.468969	0.194253	0.194253
12	0.000000	0.000000	0.000000	0.000000	0.000000	0.000000
13	0.578099	-0.578099	0.386274	0.386274	0.160000	-0.160000
14	0.000000	0.000000	-0.000000	-0.000000	0.000000	0.000000
15	0.323549	0.323549	-0.064358	0.064358	0.155373	0.155374
16	0.000000	0.000000	0.000000	0.000000	0.000000	0.000000
17	0.347530	-0.347530	-0.069128	-0.069128	0.166890	-0.166890
18	0.000000	0.000000	0.000000	0.000000	0.000000	0.000000
19	0.719107	0.719107	0.480492	-0.480492	0.199026	0.199026
20	-0.000000	-0.000000	0.000000	0.000000	0.000000	0.000000
21	-0.456888	0.456888	0.683781	0.683781	0.283231	-0.283231
22	0.000000	-0.000000	-0.000000	-0.000000	0.000000	0.000000
23	-0.059075	-0.059075	-0.296991	0.296991	0.716999	0.716999
24	0.000000	0.000000	0.000000	-0.000000	-0.000000	-0.000000
25	0.048386	-0.048386	0.243253	0.243253	-0.587265	0.587265
26	0.000000	0.000000	-0.000000	-0.000000	0.000000	-0.000000
27	0.242937	0.242937	-0.363581	0.363581	-0.150600	-0.150600
28	-0.000000	-0.000000	0.000000	-0.000000	0.000000	0.000000
29	-0.216761	0.216761	-0.144835	-0.144835	-0.059993	0.059993
30	0.000000	-0.000000	0.000000	0.000000	0.000000	-0.000000
31	-0.034108	-0.034108	0.006784	-0.006784	-0.016379	-0.016379
32	0.000000	0.000000	0.000000	0.000000	0.000000	0.000000
33	0.032041	-0.032041	-0.006373	-0.006373	0.015386	-0.015386
34	0.000000	0.000000	0.000000	0.000000	0.000000	0.000000
35	0.179602	0.179602	0.120006	-0.120006	0.049708	0.049708
36	-0.000000	-0.000000	0.000000	0.000000	0.000000	0.000000
37	-0.177278	0.177278	0.265316	0.265316	0.109897	-0.109897
38	0.000000	-0.000000	-0.000000	-0.000000	0.000000	0.000000
39	-0.031017	-0.031017	-0.155932	0.155932	0.376452	0.376452
40	0.000000	0.000000	0.000000	-0.000000	-0.000000	-0.000000
41	0.033140	-0.033140	0.166604	0.166605	-0.402219	0.402219
42	0.000000	0.000000	-0.000000	-0.000000	0.000000	-0.000000
43	0.223131	0.223131	-0.333940	0.333940	-0.138322	-0.138322
44	-0.000000	-0.000000	0.000000	-0.000000	0.000000	0.000000
45	-0.303623	0.303623	-0.202874	-0.202875	-0.084033	0.084033
46	0.000000	-0.000000	0.000000	0.000000	0.000000	-0.000000
47	-0.125702	-0.125702	0.025004	-0.025004	-0.060364	-0.060364
48	0.000000	0.000000	0.000000	0.000000	0.000000	0.000000
49	-0.099045	0.099045	0.019701	0.019701	-0.047563	0.047563
50	0.000000	-0.000000	-0.000000	-0.000000	0.000000	-0.000000

Table B-11. (continued) Fourier Coefficients of Walsh Functions

N	ANC25	BNS25	ANC27	BNS27	ANC29	BNS29
1	-0.012442	-0.012442	-0.005154	0.005154	-0.025909	-0.025909
2	0.000000	0.000000	0.000000	-0.000000	0.000000	0.000000
3	0.042066	-0.042066	-0.101555	-0.101556	0.151989	-0.151989
4	0.000000	0.000000	0.000000	0.000000	0.000000	0.000000
5	-0.095462	-0.095462	0.230467	-0.230467	0.153993	0.153993
6	0.000000	0.000000	0.000000	0.000000	0.000000	0.000000
7	0.327188	-0.327188	0.135526	0.135526	-0.026958	0.026958
8	0.000000	0.000000	0.000000	0.000000	0.000000	0.000000
9	0.336383	0.336383	0.139335	-0.139335	-0.027715	-0.027715
10	-0.000000	-0.000000	0.000000	0.000000	0.000000	0.000000
11	-0.103830	0.103830	0.250669	0.250669	0.167492	-0.167492
12	0.000000	0.000000	-0.000000	-0.000000	0.000000	0.000000
13	0.048535	0.048535	-0.117175	0.117175	0.175365	0.175365
14	0.000000	0.000000	0.000000	-0.000000	-0.000000	0.000000
15	-0.015303	0.015303	-0.006339	-0.006339	-0.031867	0.031867
16	0.000000	0.000000	0.000000	0.000000	0.000000	0.000000
17	-0.016437	-0.016437	-0.006809	0.006809	-0.034229	-0.034229
18	0.000000	0.000000	0.000000	-0.000000	0.000000	0.000000
19	0.060374	-0.060374	-0.145756	-0.145756	0.218139	-0.218139
20	0.000000	0.000000	0.000000	0.000000	0.000000	0.000000
21	-0.151390	-0.151390	0.365489	-0.365489	0.244212	0.244212
22	0.000000	0.000000	0.000000	0.000000	-0.000000	-0.000000
23	0.588426	-0.588426	0.243734	0.243734	-0.048482	0.048482
24	0.000000	0.000000	0.000000	0.000000	0.000000	0.000000
25	0.715585	0.715585	0.296405	-0.296405	-0.058959	-0.058959
26	-0.000000	-0.000000	0.000000	0.000000	0.000000	0.000000
27	-0.281753	0.281753	0.680212	0.680212	0.454503	-0.454503
28	0.000000	-0.000000	-0.000000	-0.000000	0.000000	0.000000
29	0.197769	0.197769	-0.477457	0.477457	0.714564	0.714564
30	-0.000000	-0.000000	0.000000	-0.000000	-0.000000	-0.000000
31	-0.166300	0.166300	-0.068884	-0.068884	-0.346301	0.346301
32	0.000000	-0.000000	0.000000	0.000000	0.000000	-0.000000
33	0.156221	0.156221	0.064709	-0.064709	0.325313	0.325313
34	-0.000000	-0.000000	0.000000	0.000000	-0.000000	-0.000000
35	-0.163866	0.163866	0.395607	0.395607	-0.592068	0.592067
36	0.000000	-0.000000	-0.000000	-0.000000	0.000000	-0.000000
37	0.205604	0.205604	-0.496371	0.496371	-0.331664	-0.331665
38	-0.000000	-0.000000	0.000000	-0.000000	0.000000	0.000000
39	-0.458708	0.458708	-0.190003	-0.190003	0.037794	-0.037794
40	0.000000	-0.000000	0.000000	0.000000	0.000000	0.000000
41	-0.330092	-0.330093	-0.136729	0.136729	0.027197	0.027197
42	0.000000	0.000000	0.000000	-0.000000	-0.000000	-0.000000
43	0.073935	-0.073935	-0.178494	-0.178494	-0.119266	0.119266
44	0.000000	0.000000	0.000000	0.000000	0.000000	-0.000000
45	-0.025491	-0.025491	0.061541	-0.061541	-0.092103	-0.092103
46	0.000000	0.000000	0.000000	0.000000	0.000000	0.000000
47	0.005945	-0.005945	0.002463	0.002463	0.012381	-0.012381
48	0.000000	0.000000	0.000000	0.000000	0.000000	0.000000
49	0.004685	0.004685	0.001940	-0.001940	0.009755	0.009755
50	0.000000	0.000000	0.000000	0.000000	-0.000000	0.000000

Table B-11. (continued) Fourier Coefficients of Walsh Functions

N	ANC31	BNS31	ANC33	BNS33
1	0.062550	-0.062550	-0.001535	-0.001535
2	0.000000	0.000000	0.000000	0.000000
3	0.062956	0.062956	0.004644	-0.004644
4	0.000000	0.000000	0.000000	0.000000
5	0.063786	-0.063786	-0.007867	-0.007867
6	0.000000	0.000000	0.000000	0.000000
7	0.065082	0.065082	0.011293	-0.011293
8	0.000000	0.000000	0.000000	0.000000
9	0.066911	-0.066911	-0.015025	-0.015025
10	0.000000	0.000000	0.000000	0.000000
11	0.069377	0.069377	0.019199	-0.019199
12	0.000000	0.000000	0.000000	0.000000
13	0.072638	-0.072638	-0.023996	-0.023996
14	0.000000	0.000000	0.000000	0.000000
15	0.076933	0.076933	0.029676	-0.029676
16	0.000000	0.000000	0.000000	0.000000
17	0.082635	-0.082635	-0.036630	-0.036630
18	0.000000	0.000000	0.000000	0.000000
19	0.090356	0.090356	0.045481	-0.045481
20	0.000000	0.000000	0.000000	0.000000
21	0.101156	-0.101156	-0.057304	-0.057304
22	0.000000	0.000000	0.000000	0.000000
23	0.117045	0.117045	0.074118	-0.074118
24	0.000000	0.000000	0.000000	0.000000
25	0.142339	-0.142339	-0.100246	-0.100246
26	0.000000	0.000000	0.000000	0.000000
27	0.188261	0.188261	0.146921	-0.146921
28	0.000000	0.000000	0.000000	0.000000
29	0.295982	-0.295982	-0.255316	-0.255316
30	0.000000	0.000000	0.000000	0.000000
31	0.836045	0.836045	0.795981	-0.795981
32	-0.000000	-0.000000	0.000000	0.000000
33	-0.785375	0.785375	0.824906	0.824906
34	0.000000	-0.000000	-0.000000	-0.000000
35	-0.245242	-0.245243	-0.284304	0.284304
36	0.000000	0.000000	0.000000	-0.000000
37	-0.137380	0.137380	0.176036	0.176036
38	0.000000	-0.000000	-0.000000	-0.000000
39	-0.091243	-0.091243	-0.129555	0.129555
40	0.000000	0.000000	0.000000	-0.000000
41	-0.065659	0.065659	0.103688	0.103688
42	0.000000	-0.000000	-0.000000	-0.000000
43	-0.049402	-0.049402	-0.087206	0.087206
44	0.000000	0.000000	0.000000	-0.000000
45	-0.038150	0.038150	0.075792	0.075792
46	0.000000	-0.000000	-0.000000	-0.000000
47	-0.029889	-0.029889	-0.067429	0.067429
48	0.000000	0.000000	0.000000	-0.000000
49	-0.023551	0.023551	0.061054	0.061054
50	0.000000	-0.000000	-0.000000	-0.000000

Table B-III. Fourier Series of Walsh Functions

$$
\begin{aligned}
cal(1,\theta) = {} & 1.27324\cos\theta - .42441\cos 3\theta + .25465\cos 5\theta \\
& -.18189\cos 7\theta + .14147\cos 9\theta - .11575\cos 11\theta \\
& +.09794\cos 13\theta - .08488\cos 15\theta + .07490\cos 17\theta \\
& -.06701\cos 19\theta + .06063\cos 21\theta - .05536\cos 23\theta \\
& +.05093\cos 25\theta - .04716\cos 27\theta + .04391\cos 29\theta \\
& -.04107\cos 31\theta - \cdots
\end{aligned}
$$

$$
\begin{aligned}
cal(2,\theta) = {} & 1.27324\cos 2\theta - .42441\cos 6\theta + .25465\cos 10\theta \\
& -.18189\cos 14\theta + .14147\cos 18\theta - .11575\cos 22\theta \\
& +.09794\cos 26\theta - .08488\cos 30\theta - \cdots
\end{aligned}
$$

$$
\begin{aligned}
cal(3,\theta) = {} & .52739\cos\theta + 1.02462\cos 3\theta - .61477\cos 5\theta \\
& -.07534\cos 7\theta + .05860\cos 9\theta + .27944\cos 11\theta \\
& -.23645\cos 13\theta - .03516\cos 15\theta + .03102\cos 17\theta \\
& +.16178\cos 19\theta - .14638\cos 21\theta - .02293\cos 23\theta \\
& +.02110\cos 25\theta + .11385\cos 27\theta - .10600\cos 29\theta \\
& -.01701\cos 31\theta - \cdots
\end{aligned}
$$

$$
\begin{aligned}
cal(4,\theta) = {} & 1.27324\cos 4\theta - .42441\cos 12\theta + .25465\cos 20\theta \\
& -.18189\cos 28\theta + \cdots
\end{aligned}
$$

$$
\begin{aligned}
cal(5,\theta) = {} & -.10491\cos\theta + .68463\cos 3\theta + .92008\cos 5\theta \\
& -.37877\cos 7\theta + .29460\cos 9\theta - .41822\cos 11\theta \\
& -.15799\cos 13\theta + .00699\cos 15\theta - .00617\cos 17\theta \\
& +.10810\cos 19\theta + .21907\cos 21\theta - .11528\cos 23\theta \\
& +.10606\cos 25\theta - .17038\cos 27\theta - .07082\cos 29\theta \\
& +.00338\cos 31\theta - \cdots
\end{aligned}
$$

$$
\begin{aligned}
cal(6,\theta) = {} & .52739\cos 2\theta + 1.02462\cos 6\theta - .61477\cos 10\theta \\
& -.07534\cos 14\theta + .05860\cos 18\theta + .27944\cos 22\theta \\
& -.23645\cos 26\theta - .03516\cos 30\theta + \cdots
\end{aligned}
$$

$$
\begin{aligned}
cal(7,\theta) = {} & .25326\cos\theta + .28358\cos 3\theta + .38111\cos 5\theta \\
& +.91443\cos 7\theta - .71122\cos 9\theta - .17323\cos 11\theta \\
& -.06544\cos 13\theta - .01688\cos 15\theta + .01490\cos 17\theta \\
& +.04478\cos 19\theta + .09074\cos 21\theta + .27831\cos 23\theta \\
& -.25604\cos 25\theta - .07058\cos 27\theta - .02934\cos 29\theta \\
& -.00817\cos 31\theta - \cdots
\end{aligned}
$$

$$
\begin{aligned}
cal(8,\theta) = {} & 1.27324\cos 8\theta - .42441\cos 24\theta + \cdots
\end{aligned}
$$

$$
\begin{aligned}
cal(9,\theta) = {} & -.02494\cos\theta + .08602\cos 3\theta - .20371\cos 5\theta \\
& +.75045\cos 7\theta + .86663\cos 9\theta - .32409\cos 11\theta \\
& +.21574\cos 13\theta - .17143\cos 15\theta + .15126\cos 17\theta \\
& -.14761\cos 19\theta + .16976\cos 21\theta - .33912\cos 23\theta \\
& -.21013\cos 25\theta + .03772\cos 27\theta - .00890\cos 29\theta \\
& +.00081\cos 31\theta - \cdots
\end{aligned}
$$

Table B-III. (cont'd) Fourier Series of Walsh Functions

$$cal(10,\theta) = -.10491\cos 2\theta + .68463\cos 6\theta + .92008\cos 10\theta - .37877\cos 14\theta + .29460\cos 18\theta - .41822\cos 22\theta - .15799\cos 26\theta + .00699\cos 30\theta - \cdots$$

$$cal(11,\theta) = -.01033\cos \theta - .20768\cos 3\theta + .49179\cos 5\theta + .31085\cos 7\theta + .35897\cos 9\theta + .78243\cos 11\theta - .52083\cos 13\theta - .07101\cos 15\theta + .06265\cos 17\theta + .35638\cos 19\theta - .40984\cos 21\theta - .14047\cos 23\theta - .08704\cos 25\theta - .09107\cos 27\theta + .02148\cos 29\theta + .00033\cos 31\theta - \cdots$$

$$cal(12,\theta) = .52739\cos 4\theta + 1.02462\cos 12\theta - .61477\cos 20\theta - .07534\cos 28\theta + \cdots$$

$$cal(13,\theta) = -.05194\cos \theta + .31082\cos 3\theta + .32860\cos 5\theta - .06183\cos 7\theta - .07140\cos 9\theta + .52280\cos 11\theta + .77948\cos 13\theta - .35698\cos 15\theta + .31498\cos 17\theta - .53333\cos 19\theta - .27385\cos 21\theta + .02794\cos 23\theta + .01731\cos 25\theta - .06085\cos 27\theta - .03215\cos 29\theta + .00168\cos 31\theta - \cdots$$

$$cal(14,\theta) = .25326\cos 2\theta + .28358\cos 6\theta + .38111\cos 10\theta + .91443\cos 14\theta - .71122\cos 18\theta - .17323\cos 22\theta - .06544\cos 26\theta - .01688\cos 30\theta + \cdots$$

$$cal(15,\theta) = .12540\cos \theta + .12874\cos 3\theta + .13611\cos 5\theta + .14927\cos 7\theta + .17238\cos 9\theta + .21655\cos 11\theta + .32287\cos 13\theta + .86183\cos 15\theta - .76044\cos 17\theta - .22091\cos 19\theta - .11343\cos 21\theta - .06745\cos 23\theta - .04180\cos 25\theta - .02521\cos 27\theta - .01332\cos 29\theta - .00405\cos 31\theta - \cdots$$

$$cal(16,\theta) = 1.27324\cos 16\theta - \cdots$$

$$cal(17,\theta) = -.00616\cos \theta + .01910\cos 3\theta - .03409\cos 5\theta + .05341\cos 7\theta - .08153\cos 9\theta + .12980\cos 11\theta - .23948\cos 13\theta + .78112\cos 15\theta + .83901\cos 17\theta - .29786\cos 19\theta + .18925\cos 21\theta - .14262\cos 23\theta + .11681\cos 25\theta - .10063\cos 27\theta + .08979\cos 29\theta - .08234\cos 31\theta - \cdots$$

$$cal(18,\theta) = -.02494\cos 2\theta + .08602\cos 6\theta - .20371\cos 10\theta + .75045\cos 14\theta + .86663\cos 18\theta - .32409\cos 22\theta + .21574\cos 26\theta - .17143\cos 30\theta - \cdots$$

$$cal(19,\theta) = -.00255\cos \theta - .04611\cos 3\theta + .08231\cos 5\theta + .02212\cos 7\theta - .03377\cos 9\theta - .31336\cos 11\theta + .57810\cos 13\theta + .32355\cos 15\theta + .34753\cos 17\theta + .71911\cos 19\theta - .45689\cos 21\theta - .05908\cos 23\theta + .04839\cos 25\theta + .24294\cos 27\theta - .21676\cos 29\theta - .03411\cos 31\theta - \cdots$$

Table B-III. (cont'd) Fourier Series of Walsh Functions

$$cal(20,\theta) = -.10491 \cos 4\theta + .68463 \cos 12\theta + .92008 \cos 20\theta - .37877 \cos 28\theta + \text{-----}$$

$$cal(21,\theta) = .00051 \cos \theta - .03081 \cos 3\theta - .12319 \cos 5\theta + .11122 \cos 7\theta - .16978 \cos 9\theta + .46897 \cos 11\theta + .38627 \cos 13\theta - .06436 \cos 15\theta - .06913 \cos 17\theta + .48049 \cos 19\theta + .68378 \cos 21\theta - .29699 \cos 23\theta + .24325 \cos 25\theta - .36358 \cos 27\theta - .14484 \cos 29\theta + .00678 \cos 31\theta \text{-----}$$

$$cal(22,\theta) = -.01033 \cos 2\theta - .20768 \cos 6\theta + .49179 \cos 10\theta + .31085 \cos 14\theta + .35897 \cos 18\theta + .78243 \cos 22\theta - .52083 \cos 26\theta - .07101 \cos 30\theta + \text{----}$$

$$cal(23,\theta) = -.00123 \cos \theta - .01276 \cos 3\theta - .05103 \cos 5\theta - .26852 \cos 7\theta + .40988 \cos 9\theta + .19425 \cos 11\theta + .16000 \cos 13\theta + .15537 \cos 15\theta + .16689 \cos 17\theta + .19903 \cos 19\theta + .28323 \cos 21\theta + .71700 \cos 23\theta - .58727 \cos 25\theta - .15060 \cos 27\theta - .05999 \cos 29\theta - .01638 \cos 31\theta \text{-----}$$

$$cal(24,\theta) = .52739 \cos 8\theta + 1.02462 \cos 24\theta - \text{---}$$

$$cal(25,\theta) = -.01244 \cos \theta + .04207 \cos 3\theta - .09546 \cos 5\theta + .32719 \cos 7\theta + .33638 \cos 9\theta - .10383 \cos 11\theta + .04854 \cos 13\theta - .01530 \cos 15\theta - .01644 \cos 17\theta + .06037 \cos 19\theta - .15139 \cos 21\theta + .55843 \cos 23\theta + .71559 \cos 25\theta - .28175 \cos 27\theta + .19777 \cos 29\theta - .16630 \cos 31\theta + \text{-----}$$

$$cal(26,\theta) = -.05194 \cos 2\theta + .31082 \cos 6\theta + .32860 \cos 10\theta - .06183 \cos 14\theta - .07140 \cos 18\theta + .52280 \cos 22\theta + .77948 \cos 26\theta - .35698 \cos 30\theta + \text{-----}$$

$$cal(27,\theta) = -.00515 \cos \theta - .10156 \cos 3\theta + .23047 \cos 5\theta + .13553 \cos 7\theta + .13934 \cos 9\theta + .25067 \cos 11\theta - .11718 \cos 13\theta - .00634 \cos 15\theta - .00681 \cos 17\theta - .14576 \cos 19\theta + .36549 \cos 21\theta + .24373 \cos 23\theta + .29641 \cos 25\theta + .68021 \cos 27\theta - .47748 \cos 29\theta - .06888 \cos 31\theta \text{-----}$$

$$cal(28,\theta) = .25326 \cos 4\theta + .28358 \cos 12\theta + .38111 \cos 20\theta + .91443 \cos 28\theta \text{-----}$$

$$cal(29,\theta) = -.02591 \cos \theta + .15199 \cos 3\theta + .15399 \cos 5\theta - .02696 \cos 7\theta - .02772 \cos 9\theta + .16749 \cos 11\theta + .17537 \cos 13\theta - .03187 \cos 15\theta - .03423 \cos 17\theta + .21814 \cos 19\theta + .24421 \cos 21\theta - .04848 \cos 23\theta - .05896 \cos 25\theta + .45450 \cos 27\theta + .71456 \cos 29\theta - .34630 \cos 31\theta \text{-----}$$

Table B-III. (cont'd) Fourier Series of Walsh Functions

$$cal(30,\theta) = .12540\cos 2\theta + .12874\cos 6\theta + .13611\cos 10\theta + .14927\cos 14\theta + .17238\cos 18\theta + .21655\cos 22\theta + .32287\cos 26\theta + .86183\cos 30\theta - \cdots$$

$$cal(31,\theta) = .06255\cos \theta + .06296\cos 3\theta + .06379\cos 5\theta + .06508\cos 7\theta + .06691\cos 9\theta + .06938\cos 11\theta + .07264\cos 13\theta + .07693\cos 15\theta + .08264\cos 17\theta + .09036\cos 19\theta + .10116\cos 21\theta + .11705\cos 23\theta + .14234\cos 25\theta + .18826\cos 27\theta + .29598\cos 29\theta + .83605\cos 31\theta - \cdots$$

$$cal(32,\theta) = 1.27324\cos 32\theta - \cdots$$

$$sal(1,\theta) = 1.27324\sin \theta + .42441\sin 3\theta + .25465\sin 5\theta + .18189\sin 7\theta + .14147\sin 9\theta + .11575\sin 11\theta + .09794\sin 13\theta + .08488\sin 15\theta + .07490\sin 17\theta + .06701\sin 19\theta + .06063\sin 21\theta + .05536\sin 23\theta + .05093\sin 25\theta + .04716\sin 27\theta + .04391\sin 29\theta + .04107\sin 31\theta + \cdots$$

$$sal(2,\theta) = 1.27324\sin 2\theta + .42441\sin 6\theta + .25465\sin 10\theta + .18189\sin 14\theta + .14147\sin 18\theta + .11575\sin 22\theta + .09794\sin 26\theta + .08488\sin 30\theta + \cdots$$

$$sal(3,\theta) = -.52739\sin \theta + 1.02462\sin 3\theta - .61477\sin 5\theta - .07534\sin 7\theta - .05860\sin 9\theta + .27944\sin 11\theta + .23645\sin 13\theta - .03516\sin 15\theta - .03102\sin 17\theta + .16178\sin 19\theta + .14638\sin 21\theta - .02293\sin 23\theta - .02110\sin 25\theta + .11385\sin 27\theta + .10600\sin 29\theta - .01701\sin 31\theta - \cdots$$

$$sal(4,\theta) = 1.27324\sin 4\theta + .42441\sin 12\theta + .25465\sin 20\theta + .18189\sin 28\theta + \cdots$$

$$sal(5,\theta) = -.10491\sin \theta - .68463\sin 3\theta + .92008\sin 5\theta + .37877\sin 7\theta + .29460\sin 9\theta + .41822\sin 11\theta - .15799\sin 13\theta - .00699\sin 15\theta - .00617\sin 17\theta - .10810\sin 19\theta + .21907\sin 21\theta + .11528\sin 23\theta + .10606\sin 25\theta + .17038\sin 27\theta - .07082\sin 29\theta - .00338\sin 31\theta - \cdots$$

$$sal(6,\theta) = -.52739\sin 2\theta + 1.02462\sin 6\theta + .61477\sin 10\theta - .07534\sin 14\theta - .05860\sin 18\theta + .27944\sin 22\theta + .23645\sin 26\theta - .03516\sin 30\theta - \cdots$$

$$sal(7,\theta) = -.25326\sin 2\theta + .28358\sin 3\theta - .38111\sin 5\theta + .91443\sin 7\theta + .71122\sin 9\theta - .17323\sin 11\theta + .06544\sin 13\theta - .01688\sin 15\theta - .01490\sin 17\theta + .04478\sin 19\theta - .09074\sin 21\theta + .27831\sin 23\theta + .25604\sin 25\theta - .07058\sin 27\theta + .02934\sin 29\theta - .00817\sin 31\theta - \cdots$$

Table B-III. (cont'd) Fourier Series of Walsh Functions

$$sal(8,\theta) = 1.27324 \sin 8\theta + .42441 \sin 24\theta + \text{-----}$$

$$\begin{aligned} sal(9,\theta) = {} & -.02494 \sin \theta - .08602 \sin 3\theta - .20371 \sin 5\theta \\ & -.75045 \sin 7\theta + .86663 \sin 9\theta + .32409 \sin 11\theta \\ & +.21574 \sin 13\theta + .17143 \sin 15\theta + .15126 \sin 17\theta \\ & +.14761 \sin 19\theta + .16976 \sin 21\theta + .33912 \sin 23\theta \\ & -.21013 \sin 25\theta - .03772 \sin 27\theta - .00890 \sin 29\theta \\ & -.00081 \sin 31\theta - \text{-----} \end{aligned}$$

$$\begin{aligned} sal(10,\theta) = {} & -.10491 \sin 2\theta - .68463 \sin 6\theta + .92008 \sin 10\theta \\ & +.37877 \sin 14\theta + .29460 \sin 18\theta + .41822 \sin 22\theta \\ & -.15799 \sin 26\theta - .00699 \sin 30\theta - \text{-----} \end{aligned}$$

$$\begin{aligned} sal(11,\theta) = {} & .01033 \sin \theta - .20768 \sin 3\theta - .49179 \sin 5\theta \\ & +.31085 \sin 7\theta - .35897 \sin 9\theta + .78243 \sin 11\theta \\ & +.52083 \sin 13\theta - .07101 \sin 15\theta - .06265 \sin 17\theta \\ & +.35638 \sin 19\theta + .40984 \sin 21\theta - .14047 \sin 23\theta \\ & +.08704 \sin 25\theta - .09107 \sin 27\theta - .02148 \sin 29\theta \\ & +.00033 \sin 31\theta + \text{-----} \end{aligned}$$

$$\begin{aligned} sal(12,\theta) = {} & -.52739 \sin 4\theta + 1.02462 \sin 12\theta + .61477 \sin 20\theta \\ & -.07534 \sin 28\theta \end{aligned}$$

$$\begin{aligned} sal(13,\theta) = {} & -.05194 \sin \theta - .31082 \sin 3\theta + .32860 \sin 5\theta \\ & +.06183 \sin 7\theta - .07140 \sin 9\theta - .52280 \sin 11\theta \\ & +.77948 \sin 13\theta + .35698 \sin 15\theta + .31498 \sin 17\theta \\ & +.53333 \sin 19\theta - .27385 \sin 21\theta - .02794 \sin 23\theta \\ & +.01731 \sin 25\theta + .06085 \sin 27\theta - .03215 \sin 29\theta \\ & -.00168 \sin 31\theta - \text{-----} \end{aligned}$$

$$\begin{aligned} sal(14,\theta) = {} & -.25326 \sin 2\theta + .28358 \sin 6\theta - .38111 \sin 10\theta \\ & +.91443 \sin 14\theta + .71122 \sin 18\theta - .17323 \sin 22\theta \\ & +.06544 \sin 26\theta - .01688 \sin 30\theta - \text{-----} \end{aligned}$$

$$\begin{aligned} sal(15,\theta) = {} & -.12540 \sin \theta + .12874 \sin 3\theta - .13611 \sin 5\theta \\ & +.14927 \sin 7\theta - .17238 \sin 9\theta + .21655 \sin 11\theta \\ & -.32287 \sin 13\theta + .86183 \sin 15\theta + .76044 \sin 17\theta \\ & -.22091 \sin 19\theta + .11343 \sin 21\theta - .06745 \sin 23\theta \\ & +.04180 \sin 25\theta - .02521 \sin 27\theta + .01332 \sin 29\theta \\ & -.00405 \sin 31\theta - \text{-----} \end{aligned}$$

$$sal(16,\theta) = 1.27324 \sin 16\theta + \text{-----}$$

$$\begin{aligned} sal(17,\theta) = {} & -.00616 \sin \theta - .01910 \sin 3\theta - .03409 \sin 5\theta \\ & -.05341 \sin 7\theta - .08153 \sin 9\theta - .12980 \sin 11\theta \\ & -.23948 \sin 13\theta - .78112 \sin 15\theta + .83901 \sin 17\theta \\ & +.29786 \sin 19\theta + .18925 \sin 21\theta + .14262 \sin 23\theta \\ & +.11681 \sin 25\theta + .10063 \sin 27\theta + .08979 \sin 29\theta \\ & +.08234 \sin 31\theta + \text{-----} \end{aligned}$$

$$\begin{aligned} sal(18,\theta) = {} & -.02494 \sin 2\theta - .08602 \sin 6\theta - .20371 \sin 10\theta \\ & -.75045 \sin 14\theta + .86663 \sin 18\theta + .32409 \sin 22\theta \\ & +.21574 \sin 26\theta + .17143 \sin 30\theta + \text{-----} \end{aligned}$$

Table B-III. (cont'd) Fourier Series of Walsh Functions

$$sal(19,\theta) = .00255 \sin\theta - .04611 \sin 3\theta - .08231 \sin 5\theta + .02212 \sin 7\theta + .03377 \sin 9\theta - .31336 \sin 11\theta - .57810 \sin 13\theta + .32355 \sin 15\theta - .34753 \sin 17\theta + .71911 \sin 19\theta + .45689 \sin 21\theta - .05908 \sin 23\theta - .04839 \sin 25\theta + .24294 \sin 27\theta + .21676 \sin 29\theta - .03411 \sin 31\theta - \text{-----}$$

$$sal(20,\theta) = -.10491 \sin 4\theta - .68463 \sin 12\theta + .92008 \sin 20\theta + .37877 \sin 28\theta + \text{-----}$$

$$sal(21,\theta) = .00051 \sin\theta + .03081 \sin 3\theta - .12319 \sin 5\theta - .11122 \sin 7\theta - .16978 \sin 9\theta - .46897 \sin 11\theta + .38627 \sin 13\theta + .06436 \sin 15\theta - .06913 \sin 17\theta - .48049 \sin 19\theta + .68378 \sin 21\theta + .29699 \sin 23\theta + .24325 \sin 25\theta + .36358 \sin 27\theta - .14484 \sin 29\theta - .00678 \sin 31\theta - \text{-----}$$

$$sal(22,\theta) = +.01033 \sin 2\theta - .20768 \sin 6\theta - .49179 \sin 10\theta + .31085 \sin 14\theta - .35897 \sin 18\theta + .78243 \sin 22\theta + .52083 \sin 26\theta - .07101 \sin 30\theta - \text{-----}$$

$$sal(23,\theta) = .00123 \sin\theta - .01276 \sin 3\theta + .05103 \sin 5\theta - .26852 \sin 7\theta - .40988 \sin 9\theta + .19425 \sin 11\theta - .16000 \sin 13\theta + .15537 \sin 15\theta - .16689 \sin 17\theta + .19903 \sin 19\theta - .28323 \sin 21\theta + .71700 \sin 23\theta + .58727 \sin 25\theta - .15060 \sin 27\theta + .05999 \sin 29\theta - .01638 \sin 31\theta \text{-----}$$

$$sal(24,\theta) = -.52739 \sin 8\theta + 1.02462 \sin 24\theta$$

$$sal(25,\theta) = -.01244 \sin\theta - .04207 \sin 3\theta - .09546 \sin 5\theta - .32719 \sin 7\theta + .33638 \sin 9\theta + .10383 \sin 11\theta + .04854 \sin 13\theta + .01530 \sin 15\theta - .01644 \sin 17\theta - .06037 \sin 19\theta - .15139 \sin 21\theta - .55843 \sin 23\theta + .71559 \sin 25\theta + .28175 \sin 27\theta + .19777 \sin 29\theta + .16630 \sin 31\theta + \text{-----}$$

$$sal(26,\theta) = -.05194 \sin 2\theta - .31082 \sin 6\theta + .32860 \sin 10\theta + .06183 \sin 14\theta - .07140 \sin 18\theta - .52280 \sin 22\theta + .77948 \sin 26\theta + .35698 \sin 30\theta + \text{-----}$$

$$sal(27,\theta) = .00515 \sin\theta - .10156 \sin 3\theta - .23047 \sin 5\theta + .13553 \sin 7\theta - .13934 \sin 9\theta + .25067 \sin 11\theta + .11718 \sin 13\theta - .00634 \sin 15\theta + .00681 \sin 17\theta - .14576 \sin 19\theta - .36549 \sin 21\theta + .24373 \sin 23\theta - .29641 \sin 25\theta + .68021 \sin 27\theta + .47748 \sin 29\theta - .06888 \sin 31\theta \text{-----}$$

$$sal(28,\theta) = -.25326 \sin 4\theta + .28358 \sin 12\theta - .38111 \sin 20\theta + .91443 \sin 28\theta + \text{-----}$$

Table B-111. (cont'd) Fourier Series of Walsh Functions

$$
\begin{aligned}
sal(29,\theta) = {} & -.02591 \sin\theta - .15199 \sin 3\theta + .15399 \sin 5\theta \\
& +.02696 \sin 7\theta - .02772 \sin 9\theta - .16749 \sin 11\theta \\
& +.17537 \sin 13\theta + .03187 \sin 15\theta - .03423 \sin 17\theta \\
& -.21814 \sin 19\theta + .24421 \sin 21\theta + .04848 \sin 23\theta \\
& -.05896 \sin 25\theta - .45450 \sin 27\theta + .71456 \sin 29\theta \\
& +.34630 \sin 31\theta + \text{-----}
\end{aligned}
$$

$$
\begin{aligned}
sal(30,\theta) = {} & -.12540 \sin 2\theta + .12874 \sin 6\theta - .13611 \sin 10\theta \\
& +.14927 \sin 14\theta - .17238 \sin 18\theta + .21655 \sin 22\theta \\
& -.32287 \sin 26\theta + .86183 \sin 30\theta + \text{-----}
\end{aligned}
$$

$$
\begin{aligned}
sal(31,\theta) = {} & -.06255 \sin\theta + .06296 \sin 3\theta - .06379 \sin 5\theta \\
& +.06508 \sin 7\theta - .06691 \sin 9\theta + .06938 \sin 11\theta \\
& -.07264 \sin 13\theta + .07693 \sin 15\theta - .08264 \sin 17\theta \\
& +.09036 \sin 19\theta - .10116 \sin 21\theta + .11705 \sin 23\theta \\
& -.14324 \sin 25\theta + .18826 \sin 27\theta - .29598 \sin 29\theta \\
& +.83605 \sin 31\theta \text{-----}
\end{aligned}
$$

$$
sal(32,\theta) = 1.27324 \sin 32\theta + \text{-----}
$$

Table B-IV. Fourier Coefficients of f(t) for Given Walsh-Fourier Coefficients

$$a_0 = 2A_0$$

$$\begin{aligned} a_1 = {} & 1.27324\,A_1 + .52739\,A_3 - .10491\,A_5 + .25326\,A_7 \\ & -.02494\,A_9 - .01033\,A_{11} - .05194\,A_{13} + .12540\,A_{15} \\ & -.00616\,A_{17} - .00255\,A_{19} + .00051\,A_{21} - .00123\,A_{23} \\ & \pm.01244\,A_{25} - .00515\,A_{27} - .02591\,A_{29} + .06255\,A_{31} \end{aligned}$$

$$\begin{aligned} a_2 = {} & 1.27324\,A_2 + .52739\,A_6 - .10491\,A_{10} + .25326\,A_{14} \\ & \pm.02494\,A_{18} - .01033\,A_{22} - .05194\,A_{26} + .12540\,A_{30} \end{aligned}$$

$$\begin{aligned} a_3 = {} & -.42441\,A_1 + 1.02462\,A_3 + .68463\,A_5 + .28358\,A_7 \\ & +.08602\,A_9 - .20768\,A_{11} + .31082\,A_{13} + .12874\,A_{15} \\ & +.01910\,A_{17} - .04611\,A_{19} - .03081\,A_{21} - .01276\,A_{23} \\ & \pm.04207\,A_{25} - .10156\,A_{27} + .15199\,A_{29} + .06296\,A_{31} \end{aligned}$$

$$a_4 = 1.27324\,A_4 + .52739\,A_{12} - .10491\,A_{20} + .25326\,A_{28} \text{ -----}$$

$$\begin{aligned} a_5 = {} & .25465\,A_1 - .61477\,A_3 + .92008\,A_5 + .38111\,A_7 \\ & -.20371\,A_9 + .49179\,A_{11} + .32860\,A_{13} + .13611\,A_{15} \\ & -.03409\,A_{17} + .08231\,A_{19} - .12319\,A_{21} - .05103\,A_{23} \\ & -.09546\,A_{25} + .23047\,A_{27} + .15399\,A_{29} + .06379\,A_{31} \\ & \text{-----} \end{aligned}$$

$$\begin{aligned} a_6 = {} & -.42441\,A_2 + 1.02462\,A_6 + .68463\,A_{10} + .28358\,A_{14} \\ & +.08602\,A_{18} - .20768\,A_{22} + .31082\,A_{26} + .12874\,A_{30} \\ & \text{-----} \end{aligned}$$

$$\begin{aligned} a_7 = {} & -.18189\,A_1 - .07534\,A_3 - .37877\,A_5 + .91443\,A_7 \\ & +.75045\,A_9 + .31085\,A_{11} - .06183\,A_{13} + .14927\,A_{15} \\ & +.05341\,A_{17} + .02212\,A_{19} + .11122\,A_{21} - .26852\,A_{23} \\ & +.32719\,A_{25} + .13553\,A_{27} - .02696\,A_{29} + .06508\,A_{31} \\ & \text{-----} \end{aligned}$$

$$a_8 = 1.27324\,A_8 + .52739\,A_{24} \text{ -----}$$

$$\begin{aligned} a_9 = {} & .14147\,A_1 + .05860\,A_3 + .29460\,A_5 - .71122\,A_7 \\ & +.86663\,A_9 + .35897\,A_{11} - .07140\,A_{13} + .17238\,A_{15} \\ & -.08153\,A_{17} - .03377\,A_{19} - .16978\,A_{21} + .40988\,A_{23} \\ & +.33638\,A_{25} + .13934\,A_{27} - .02772\,A_{29} + .06691\,A_{31} \\ & \text{-----} \end{aligned}$$

Table B-IV. (cont'd) Fourier Coefficients of f(t) for given Walsh-Fourier Coefficients

$$a_{10} = .25465\,A_2 - .61477\,A_6 + .92008\,A_{10} + .38111\,A_{14} - .20371\,A_{18} + .49179\,A_{22} + .32860\,A_{26} + .13611\,A_{30}$$

$$a_{11} = -.11575\,A_1 + .27944\,A_3 - .41822\,A_5 - .17323\,A_7 - .32409\,A_9 + .78243\,A_{11} + .52280\,A_{13} + .21655\,A_{15} + .12980\,A_{17} - .31336\,A_{19} + .46897\,A_{21} + .19425\,A_{23} - .10383\,A_{25} + .25067\,A_{27} + .16749\,A_{29} + .06938\,A_{31}$$

$$a_{12} = -.42441\,A_4 + 1.02462\,A_{12} + .68463\,A_{20} + .28358\,A_{28}$$

$$a_{13} = +.09794\,A_1 - .23645\,A_3 - .15799\,A_5 - .06544\,A_7 + .21574\,A_9 - .52083\,A_{11} + .77948\,A_{13} + .32287\,A_{15} - .23948\,A_{17} + .57810\,A_{19} + .38627\,A_{21} + .16000\,A_{23} + .04854\,A_{25} - .11718\,A_{27} + .17537\,A_{29} + .07264\,A_{31}$$

$$a_{14} = -.18189\,A_2 - .07534\,A_6 - .37877\,A_{10} + .91443\,A_{14} + .75045\,A_{18} + .31085\,A_{22} - .06183\,A_{26} + .14927\,A_{30}$$

$$a_{15} = -.08488\,A_1 - .03516\,A_3 + .00699\,A_5 - .01688\,A_7 - .17143\,A_9 - .07101\,A_{11} - .35698\,A_{13} + .86183\,A_{15} + .78112\,A_{17} + .32355\,A_{19} - .06436\,A_{21} + .15537\,A_{23} - .01530\,A_{25} - .00634\,A_{27} - .03187\,A_{29} + .07693\,A_{31}$$

$$a_{16} = 1.27324\,A_{16} + \text{-----}$$

$$a_{17} = .07490\,A_1 + .03102\,A_3 - .00617\,A_5 + .01490\,A_7 + .15126\,A_9 + .06265\,A_{11} + .31498\,A_{13} - .76044\,A_{15} + .83901\,A_{17} + .34753\,A_{19} - .06913\,A_{21} + .16689\,A_{23} - .01644\,A_{25} + .00681\,A_{27} - .03423\,A_{29} + .08264\,A_{31}$$

$$a_{18} = .14147\,A_2 + .05860\,A_6 + .29460\,A_{10} - .71122\,A_{14} + .86663\,A_{18} + .35897\,A_{22} - .07140\,A_{26} + .17238\,A_{30}$$

$$a_{19} = -.06701\,A_1 + .16178\,A_3 + .10810\,A_5 + .04478\,A_7 - .14761\,A_9 + .35638\,A_{11} - .53333\,A_{13} - .22091\,A_{15} - .29786\,A_{17} + .71911\,A_{19} + .48049\,A_{21} + .19903\,A_{23} + .06037\,A_{25} - .14576\,A_{27} + .21814\,A_{29} + .09036\,A_{31}$$

$$a_{20} = .25465\,A_4 - .61477\,A_{12} + .92008\,A_{20} + .38111\,A_{28}$$

Table B-IV. (cont'd) Fourier Coefficients of f(t) for given Walsh-Fourier Coefficients

$$a_{21} = .06063\,A_1 - .14638\,A_3 + .21907\,A_5 + .09074\,A_7 + .16976\,A_9 - .40984\,A_{11} - .27385\,A_{13} - .11343\,A_{15} + .18925\,A_{17} - .45689\,A_{19} + .68378\,A_{21} + .28323\,A_{29} - .15139\,A_{25} + .36549\,A_{27} + .24421\,A_{29} + .10116\,A_{31}$$

$$a_{22} = -.11575\,A_2 + .27944\,A_6 - .41822\,A_{10} - .17323\,A_{14} - .32409\,A_{18} + .78243\,A_{22} + .52280\,A_{26} + .21655\,A_{30}$$

$$a_{23} = -.05536\,A_1 - .02293\,A_3 - .11528\,A_5 + .27831\,A_7 - .33912\,A_9 - .14047\,A_{11} + .02794\,A_{13} - .06745\,A_{15} - .14262\,A_{17} - .05908\,A_{19} - .29699\,A_{21} + .71700\,A_{23} + .55843\,A_{25} + .24373\,A_{27} - .04848\,A_{29} + .11705\,A_{31}$$

$$a_{24} = -.42441\,A_8 + 1.02462\,A_{24} + \text{-----}$$

$$a_{25} = +.05093\,A_1 + .02110\,A_3 + .10606\,A_5 - .25604\,A_7 - .21013\,A_9 - .08704\,A_{11} + .01731\,A_{13} - .04180\,A_{15} + .11683\,A_{17} + .04839\,A_{19} + .24325\,A_{21} - .58727\,A_{23} + .71559\,A_{25} + .29641\,A_{27} - .05896\,A_{29} + .14234\,A_{31}$$

$$a_{26} = .09794\,A_2 - .23645\,A_6 - .15799\,A_{10} - .06544\,A_{14} + .21574\,A_{18} - .52083\,A_{22} + .77948\,A_{26} + .32287\,A_{30}$$

$$a_{27} = -.04716\,A_1 + .11385\,A_3 - .17038\,A_5 - .07058\,A_7 + .03772\,A_9 - .09107\,A_{11} - .06085\,A_{13} - .02521\,A_{15} - .10063\,A_{17} + .24294\,A_{19} - .36358\,A_{21} - .15060\,A_{23} - .28175\,A_{25} + .68021\,A_{27} + .45450\,A_{29} + .18826\,A_{31}$$

$$a_{28} = -.18189\,A_4 - .07534\,A_{12} - .37877\,A_{20} + .91443\,A_{28} + \text{-----}$$

$$a_{29} = .04391\,A_1 - .10600\,A_3 - .07082\,A_9 - .02934\,A_7 - .00890\,A_9 + .02148\,A_{11} - .03215\,A_{13} - .01332\,A_{15} + .08979\,A_{17} - .21676\,A_{19} - .14484\,A_{21} - .05999\,A_{23} + .19777\,A_{25} - .47748\,A_{27} + .71456\,A_{29} + .29598\,A_{31}$$

$$a_{30} = -.08488\,A_2 - .03516\,A_6 + .00699\,A_{10} - .01688\,A_{14} - .17143\,A_{18} - .07101\,A_{22} - .35698\,A_{26} + .86183\,A_{30}$$

Table B-IV. (cont'd) Fourier Coefficients of f(t) for given Walsh-Fourier Coefficients

$$a_{31} = -.04107\,A_1 - .01701\,A_3 + .00338\,A_5 - .00817\,A_7$$
$$+.00081\,A_9 + .00033\,A_{11} + .00168\,A_{13} - .00405\,A_{15}$$
$$-.08234\,A_{17} - .03411\,A_{19} + .00678\,A_{21} - .01638\,A_{23}$$
$$-.16630\,A_{25} - .06888\,A_{27} - .34630\,A_{29} + .83605\,A_{31}$$
$$-----$$

$$a_{32} = 1.27324\,A_{32} + -----$$

$$b_1 = 1.27324\,B_1 - .52739\,B_3 - .10491\,B_5 - .25326\,B_7$$
$$-.02494\,B_9 + .01033\,B_{11} - .05194\,B_{13} - .12540\,B_{15}$$
$$-.00616\,B_{17} + .00255\,B_{19} + .00051\,B_{21} + .00123\,B_{23}$$
$$-.01244\,B_{25} + .00515\,B_{27} - .02591\,B_{29} - .06255\,B_{31}$$
$$-----$$

$$b_2 = 1.27324\,B_2 - .52739\,B_6 - .10491\,B_{10} - .25326\,B_{14}$$
$$-.02494\,B_{18} + .01033\,B_{22} - .05194\,B_{26} - .12540\,B_{30}$$
$$----$$

$$b_3 = .42441\,B_1 + 1.02462\,B_3 - .68463\,B_5 + .28358\,B_7$$
$$-.08602\,B_9 - .20768\,B_{11} - .31082\,B_{13} + .12874\,B_{15}$$
$$-.01910\,B_{17} - .04611\,B_{19} + .03081\,B_{21} - .01276\,B_{23}$$
$$-.04207\,B_{25} - .10156\,B_{27} - .15199\,B_{29} + .06296\,B_{31}$$
$$-----$$

$$b_4 = 1.27324\,B_4 - .52739\,B_{12} - .10491\,B_{20} - .25326\,B_{28}$$
$$-----$$

$$b_5 = .25465\,B_1 + .61477\,B_3 + .92008\,B_5 - .38111\,B_7$$
$$-.20371\,B_9 - .49179\,B_{11} + .32860\,B_{13} - .13611\,B_{15}$$
$$-.03409\,B_{17} - .08231\,B_{19} - .12319\,B_{21} + .05103\,B_{23}$$
$$-.09546\,B_{25} - .23047\,B_{27} + .15399\,B_{29} - .06379\,B_{31}$$
$$-----$$

$$b_6 = .42441\,B_2 + 1.02462\,B_6 - .68463\,B_{10} + .28358\,B_{14}$$
$$-.08602\,B_{18} - .20768\,B_{22} - .31082\,B_{26} + .12874\,B_{30}$$
$$-----$$

$$b_7 = .18189\,B_1 - .07534\,B_3 + .37877\,B_5 + .91443\,B_7$$
$$-.75045\,B_9 + .31085\,B_{11} + .06183\,B_{13} + .14927\,B_{15}$$
$$-.05341\,B_{17} + .02212\,B_{19} - .11122\,B_{21} - .26852\,B_{23}$$
$$-.32719\,B_{25} + .13553\,B_{27} + .02696\,B_{29} + .06508\,B_{31}$$
$$-----$$

$$b_8 = 1.27324\,B_8 - .52739\,B_{24} -----$$

$$b_9 = .14147\,B_1 - .05860\,B_3 + .29460\,B_5 + .71122\,B_7$$
$$+.86663\,B_9 - .35897\,B_{11} - .07140\,B_{13} - .17238\,B_{15}$$
$$-.08153\,B_{17} + .03377\,B_{19} - .16978\,B_{21} - .40988\,B_{23}$$
$$+.33638\,B_{25} - .13934\,B_{27} - .02772\,B_{29} - .06691\,B_{31}$$
$$-----$$

Table B-IV. (cont'd) Fourier Coefficients of f(t) for given Walsh-Fourier Coefficients

$$b_{10} = .25465\,B_2 + .61477\,B_6 + .92008\,B_{10} - .38111\,B_{14} - .20371\,B_{18} - .49179\,B_{22} + .32860\,B_{26} - .13611\,B_{30}$$

$$b_{11} = .11575\,B_1 + .27944\,B_3 + .41822\,B_5 - .17323\,B_7 + .32409\,B_9 + .78243\,B_{11} - .52280\,B_{13} + .21655\,B_{15} - .12980\,B_{17} - .31336\,B_{19} - .46897\,B_{21} + .19425\,B_{23} + .10383\,B_{25} + .25067\,B_{27} - .16749\,B_{29} + .06938\,B_{31}$$

$$b_{12} = .42441\,B_4 + 1.02462\,B_{12} - .68463\,B_{20} + .28358\,B_{28}$$

$$b_{13} = .09794\,B_1 + .23645\,B_3 - .15799\,B_5 + .06544\,B_7 + .21574\,B_9 + .52083\,B_{11} + .77948\,B_{13} - .32287\,B_{15} - .23948\,B_{17} - .57810\,B_{19} + .38627\,B_{21} - .16000\,B_{23} + .04854\,B_{25} + .11718\,B_{27} + .17537\,B_{29} - .07264\,B_{31}$$

$$b_{14} = .18189\,B_2 - .07534\,B_6 + .37877\,B_{10} + .91443\,B_{14} - .75045\,B_{18} + .31085\,B_{22} + .06183\,B_{26} + .14927\,B_{30}$$

$$b_{15} = .08488\,B_1 - .03516\,B_3 - .00699\,B_5 - .01688\,B_7 + .17143\,B_9 - .07101\,B_{11} + .35698\,B_{13} + .86183\,B_{15} - .78112\,B_{17} + .32355\,B_{19} + .06436\,B_{21} + .15537\,B_{23} + .01530\,B_{25} - .00634\,B_{27} + .03187\,B_{29} + .07693\,B_{31}$$

$$b_{16} = 1.27324\,B_{16}$$

$$b_{17} = .07490\,B_1 - .03102\,B_3 - .00617\,B_5 - .01490\,B_7 + .15126\,B_9 - .06265\,B_{11} + .31498\,B_{13} + .76044\,B_{15} + .83901\,B_{17} - .34753\,B_{19} - .06913\,B_{21} - .16689\,B_{23} - .01644\,B_{25} + .00681\,B_{27} - .03423\,B_{29} - .08264\,B_{31}$$

$$b_{18} = .14147\,B_2 - .05860\,B_6 + .29460\,B_{10} + .71122\,B_{14} + .86663\,B_{18} - .35897\,B_{22} - .07140\,B_{26} - .17238\,B_{30}$$

$$b_{19} = .06701\,B_1 + .16178\,B_3 - .10810\,B_5 + .04478\,B_7 + .14761\,B_9 + .35638\,B_{11} + .53333\,B_{13} - .22091\,B_{15} + .29786\,B_{17} + .71911\,B_{19} - .48049\,B_{21} + .19903\,B_{23} - .06037\,B_{25} - .14576\,B_{27} - .21814\,B_{29} + .09036\,B_{31}$$

$$b_{20} = .25465\,B_4 + .61477\,B_{12} + .92008\,B_{20} - .38111\,B_{28}$$

Table B-IV. (cont'd) Fourier Coefficients of f(t) for given Walsh-Fourier Coefficients

$$b_{21} = .06063\,B_1 + .14638\,B_3 + .21907\,B_5 - .09074\,B_7 + .16976\,B_9 + .40984\,B_{11} - .27385\,B_{13} + .11343\,B_{15} + .18925\,B_{17} + .45689\,B_{19} + .68378\,B_{21} - .28323\,B_{23} - .15139\,B_{25} - .36549\,B_{27} + .24421\,B_{29} - .10116\,B_{31}$$

$$b_{22} = .11575\,B_2 + .27944\,B_6 + .41822\,B_{10} - .17323\,B_{14} + .32409\,B_{18} + .78243\,B_{22} - .52280\,B_{26} + .21655\,B_{30}$$

$$b_{23} = .05536\,B_1 - .02293\,B_3 + .11528\,B_5 + .27831\,B_7 + .33912\,B_9 - .14047\,B_{11} - .02794\,B_{13} - .06745\,B_{15} + .14262\,B_{17} - .05908\,B_{19} + .29699\,B_{21} + .71700\,B_{23} - .55843\,B_{25} + .24373\,B_{27} + .04848\,B_{29} + .11705\,B_{31}$$

$$b_{24} = .42441\,B_8 + 1.02462\,B_{24}$$

$$b_{25} = .05093\,B_1 - .02110\,B_3 + .10606\,B_5 + .25604\,B_7 - .21013\,B_9 + .08704\,B_{11} + .01731\,B_{13} + .04180\,B_{15} + .11683\,B_{17} - .04839\,B_{19} + .24325\,B_{21} + .58727\,B_{23} + .71559\,B_{25} - .29641\,B_{27} - .05896\,B_{29} - .14234\,B_{31}$$

$$b_{26} = .09794\,B_2 + .23645\,B_6 - .15799\,B_{10} + .06544\,B_{14} + .21574\,B_{18} + .52083\,B_{22} + .77948\,B_{26} - .32287\,B_{30}$$

$$b_{27} = .04716\,B_1 + .11385\,B_3 + .17038\,B_5 - .07058\,B_7 - .03772\,B_9 - .09107\,B_{11} + .06085\,B_{13} - .02521\,B_{15} + .10063\,B_{17} + .24294\,B_{19} + .36358\,B_{21} - .15060\,B_{23} + .28175\,B_{25} + .68021\,B_{27} - .45450\,B_{29} + .18826\,B_{31}$$

$$b_{28} = .18189\,B_4 - .07534\,B_{12} + .37877\,B_{20} + .91443\,B_{28}$$

$$b_{29} = .04391\,B_1 + .10600\,B_3 - .07082\,B_5 + .02934\,B_7 - .00890\,B_9 - .02148\,B_{11} - .03215\,B_{13} + .01332\,B_{15} + .08979\,B_{17} + .21676\,B_{19} - .14484\,B_{21} + .05999\,B_{23} + .19777\,B_{25} + .47748\,B_{27} + .71456\,B_{29} - .29598\,B_{31}$$

$$b_{30} = .08488\,B_2 - .03516\,B_6 - .00699\,B_{10} - .01688\,B_{14} + .17143\,B_{18} - .01701\,B_{22} + .35698\,B_{26} + .86183\,B_{30}$$

Table B-IV. (cont'd) Fourier Coefficients of f(t) for given Walsh Fourier Coefficients

$$b_{31} = .04107\,B_1 - .01701\,B_3 - .00338\,B_5 - .00817\,B_7 - .00081\,B_9 + .00033\,B_{11} - .00168\,B_{13} - .00405\,B_{15} + .08234\,B_{17} - .03411\,B_{19} - .00678\,B_{21} - .01638\,B_{23} + .16630\,B_{25} - .06888\,B_{27} + .34630\,B_{29} + .83605\,B_{31}$$

$$b_{32} = 1.27324\,B_{32}$$

Appendix C. Layout of Circuit Boards

The following diagrams show the layout of the integrated circuit chips on the 3 boards of the Walsh Function Generator and the 2 boards of the Pulse Burst Generator. Each of the integrated circuits is labelled with the type number and a letter designation. Only Figure C-1 shows the input-output terminals. On all boards, terminal Ⓐ is Vcc and Ⓩ is ground. Table C-1 below lists each of the integrated circuits that are used on the boards.

Table C-1. List of Integrated Circuits

Type No.	Circuit Function
SN7400N	Quadruple 2-input positive NAND gate
SN7401N	Quad 2-input NAND gate w/open collector output
SN7430N	8-input positive NAND gate
SN7440N	Dual 4-input positive NAND "power" gate
SN7451N	Dual AND-OR-invert gate
SN7473N	Dual master/slave J-K Flip-flop

Type number SN7473N has Vcc on pin 4 and ground on pin 11. All other chips have Vcc on pin 14 and ground on pin 7. Fan-out for SN7440N is 30 units. All other chips have a fan-out of 10. All input leads have a fan-in of 1. Schematic diagrams of each integrated circuit listed in Table C-1 are shown in Figure C-5 on page 111.

Figure C-1. Walsh Function Generator - Card I

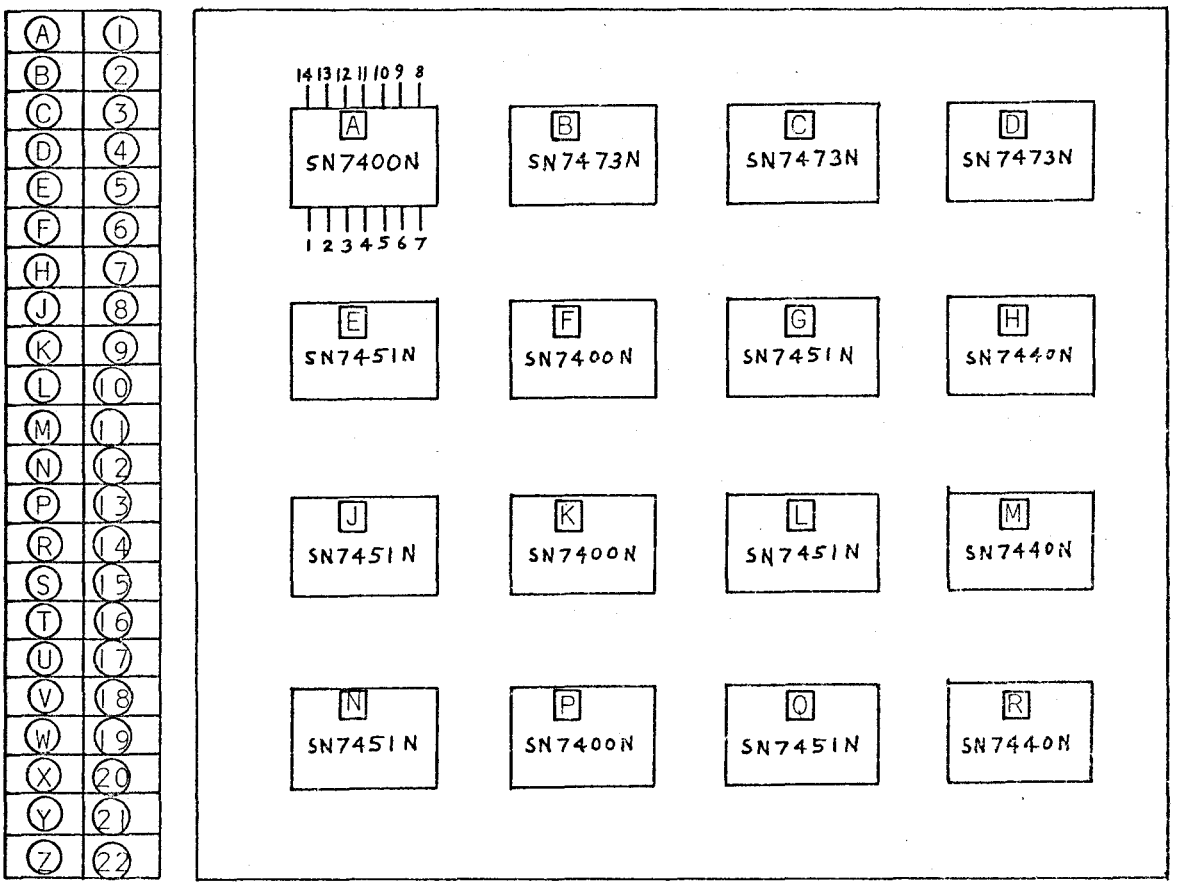

Note: Only integrated circuit [A] shows pin locations.

Figure C-2. Walsh Function Generator - Cards 2 and 3

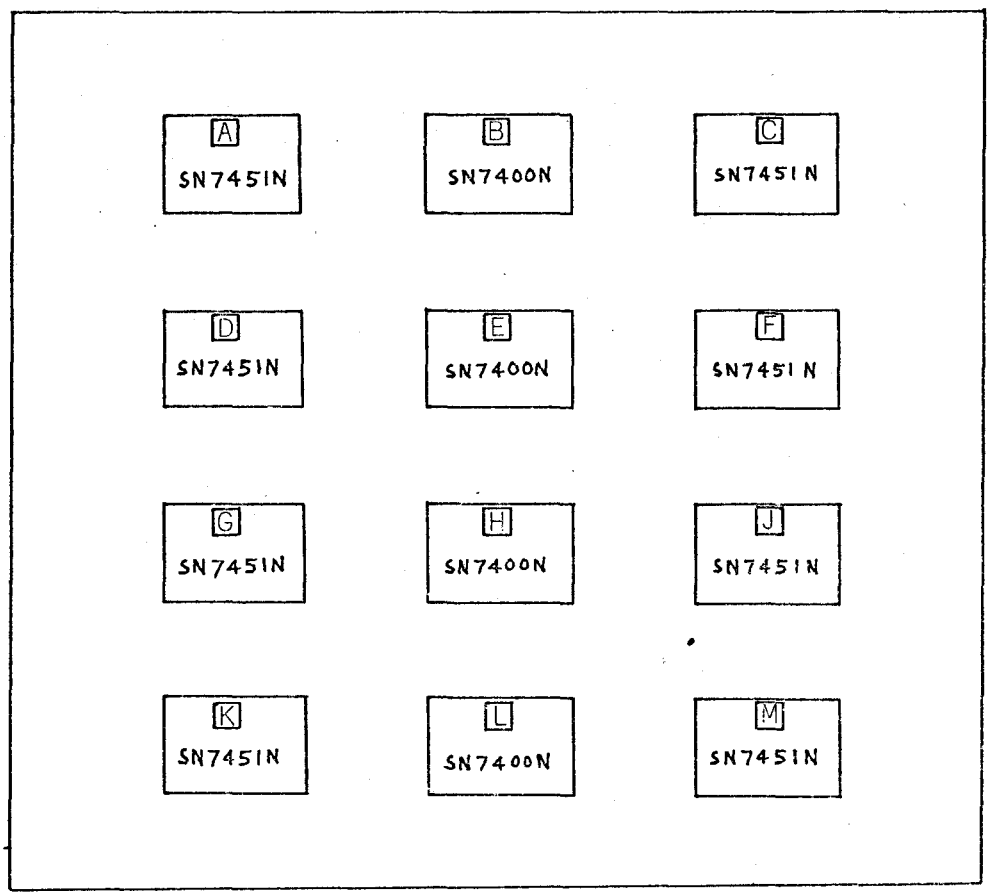

Cards 2 and 3 of the Walsh Function Generator are identical in layout.

Figure C-3. Pulse Burst Generator - Card I

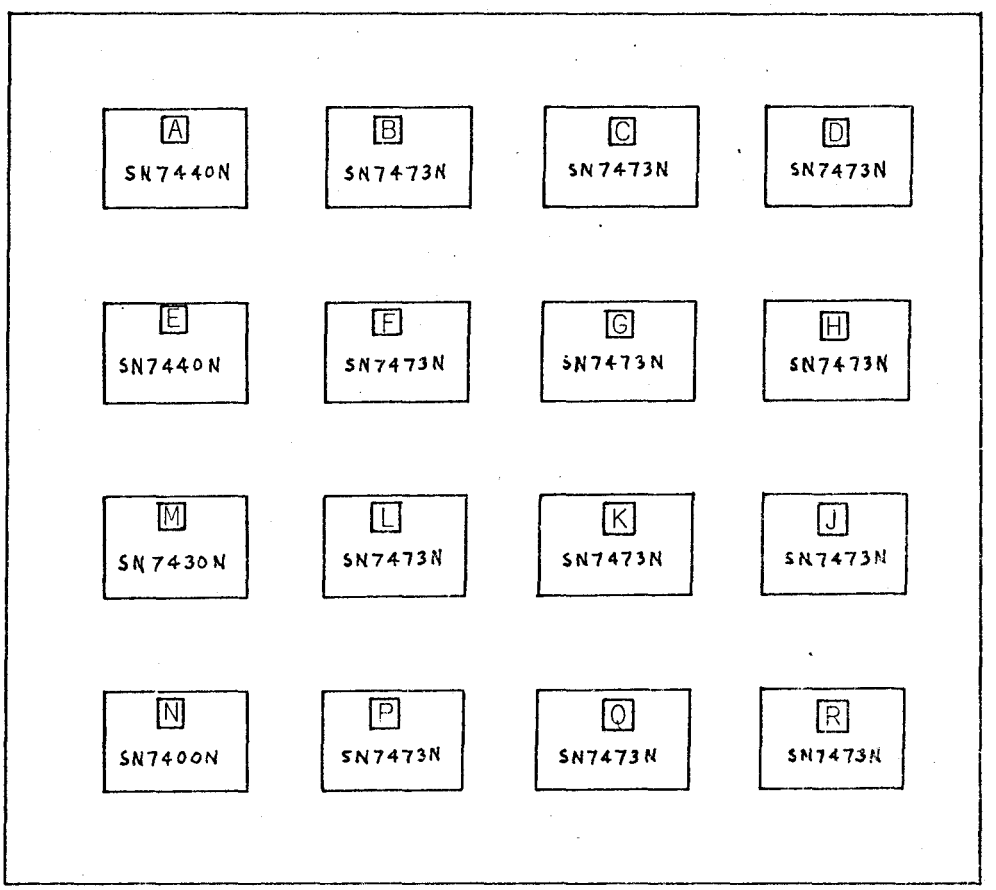

Figure C-4. Pulse Burst Generator - Card 2

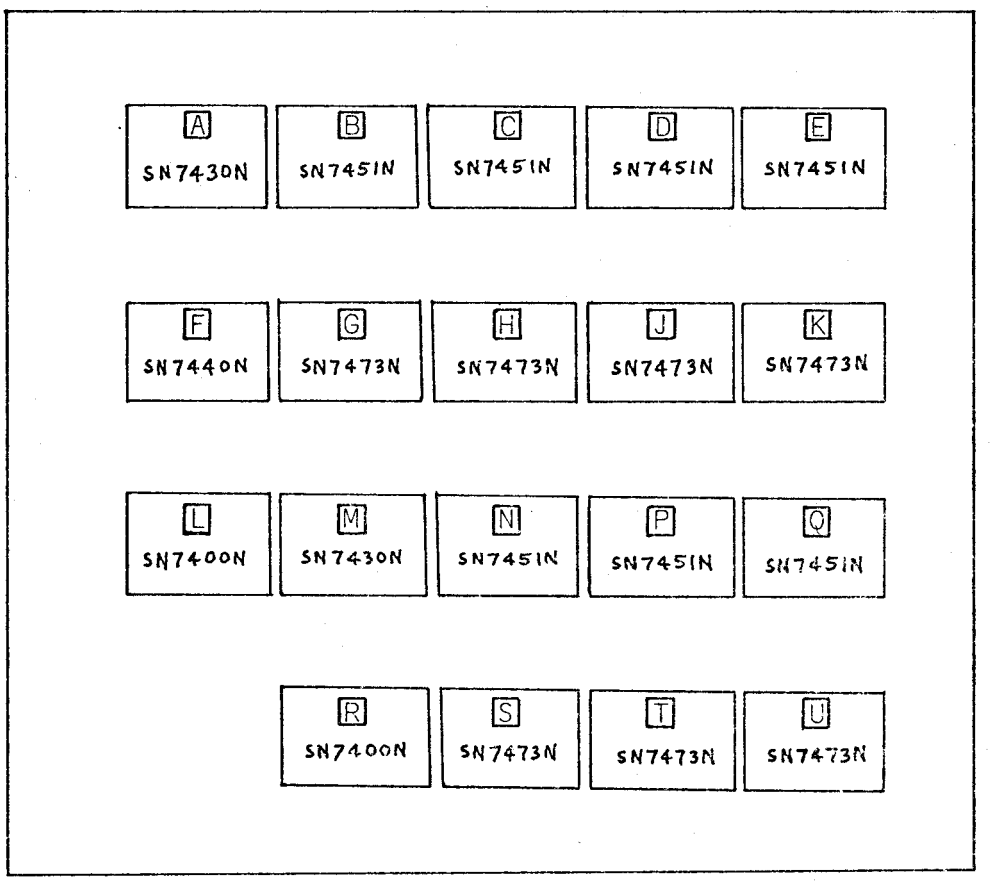

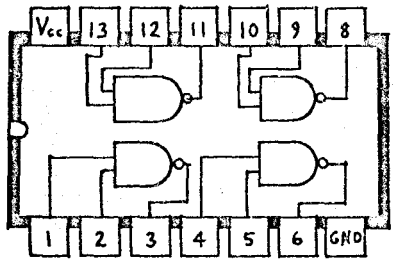

SN7400N
Quadruple 2-input NAND

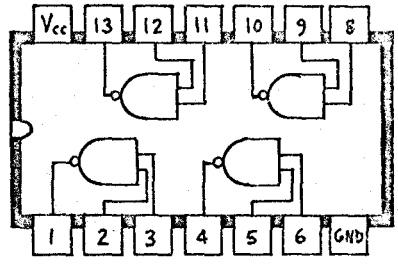

SN7401N
Quadruple Open Collector 2-input NAND

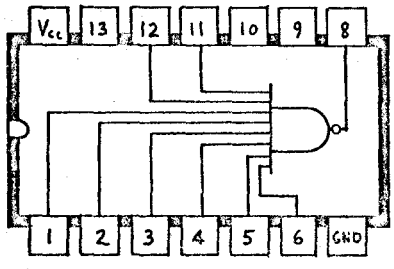

SN7430N
8-input NAND

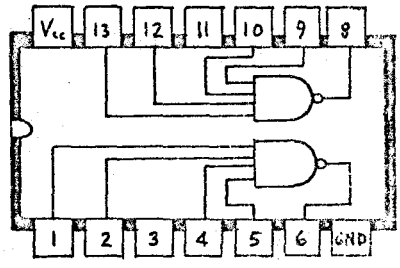

SN7440N
Dual 4-input NAND Buffer

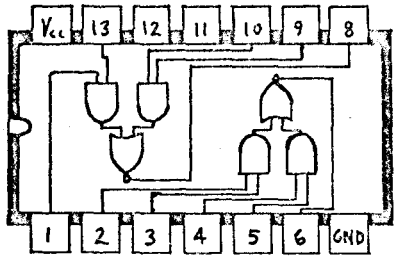

SN7451N
Dual AND-OR-Invert

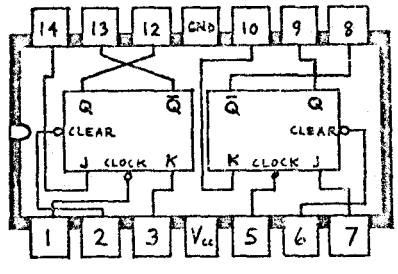

SN7473N
Dual J-K Flip-Flop

Figure C-5. TTL Integrated Circuits

Appendix D. Errors in Walsh-Fourier to Fourier Series Conversion when Walsh-Fourier Series is Limited to sal(32,θ) and cal(31,θ)

Table D-1. Square Wave (Amplitude, 10 Volts)

N	A_n	B_n	a_n	b_n
1	0.0	10.0	0.0	12.732
2	0.0	0.0	0.0	0.000
3	0.0	0.0	0.0	4.244
4	0.0	0.0	0.0	0.000
5	0.0	0.0	0.0	2.547
6	0.0	0.0	0.0	0.000
7	0.0	0.0	0.0	1.819
8	0.0	0.0	0.0	0.000
9	0.0	0.0	0.0	1.415
10	0.0	0.0	0.0	0.000

True values of coefficients

N	a_n	Error	% Error	b_n	Error	% Error
1	0.0	0.0	undefined	12.732	0.0	0.0
2	0.0	0.0	"	0.000	0.0	undefined
3	0.0	0.0	"	4.244	0.0	0.0
4	0.0	0.0	"	0.000	0.0	undefined
5	0.0	0.0	"	2.547	0.0	0.0
6	0.0	0.0	"	0.000	0.0	undefined
7	0.0	0.0	"	1.819	0.0	0.0
8	0.0	0.0	"	0.000	0.0	undefined
9	0.0	0.0	"	1.415	0.0	0.0
10	0.0	0.0	"	0.000	0.0	undefined

Calculated values of a_n and b_n using Walsh-Fourier Coefficients

Table D-II. 10 Volt Pulse (Duty cycle = 1/3)

N	A_n	B_n	a_n	b_n
1	1.667	3.333	2.756	4.775
2	-.833	1.667	-1.378	2.387
3	.833	-.833	0.0	0.0
4	.417	.833	.689	1.194
5	-.417	.417	-.551	.955
6	-.417	-.417	0.0	0.0
7	.417	-.417	.394	.682
8	-.208	.417	-.345	.597
9	.208	-.208	0.0	0.0
10	.208	.208	.276	.477

True values of coefficients

N	a_n	Error	% Error	b_n	Error	% Error
1	2.754	.003	.106	4.773	.002	.036
2	-1.372	-.006	.433	2.384	.003	.137
3	.000	.000	undefined	.010	.010	undefined
4	.678	.011	1.663	1.186	.007	.612
5	-.536	-.015	2.744	.947	.008	.801
6	-.001	-.001	undefined	.020	.020	undefined
7	.374	.019	4.950	.669	.013	1.955
8	-.320	-.024	7.077	.585	.011	1.906
9	-.003	-.003	undefined	.030	.030	undefined
10	.249	.027	9.771	.458	.020	4.131

Calculated Values of a_n and b_n using Walsh-Fourier Coefficients

Table D-III. 10 Volt Pulse (Duty cycle = 1/5)

N	A_n	B_n	a_n	b_n
1	2.0	2.0	3.027	2.199
2	.5	2.0	.935	2.879
3	.5	.5	-.624	1.919
4	-.5	.5	-.757	.550
5	-.5	-.5	0.0	0.0
6	.5	-.5	.505	.367
7	.5	.5	.267	.823
8	-.125	.5	-.234	.720
9	-.125	-.125	-.336	.244
10	.125	-.125	0.0	0.0

True values of coefficients

N	a_n	Error	% Error	b_n	Error	% Error
1	3.025	.002	.077	2.200	-.001	-.037
2	.932	.003	.325	2.875	.004	.133
3	-.620	-.004	.636	1.913	.006	.322
4	-.747	-.010	1.257	.552	-.002	-.416
5	.001	.001	undefined	.012	.012	undefined
6	.491	.013	2.637	.373	-.006	-1.657
7	.256	.012	4.403	.810	.012	1.489
8	-.225	-.009	3.760	.703	.017	2.395
9	-.315	-.021	6.387	.247	-.003	-1.219
10	.005	.005	undefined	.024	.024	undefined

Calculated values of a_n and b_n using Walsh-Fourier Coefficients

Table D-IV. 10 Volt Pulse (Duty cycle = 1/8)

N	A_n	B_n	a_n	b_n
1	1.25	1.25	2.251	.932
2	1.25	1.25	1.592	1.592
3	1.25	1.25	.750	1.811
4	0.0	1.25	0.000	1.592
5	0.0	0.0	-.450	1.087
6	0.0	0.0	-.531	.531
7	0.0	0.0	-.322	.133
8	0.0	0.0	0.000	0.000
9	0.0	0.0	.250	.104
10	0.0	0.0	.318	.318

True values of coefficients

N	a_n	Error	% Error	b_n	Error	% Error
1	2.251	0.0	0.0	.932	0.0	0.0
2	1.592	0.0	0.0	1.592	0.0	0.0
3	.750	0.0	0.0	1.811	0.0	0.0
4	0.000	0.0	undefined	1.592	0.0	0.0
5	-.450	0.0	0.0	1.087	0.0	0.0
6	-.531	0.0	0.0	.531	0.0	0.0
7	-.322	0.0	0.0	.133	0.0	0.0
8	0.000	0.0	undefined	0.000	0.0	undefined
9	.250	0.0	0.0	.104	0.0	0.0
10	.318	0.0	0.0	.318	0.0	0.0

Calculated values of a_n and b_n using Walsh-Fourier Coefficients

Table D-V. 10 sin $2\pi ft$

N	A_n	B_n	a_n	b_n
1	0.0	6.366	0.0	10.0
2	0.0	0.000	0.0	0.0
3	0.0	-2.637	0.0	0.0
4	0.0	0.000	0.0	0.0
5	0.0	-.525	0.0	0.0
6	0.0	0.000	0.0	0.0
7	0.0	-1.266	0.0	0.0
8	0.0	0.000	0.0	0.0
9	0.0	-.125	0.0	0.0
10	0.0	0.000	0.0	0.0

True values of coefficients

N	a_n	Error	% Error	b_n	Error	% Error
1	0.0	0.0	undefined	9.992	.008	.080
2	0.0	0.0	"	0.0	0.0	undefined
3	0.0	0.0	"	0.0	0.0	"
4	0.0	0.0	"	0.0	0.0	"
5	0.0	0.0	"	0.0	0.0	"
6	0.0	0.0	"	0.0	0.0	"
7	0.0	0.0	"	0.0	0.0	"
8	0.0	0.0	"	0.0	0.0	"
9	0.0	0.0	"	0.0	0.0	"
10	0.0	0.0	"	0.0	0.0	"

Calculated values of a_n and b_n using Walsh-Fourier Coefficients

Table D-VI. Sum of 10 Sines Waves (First 10 Harmonics of Fourier Series are Equal)

N	A_n	B_n	a_n	b_n
1	0.0	1.138	0.0	1.0
2	0.0	.976	0.0	1.0
3	0.0	.489	0.0	1.0
4	0.0	.637	0.0	1.0
5	0.0	.402	0.0	1.0
6	0.0	.556	0.0	1.0
7	0.0	.637	0.0	1.0
8	0.0	.637	0.0	1.0
9	0.0	-.099	0.0	1.0
10	0.0	-.065	0.0	1.0

True values of coefficients

N	a_n	Error	% Error	b_n	Error	% Error
1	0.0	0.0	undefined	.999	.001	.080
2	0.0	0.0	"	.997	.003	.321
3	0.0	0.0	"	.992	.007	.721
4	0.0	0.0	"	.987	.013	1.279
5	0.0	0.0	"	.980	.020	1.992
6	0.0	0.0	"	.971	.029	2.854
7	0.0	0.0	"	.961	.039	3.874
8	0.0	0.0	"	.950	.050	5.036
9	0.0	0.0	"	.937	.064	6.339
10	0.0	0.0	"	.922	.078	7.778

Calculated values of a_n and b_n using Walsh-Fourier coefficients

Table D-VII. Triangular Wave (Peak Amplitude, 10 Volts)

N	A_n	B_n	a_n	b_n
1	0.0	5.0	0.0	8.106
2	0.0	0.0	0.0	.000
3	0.0	-2.5	0.0	-.901
4	0.0	0.0	0.0	.000
5	0.0	0.0	0.0	.324
6	0.0	0.0	0.0	.000
7	0.0	-1.25	0.0	-.165
8	0.0	0.0	0.0	.000
9	0.0	0.0	0.0	.100
10	0.0	0.0	0.0	.000

True values of coefficients

N	a_n	Error	% Error	b_n	Error	% Error
1	0.0	0.0	undefined	8.099	.007	.080
2	0.0	0.0	"	.000	.000	undefined
3	0.0	0.0	"	-.894	.007	.724
4	0.0	0.0	"	.000	.000	undefined
5	0.0	0.0	"	.318	.007	2.009
6	0.0	0.0	"	.000	.000	undefined
7	0.0	0.0	"	-.159	.007	3.962
8	0.0	0.0	"	.000	.000	undefined
9	0.0	0.0	"	.093	.007	6.594
10	0.0	0.0	"	.000	.000	undefined

Calculated values of a_n and b_n using Walsh-Fourier coefficients

Bibliography

1. William S. Burdic, "Radar Signal Analysis", Prentice-Hall, Inc., Englewood Cliffs, N.Y., 1968.

2. "Digital Logic Handbook", Digital Equipment Corporation, Maynard, Mass., 1968.

3. Henning F. Harmuth, "Sequency Multiplex Systems for Telephony and Data Transmission", International Electronics Conference, I.E.E.E., Toronto, Sept. 1967.

4. _____, "A Generalized Concept of Frequency and Some Applications", I.E.E.E. Transactions on Information Theory, Vol. IT-14, No. 3, May 1968.

5. G. W. Morgenthaler, "On Walsh-Fourier Series", Trans. Am. Math. Soc., Vol. 65, 1949.

6. "TTL Integrated Circuits from Texas Instruments", 1968 Catalogue.